15

NASA CR 72259
AMS TR 798

Axial Mode Shock Wave Combustion Instability in Liquid Propellant Rocket Engines

by

Charles E. Mitchell

prepared for

NATIONAL AERONAUTICS AND SPACE ADMINISTRATION
Contract NASr 217

July 1967

Department of Aerospace
and Mechanical Sciences
PRINCETON UNIVERSITY

NASA CR 72259
AMS TR-798

TECHNICAL REPORT

AXIAL MODE SHOCK WAVE COMBUSTION INSTABILITY IN LIQUID PROPELLANT ROCKET ENGINES

by

Charles E. Mitchell

approved by

Luigi Crocco and William A. Sirignano

prepared for

NATIONAL AERONAUTICS AND SPACE ADMINISTRATION

July 1967

CONTRACT NASr-217

Technical Management
NASA Lewis Research Center
Cleveland, Ohio
Chemistry and Energy Conversion Division
Marcus F. Heidmann

Guggenheim Laboratories for the Aerospace Propulsion Sciences
Department of Aerospace and Mechanical Sciences
Princeton University
Princeton, New Jersey

ABSTRACT

Axial mode combustion instability in liquid rocket combustors is investigated, analytically, with the combustion processes represented using the Crocco time-lag concept. Periodic oscillations of finite amplitude, both continuous and discontinuous in form, are studied.

Two types of combustion distribution are considered. The first is the limiting case where the combustion can be taken to be concentrated at the injector face. The second occurs when the combustion is sufficiently distributed so that the derivative of the steady-state velocity is of the same order as the steady-state velocity itself.

For either type of combustion distribution both continuous and discontinuous pressure waves are predicted for values of the combustion feedback parameters that are in the range of practical interest. Small amplitude continuous oscillations are found to exist near the stability limit predicted by previous linear analyses. Larger amplitude discontinuous, shock-type oscillations are found at larger displacements into the region of linear instability. Discontinuous oscillations are also found for some values of the combustion parameters for which linear stability is predicted. In this latter case the periodic discontinuous oscillations are considered to be the form that oscillations take when triggered by a finite amplitude disturbance.

The distinctive form of the discontinuous pressure waves predicted, and their clear-cut dependence on the combustion feedback parameters, offer a potential means of relating the stability behavior of a given combustor to the two combustion feedback parameters through experimental techniques.

ACKNOWLEDGEMENTS

It is a pleasure to acknowledge the invaluable guidance given by Professor Luigi Crocco throughout the course of this investigation. The many valuable suggestions given by him made the completion of this report possible; the discussions of the work held with him made the endeavor stimulating and pleasurable.

I am very grateful to Dr. William A. Sirignano who generously gave of his time in many fruitful discussions. His knowledge in the area of nonlinear mechanics was often drawn upon.

The help of Mr. David T. Harrje, Senior Research Engineer, in the understanding of the experimental combustion instability program at Princeton is sincerely appreciated. Mr. Lanny Hoffman of the Guggenheim Computing Group gave many helpful suggestions concerning the numerical work carried out in this investigation.

Support for this research was provided by NASA under Grant NsG-99-60 and Contract NASr-217. The work also made use of computer facilities supported in part by National Science Foundation Grant NSF-GP579.

TABLE OF CONTENTS

NOMENCLATURE

General

x = longitudinal space dimension

t = time

u = gas velocity

a = speed of sound

p = pressure

ρ = density

T = temperature

s = entropy

h = enthalpy

γ = ratio of specific heats

$\mathcal{R}$ = gas constant

M = Mach number

n = interaction index

τ = time-lag

$\mathcal{T}$ = period of oscillation

ϵ = perturbation parameter

U = shock velocity

θ = stretched time coordinate

μ = stretched time-lag

Δ = normal displacement from linear stability curve

$\mathcal{D}$ = displacement factor

c_p = specific heat at constant pressure

g_r = function of the argument $t - \frac{x}{1 + M}$ of $O(\epsilon)$

g_s = function of the argument $t + \frac{x}{1 - M}$ of $O(\epsilon)$

f_r = function of the argument $\theta - x$ of $O(M)$

f_s = function of the argument $\theta + x$ of $O(M)$

f_r = function of the argument $\theta - x$ of $O(M^2)$

f_s = function of the argument $\theta + x$ of $O(M^2)$

δ = perturbation parameter

$\bar{\bar{T}}_1 = \frac{T_1}{M}$

$g = \frac{(\gamma + 1) f_r}{M} = \frac{\gamma + 1}{2\gamma M} \quad p_1(x = 0)$

$\dot{m}$ = mass flow per unit area per unit time

Subscripts

$i = 0, 1, 2, \ldots$etc. - i^{th} term in series expansion (in M or M_E)

I, II - quantities in region I or II respectively (see Figure 1)

ℓ - indicates property of liquid propellant

E - quantities at $x = 1$ (exit to cylindrical part of combustion chamber)

s - stagnation quantity (except for f_s , F_s , g_s)

r - reference quantity

Superscripts

(1) (2) (3) ....etc. - i^{th} term in series expansion in δ

$\longrightarrow$ - vector quantity

' - (primes) indicate deviation of quantity from its steady-state value

* - dimensional quantity

$\bar{}$ - steady-state quantity

Note: Superscripts appearing in the text without brackets around them signify the numerbered references given at the end of the text.

INTRODUCTION

During operation, a liquid propellant rocket engine may exhibit organized oscillations of physical quantities, such as pressure and velocity, in the combustion chamber. This phenomenon is designated combustion instability and is to be distinguished from rough combustion, in which the gas field properties in the chamber fluctuate in a random manner.

The most destructive kind of combustion instability is characterized by frequencies of oscillation which are close to the frequencies of the organ pipe or acoustic modes characteristic of the given combustion chamber. This instability is thought to be generated by a more or less in phase coupling between energy addition from the combustion process and the pressure oscillations in the chamber.

Other kinds of combustion instability which are observed have lower characteristic frequencies and are caused either by coupling between the propellant feed system dynamics and the pressure oscillations in the chamber or by coupling between entropy waves (caused by local mixture ratio variations) and pressure oscillations in the chamber.

The first mentioned type of instability, usually called high frequency instability, is the problem toward which the present investigation is directed.

In order to successfully analyze the general problem of high frequency instability it is necessary to first understand three sub problems associated with unsteady operation of a liquid propellant rocket engine. The three areas which must be examined are:

1) The behavior of the combustion processes in the chamber under oscillatory conditions This includes understanding such phenomena as liquid jet mixing, vaporization and chemical kinetics.

2) The behavior of the supercritical nozzle flow under oscillatory conditions. This problem involves studying the effects of varying cross-sectional area on gasdynamic oscillations, including the effects of nonlinear wave interactions.

3) The character of the wave-type oscillations in the chamber. The gasdynamic field which must be studied and in which the oscillations occur has sources of mass and energy distributed throughout it. The oscillations themselves may exhibit discontinuities or shocks and will certainly be determined by nonlinear interactions, at least for established oscillations.

Strictly speaking, these three problems are related to each other to varying degrees. For example, the presence of combustion in the nozzle or in the chamber will cause the gasdynamic flows there to depend upon the way in which combustion takes place. It is often convenient, however, to separate these problems initially and then to combine them in a stability analysis at a later time. An illustration of this is the case in which the combustion zone can be considered to be concentrated at the injector. In this situation the chamber and nozzle flow fields are naturally separated from the combustion processes. Indeed, the combustion and nozzle flow characteristics only appear as boundary conditions for the chamber flow equations in this case.

At the present time not one of these three problems has been analyzed with complete success. The situation in the case of the first

problem area, that of the combustion process itself, is probably the worst. Here, even the steady-state combustion of liquid propellants in rocket combustors is not well understood. In the absence of detailed knowledge of the combustion processes, it has proved useful in the study of combustion instability to devise and employ certain heuristic models of combustion which, it is hoped, represent sufficiently well those characteristics of the combustion process which are essential to the energy feedback loop supporting the oscillations of the gas in the rocket combustion chamber. Of these heuristic models for the combustion in the chamber, the Crocco sensitive time-lag theory has been most successfully employed in the analysis of high frequency instability.

Essentially, this model assumes that during a certain period of time (the sensitive time-lag) before the instant of combustion, the propellants are affected by the conditions in the chamber to the extent that the moment of combustion for a given propellant element may be advanced or retarded according to the varying pressure, temperature, etc. in the chamber. The sensitivity of the propellant element to the oscillating chamber conditions is measured through the use of a second parameter, the interaction index, which correlates variations in temperature and other chamber properties to the pressure variations in the chamber. Detailed descriptions of Crocco's model appear at length in the literature on combustion instability.[1,14]

The investigation of the second problem area, the behavior of the exhaust nozzle under oscillatory conditions, is considerably more advanced. In fact, when the amplitude of the oscillations in the nozzle is small enough so that nonlinear interactions are not too important, the

problem has been extensively and successfully treated. Tsien [13] and, later, Crocco [6] studied linear axial oscillations in the convergent parts of nozzle more than fifteen years ago. Since that time the linear theory has been extended to consider three dimensional oscillations in nozzles of varying geometry. A monograph [9] by Crocco and Sirignano gives a complete description of the three dimsensional linear theory, as well as extensive tables of numerical results obtained using the theory.

For oscillations in the nozzle with amplitudes large enough so that nonlinear interactions must be considered important, the theory is not nearly so well developed. Zinn's work [16] considers nonlinear effects up to third order in the amplitude of the pressure waves. Zinn, however, did not examine the case where shock waves might occur in the nozzle. Indeed, his analysis required that the nonlinear waves be continuous in form.

For the case where shock waves are present in the chamber and undergo some kind of complex reflection at the nozzle, no successful analysis of the nozzle flow has been forthcoming so far. However, if axial shock waves are considered and the nozzle is taken to be vanishingly short compared with the chamber length, then it has proved reasonable to approximate the nozzle's behavior by assuming that it is in a state of quasi-steady operation such that the Mach number at the entrance to the nozzle remains constant. In other words, a shock wave incident on the entrance to the nozzle will be partially transmitted and partially reflected, but no phasing or wave distortion will be effected. This approximation is usually referred to as the short nozzle assumption.

The last of the three problems, that of the propagation of waves

in the chamber itself, is dependent upon the behavior of the combustion process and the nozzle flow. In fact, if some particular combustion mechanism and nozzle behavior is assumed, the study of the propagation of waves in the chamber is identical to the examination of the stability of the chamber, or the rocket engine as a whole.

The study of chamber oscillations of small amplitude with the combustion process represented by the time-lag model has been extensively pursued. Crocco and Cheng[1] first treated linear longitudinal oscillations. Later Scala[15] and Reardon[14] extended the linear analysis to include transverse and three dimensional oscillations. These linear studies all resulted in the prediction of certain linear stability limits dependent upon the combustion parameters n, the interaction index, and τ, the time-lag. On one side of these curves in the n, τ plane, the theories predict that small perturbations from steady operation of the chamber will grow in time. On the other side decay of small perturbations in time is predicted. These theoretically determined stability limits have been verified experimentally. For both longitudinal and transverse oscillations the agreement between theory and experiment is quite good.[7,8]

Despite the apparent successes of the linear theories, they leave much to be desired. First of all, they are only applicable to instability initiated by infinitesimally small disturbances to the steady-state chamber operation. Experimentally it is observed, however, that many rockets, though intrinsically stable, can be sent into unstable operation by sudden finite amplitude disturbances. These may occur either accidentally, as by sudden violent mixture ratio variation, or purposely, as by the introduction of charges of high energy gas produced by means such as gunpowder charges.

Clearly, linear analyses cannot predict or explain such behavior. Secondly, most established instability observed experimentally exhibits waveforms that are quite different from the predictions of simple acoustic theory. The waveforms in general are distorted to forms with steep peaks or even discontinuities. Here again it is impossible for linear theories to predict this aspect of the instability; the regime form the oscillations take. Finally, because of the very nature of linear analysis, linear studies of instability can predict nothing about the dependence of the amplitude of the chamber oscillations on the combustion parameters n and τ .

Nonlinear extensions to the linear theory have been successful in explaining some of the phenomena just mentioned. Two nonlinear investigations by Sirignano[2] and Zinn[16] studied, respectively, longitudinal and transverse mode combustion instability for the case of continuous pressure waves of finite amplitude. Both authors employed the time-lag combustion model and assumed that mass and energy addition occurred only in an arbitrarily thin region next to the injector face. The last assumption is equivalent to saying that the chamber is long compared to the zone where combustion occurs. Sirignano also invoked the short nozzle assumption in his work, while Zinn used his previously mentioned nonlinear results for three dimensional oscillations in the nozzle. For both longitudinal and transverse modes of oscillation, periodic finite amplitude waves are found to exist near the linear stability limits. The amplitude of the periodic waves is proportional to the square root of the normal displacement from the linear stability limit in the n , τ plane. It is predicted that the periodic oscillations found for displacements into regions of linear insta-

bility on the n, τ plane are stable periodic oscillations, while the periodic oscillations found for normal displacements into regions of linear stability are unstable periodic oscillations. The existence of unstable periodic solutions in regions of the n, τ plane that are linearly stable is interpreted as indicating that triggering of finite amplitude oscillations is possible. For oscillations with amplitudes less than that of the periodic unstable solution, decay of the amplitude in time is predicted, in agreement with the linear theory. For oscillations with amplitudes greater than that of the unstable periodic solution, however, growth of the amplitude in time is predicted. This means that for some values of n and τ it should be possible to "bomb" an intrinsically stable rocket engine into unstable operation. This is, of course, in agreement with the experimental observations mentioned earlier. The waveforms of the stable periodic oscillations predicted by both Sirignano and Zinn also exhibit the sharp peaks observed in experiments.

Clearly, the nonlinear studies just mentioned add considerable information about instability not obtainable from linear analysis. However, there are some important drawbacks in these analyses. The first, and rather mundane difficulty, is the sheer algebraic complexity involved. This is because the method of eigenfunction expansion is used in the solution of the equations describing the physical situation, and though mathematically correct, this method requires considerable algebraic manipulation. A second, more basic shortcoming in these analyses, is their inability to consider discontinuous waveforms. The final drawback to this method of analysis used by Sirignano and Zinn is that it is only possible to predict the waveforms and nonlinear behavior for values of n and τ that are very

close to the linear stability limit. Nothing can be said about what forms instability might take far from this limit. In particular, though the phenomena of triggering can be predicted, the form that the triggered instability takes cannot be found.

Sirignano[24] also studied longitudinal instability using a different method of analysis that allowed the consideration of discontinuous waveforms. In this case, though the assumptions of combustion concentrated at the injector and short nozzle were employed, the time-lag model was not used to represent the combustion process. Instead a model predicting instantaneous response of the burning rate to pressure fluctuations was used. This meant that the energy addition to the gas-dynamic field was in phase with the pressure oscillations and that no off resonant oscillations associated with out of phase energy addition could be considered. This kind of combustion mechanism can only be valid as a limiting case for liquid propellant rockets, since experimental evidence clearly indicates that a time-lag of the order of the period of oscillation does exist for this type of combustor.[7] Indeed, this kind of combustion mechanism is more descriptive of the situation in a pre-mixed gas rocket, since in this case chemical kinetics are the controlling factor in combustion, and the response of the burning rate to pressure fluctuations is practically instantaneous.

Sirignano solved the problem thus posed using the characteristic coordinate perturbation technique.[17,18,19] He carried out his analysis through second order in an amplitude parameter dependent upon the difference between the energy input at the combustion zone and energy removal at the nozzle. The first order pressure waveforms that resulted were found to

take the form of a shock followed by an exponential decay. This wave form qualitatively agrees with observations of pressure waves in premixed gas rockets.[20]

From this brief summary of accomplishments in the solution of the three problems mentioned earlier, it is seen that there are many challenging areas in the field of combustion instability that are ripe for analytical investigation. The present study will be directed toward the investigation of shock wave combustion instability in the longitudinal mode. The combustion processes will be represented by the Crocco time-lag model. The sources of mass and energy due to combustion will be considered both for the case when they are concentrated at the injector (Chapter I) and for arbitrary axial distributions (Chapter II). The short nozzle approximation will be employed throughout.

The method of analysis will follow the ideas used by Chester in his work on forced oscillation in closed tubes[3] rather than the characteristic coordinate perturbation approach used by Sirignano. The purpose of the analysis is to find the dependence of the waveform and amplitude of discontinuous periodic oscillations on the combustion parameters n and τ when the time-lag model represents the combustion. In this way a nonlinear stability limit will be constructed in the n, τ plane separating regions where finite amplitude discontinuous oscillations are possible from regions where they are not. The form of the regime oscillations produced by triggering an engine that is linearly stable will also be determined. Finally, the wave shape and amplitude of oscillations with n and τ values far from the linear stability limit, beyond the limit of applicability of earlier analyses, will be found.

CHAPTER I

CONCENTRATED COMBUSTION MODEL

A. Assumptions

In general the combustion of liquid propellant elements and the attendant release of mass and energy to the flow field in the combustion chamber of a liquid propellant rocket engine are distributed throughout the combustor in an arbitrary, three dimensional manner dependent upon injector design, propellants employed,etc.

If, however, the rocket chamber is taken to be long compared to the region where combustion takes place,then the combustion can be considered to be concentrated at the injector face. This assumption separates the gasdynamic flow field from the combustion processes and leads to considerable analytical simplification since the combustion appears only as a boundary condition for the flow in the chamber and not in the partial differential equations governing that flow.

Since this assumption will be relaxed in the next chapter,and since using it makes it easy to compare the results of the present analysis with the earlier work of Sirignano,[2] the concentrated combustion model will be adopted for the purpose of the analysis to be presented in this first chapter.

Other assumptions necessary to define and delineate the problem under study are:

1) The nozzle is assumed to be so short compared to the chamber length that quasi-steady operation of the nozzle can be assumed and a constant Mach number condition at the entrance to the nozzle results.

2) The chamber is taken to have a constant cross-sectional area.

3) The flow in the chamber is assumed homentropic through second order in the wave amplitude. Entropy waves are thus ignored.

4) The flow is assumed one dimensional.

5) The chamber gas is taken to be homocompositional and calorically perfect.

Using the above assumptions the governing equations for any region in the chamber that does not contain a shock may be written as follows:

conservation of mass:

$$\frac{\partial \rho^*}{\partial t^*} + \frac{\partial \rho^* u^*}{\partial x^*} = 0 \qquad \text{(I-1)}$$

momentum:

$$\frac{\partial u^*}{\partial t^*} + u^* \frac{\partial u^*}{\partial x^*} = -\frac{1}{\rho^*} \frac{\partial p^*}{\partial x^*} \qquad \text{(I-2)}$$

homentropic condition:

$$S^* = \text{const.} \qquad \text{(I-3)}$$

At this point it is convenient to put the equations in a nondimensional form. This is done using the following nondimensional variables:

$$\rho = \frac{\rho^*}{\bar{\rho}^*} \qquad p = \frac{p^*}{\bar{p}^*} \qquad u = \frac{u^*}{\bar{a}^*} \qquad a = \frac{a^*}{\bar{a}^*} \qquad S = \frac{S^*}{\bar{S}^*}$$

$$t = \frac{t^*}{L^*} \bar{a}^* \qquad x = \frac{x^*}{L^*}$$

Using these nondimensional variables Equations (I-1), (I-2), and (I-3) become

$$\frac{\partial \rho}{\partial t} + \frac{\partial \rho u}{\partial x} = 0 \tag{I-4}$$

$$\frac{\partial u}{\partial t} + u \frac{\partial u}{\partial x} = -\frac{1}{\gamma \rho} \frac{\partial p}{\partial x} \tag{I-5}$$

$$S = 1 \tag{I-6}$$

Also, the perfect gas relation is written

$$p = \rho T \tag{I-7}$$

By combining the perfect gas law and the homentropic condition, the pressure and density may be expressed as the following functions of the local sound velocity

$$p = a^{\frac{2\gamma}{\gamma-1}} \qquad \rho = a^{\frac{2}{\gamma-1}}$$

Substituting these expressions into Equations (I-5) and (I-4) yields

$$\frac{2}{\gamma-1} \frac{\partial a}{\partial t} + \frac{2u}{\gamma-1} \frac{\partial a}{\partial x} + a \frac{\partial u}{\partial x} = 0 \tag{I-8}$$

$$\frac{\partial u}{\partial t} + u \frac{\partial u}{\partial x} + \frac{2a}{\gamma-1} \frac{\partial a}{\partial x} = 0 \tag{I-9}$$

Adding and subtracting (I-8) to (I-9) produces the following two equations

$$\frac{\partial}{\partial t}\left(u + \frac{2}{\gamma-1} a\right) + (u+a) \frac{\partial}{\partial x}\left(u + \frac{2}{\gamma-1} a\right) = 0 \tag{I-10}$$

$$\frac{\partial}{\partial t}\left(u-\frac{2}{\gamma-1}a\right)+(u-a)\frac{\partial}{\partial x}\left(u-\frac{2}{\gamma-1}a\right)=0 \qquad \text{(I-11)}$$

Of course these equations are recognized to be in the well known form due to Riemann and to imply the following relationships

$$u+\frac{2}{\gamma-1}a=\mathcal{P}(\beta)$$

$$u-\frac{2}{\gamma-1}a=Q(\alpha)$$

where P and Q are arbitrary functions of their arguments, β is constant along $\frac{dx}{dt} = u + a$ and α is constant along $\frac{dx}{dt} = u - a$. β and α together form a characteristic coordinate system. It may be possible to solve the present problem as formulated in this characteristic coordinate system following the method used by Sirignano.[2] In the current study, however, this will not be done. Instead the equations will be solved in physical coordinates following a method developed by Chester.[3]

There are two boundary conditions on Equations (I-10) and (I-11). The short nozzle boundary condition is applied at $x = 1$, the nozzle entrance, and requires that the Mach number be constant there, i.e.

$$u = Ma$$

$$M = \frac{\bar{u}^*}{\bar{a}^*} \qquad \text{(I-12)}$$

At the injector face, $x = 0$, on the other hand, the boundary condition is derived from the use of the time-lag model to represent the combustion occurring there. According to this model, the rate of mass generation due to combustion is related to the steady-state mass flow as follows

$$\dot{m} = \bar{\dot{m}} \left(1 - \frac{d\tau}{dt}\right) \tag{I-13}$$

Here $\frac{d\tau}{dt}$ represents the rate of change of the sensitive time-lag. This expression assumes a constant injection rate even under oscillatory conditions. A linearized expression for $\frac{d\tau}{dt}$ was originally devised by Crocco.[1] Nonlinear extensions have been developed by Sirignano and Zinn.[16] For reasons that will become apparent shortly, only the linear expression for $\frac{d\tau}{dt}$ is needed in the present analysis.

The linearized derivation of $\frac{d\tau}{dt}$ will not be repeated here because it is readily available and clearly presented in Crocco's original work.[1] For the purpose of analysis the final result of his linearized treatment will be accepted as a postulate in this thesis. This relationship is

$$\frac{d\tau}{dt} = -n\left(p'(t) - p'(t-\tau)\right) \tag{I-14}$$

$$p' = p - 1$$

where terms of order p'^2 and higher are not considered.

To completely specify the problem some initial conditions would normally be given. Instead of this, however, a cyclic condition will be applied in the present analysis. That is, u and a will be required to be periodic in time. This allows the regime oscillatory condition to be sought rather than the behavior of a particular initial disturbance.

B. Solution of the Partial Differential Equations

A power series expansion technique will be used to solve the equations. The choice of the expansion parameter is critical.

Crocco's linear analysis of the longitudinal mode uses an arbitrary expansion parameter that is small compared with and unrelated to the Mach number. This is because the combustion and nozzle boundary conditions for the unsteady problem differ from zero by an amount of order (Mp'). Necessarily then, if the linear analysis is to consider these two sources of energy addition or subtraction, the expansion parameter must be able to go to zero independent of the Mach number. Periodic neutral oscillations which result from such a linear analysis occur where there is a balance to first order between the energy input due to combustion and the energy removal by the nozzle. If energy input is larger than removal, growth of small perturbations is predicted, if energy removal is larger than input, decay of small perturbations is predicted.

Sirignano successfully employed a similar expansion parameter in his nonlinear study of finite amplitude continuous waves. Here the balancing of the combustion and nozzle effects was carried to third order. Also, in his study of longitudinal shock wave instability with no time-lag this principle of balancing nozzle and combustion effects to lowest order was used. In this case Sirignano defined the expansion parameter (amplitude of the shock wave) to be proportional to the first order difference between the combustion and nozzle admittances. The constant of proportionality chosen happened to be the steady-state Mach number, however, the ordering system was not dependent on the Mach number. That is, terms of order Mp' were taken to be of the same order as terms of order p'.

Because of the success of these techniques which used an expansion parameter that required balancing of combustion and nozzle effects to lowest order, one might expect that such a method of expansion should

be successful in analyzing shock wave instability when a time-lag characterizes the combustion model. This, however, is not the case. It is instructive to perform a brief analysis showing how this technique fails.

First, u and a are expressed as the sum of a steady-state part (denoted by a superposed bar) and a time variant perturbation. The time variant parts of u and a , u' and a', are then expressed as power series in ϵ , an arbitrary amplitude parameter

$$u = \bar{u} + u_1 + u_2 + \cdots$$
$$u_1 = O(\epsilon) , \quad u_2 = O(\epsilon^2) \cdots \tag{I-15}$$

$$a = 1 + a_1 + a_2 + \cdots$$
$$a_1 = O(\epsilon) , \quad a_2 = O(\epsilon^2) \cdots \tag{I-16}$$

These expansions are then substituted in Equations (I-10) and (I-11). The final equations obtained, correct to first order in ϵ are

$$\frac{\partial}{\partial t}\left(u_1 + \frac{2}{\gamma-1} a_1\right) + (M+1)\frac{\partial}{\partial x}\left(u_1 + \frac{2}{\gamma-1} a_1\right) = 0 \tag{I-17}$$

$$\frac{\partial}{\partial t}\left(u_1 - \frac{2}{\gamma-1} a_1\right) + (M-1)\frac{\partial}{\partial x}\left(u_1 - \frac{2}{\gamma-1} a_1\right) = 0 \tag{I-18}$$

These equations have the general solutions

$$u_1 + \frac{2}{\gamma-1} a_1 = g_r\left(t - \frac{x}{M+1}\right) \tag{I-19}$$

$$u_1 - \frac{2}{\gamma-1} a_1 = g_s \left(t - \frac{x}{M-1}\right) \tag{I-20}$$

The first order boundary condition at $x = 1$ is taken directly from Equation (I-12)

$$u_1 = M a_1 \tag{I-21}$$

The first order boundary condition at $x = 0$ is derived by combining Equations (I-13) and (I-14)

$$u_1 = \frac{2}{\gamma-1} M \left[(\gamma n - 1)\, a_1(t) - \gamma n\, a_1(t-\tau)\right] \tag{I-22}$$

Because of the fact that $u + \frac{2}{\gamma - 1} a$ is continuous through second order across a shock moving toward the injector and $u - \frac{2}{\gamma - 1} a$ is continuous to second order across a shock moving toward the nozzle, (I-19) and (I-20) may be substituted directly in (I-21) and (I-22) even when a shock is present. The procedure employed here will be examined in greater detail later. This substitution yields the following equation for $g \equiv g_r$

$$\frac{g(t)}{1-\nu} - \frac{g(t-T_0)}{1+\nu} = M\left[(\gamma n - 1)\left(\frac{g(t)}{1-\nu} + \frac{g(t-T_0)}{1+\nu}\right) - \gamma n\left(\frac{g(t-\tau)}{1-\nu} + \frac{g(t-\tau-T_0)}{1+\nu}\right)\right]$$

$$\nu = \frac{\gamma-1}{2} M \qquad T_0 = \frac{2}{1-M^2} \tag{I-23}$$

If a periodic shock wave solution is to be considered, then the first approximation to its period is just the wave travel time of an acoustic wave, T_0. It follows that the cyclic condition to first order may be written

$$g(t) = g(t - T_0) \tag{I-24}$$

Substituting this expression in Equation (I-23) yields

$$g(t) = K\, g(t-\tau)$$
$$K = \frac{2\gamma n}{2\gamma n - \gamma - 1} \qquad \text{(I-25)}$$

If $|K| > 1$ then $|g|$ will increase without limit with increasing time. If $|K| < 1$ then $|g|$ will decrease in time with the limiting value $|g| = 0$. Either situation is not acceptable since it has already been required that g be periodic. Thus $|K| \equiv 1$. $K = 1$ only as $n \rightarrow \infty$. The n values of physical interest are usually less than 2 or 3,[7] hence this value of K must also be discarded. The only acceptable value of K is, then, $K = -1$. For this case $n = \frac{\gamma + 1}{4\gamma}$, which is in agreement with the value of n obtained using Crocco's linear analysis when the first order period is the acoustic period.

For $K = -1$ Equation (I-25) becomes

$$g(t) = -g(t-\tau) \qquad \text{(I-26)}$$

Unless $\tau = \frac{T_0}{2k}$, k an integer, the cyclic condition $g(t) = g(t + T_0)$ is, again, apparently not satisfied. Thus τ must equal $T_0/2k$. This result also agrees with the predictions of the linear theory.

Unfortunately, it can easily be seen that the relationship (I-26) precludes the possibility of discontinuous solutions. For, if g undergoes a positive discontinuous jump at time t, then g at time $t + \tau$ undergoes a negative discontinuous jump. At $x = 0$ Equations (I-19) and (I-20) together with the isentropic relation between a and p imply $p(t) = 2\gamma g(t)$. Consequently, a negative jump in g corresponds to a discontinuous decrease in pressure, or a rarefaction shock. This is not physically reasonable.

The conclusion must be drawn that periodic shock wave solutions to the problem as formulated are impossible.

The analysis just presented considers the combustion and nozzle conditions to first order. The lowest order solution corresponds to the linearized treatment of Crocco. Since the second order modification must be small compared with the first order result, the deviation from the balance in combustion and nozzle effects that produces the linear neutral stability curve must be small, indeed must be an order of magnitude smaller than the first order wave amplitude. Because in general a small difference in energy balance must mean a small change from the linearly stable values of the combustion parameters n and τ, this implies that the region of validity of higher order results obtained using the technique just employed is restricted to a region close to the neutral stability curve in the n, τ plane. In other words, shockless solutions for periodic pressure waves are to be anticipated close to the linear stability limit.

There is another way of approaching the problem, which allows consideration of regions on the n, τ plane far from the linear stability limit and which predicts discontinuous pressure waveforms in most of these regions. In this method the combustion and nozzle effects are not balanced to lowest order. Rather, the lowest order solution is taken to be the simple acoustic solution for the given chamber.

The fact that the steady-state Mach number acts as a measure of the level of steady-state combustion in the chamber and mean nozzle outflow is used to accomplish this. It is required that the expansion parameter ϵ, be of the order of the steady-state Mach number. This causes

the combustion and nozzle admittances, which are of order $M \cdot p'$ or smaller, to be considered as being of the same order of magnitude as terms of order p'^2 and thus not first order effects.

To put this in mathematical terms, ϵ, the expansion parameter is assumed to have the following form

$$\epsilon = M H(n, \tau) \tag{I-27}$$

$H(n, \tau)$ is, for the moment, an undetermined function of n and τ that must be of order unity or less. It is obvious that as $M \rightarrow 0$, $\epsilon \rightarrow 0$ also. However, it is not necessarily true that as ϵ goes to zero the Mach number must also tend to zero at the same time. This is because in some region of the n, τ plane it is possible for $H(n, \tau)$ to tend to zero independent of the Mach number. The region where this is possible turns out to be the area close to the neutral stability curve.

To summarize, then, in this method of ordering the terms in the governing equations and boundary conditions, the combustion and nozzle effects themselves are considered small to first order, in contrast with the first technique, which considered that only the difference in energy input and removal was small.

The partial differential Equations (I-10) and (I-11) will now be solved using a power series representation of the dependent variables u and a, with the expansion parameter given by definition (I-27). u and a are represented as follows

$$u = M + u_1 + u_2 + \cdots$$

$$u_1 = O(\epsilon) = O(M), \quad u_2 = O(\epsilon^2) = O(M^2)$$

$$a = 1 + a_1 + a_2 + \cdots$$

$$a_1 = O(\epsilon) = O(M), \quad a_2 = O(\epsilon^2) = O(M^2)$$

These definitions are substituted into Equations (I-10) and (I-11). Then, using the fact that $\epsilon = O(M)$, the equations are separated into systems of first and second order equations. The first order equations are (correct to $O(M)$)

$$\frac{\partial}{\partial t}\left(u_1 + \frac{2}{\gamma-1} a_1\right) + \frac{\partial}{\partial x}\left(u_1 + \frac{2}{\gamma-1} a_1\right) = 0 \qquad \text{(I-28)}$$

$$\frac{\partial}{\partial t}\left(u_1 - \frac{2}{\gamma-1} a_1\right) - \frac{\partial}{\partial x}\left(u_1 - \frac{2}{\gamma-1} a_1\right) = 0 \qquad \text{(I-29)}$$

The second order equations are (correct to $O(M^2)$)

$$\frac{\partial}{\partial t}\left(u_2 + \frac{2}{\gamma-1} a_2\right) + \frac{\partial}{\partial x}\left(u_2 + \frac{2}{\gamma-1} a_2\right) = -\left(u_1 + a_1 + M\right) \frac{\partial}{\partial x}\left(u_1 + \frac{2}{\gamma-1} a_1\right) \qquad \text{(I-30)}$$

$$\frac{\partial}{\partial t}\left(u_2 - \frac{2}{\gamma-1} a_2\right) - \frac{\partial}{\partial x}\left(u_2 - \frac{2}{\gamma-1} a_2\right) = -\left(u_1 - a_1 + M\right) \frac{\partial}{\partial x}\left(u_1 - \frac{2}{\gamma-1} a_1\right) \qquad \text{(I-31)}$$

The boundary conditions on the first order equations are homogeneous when $\epsilon = O(M)$

$$x = 1: \quad u_1 = 0 \qquad \text{(I-32)}$$

$$\chi = 0: \quad u_1 = 0 \tag{I-33}$$

The second order boundary conditions are

$$\chi = 1: \quad u_2 = M a_1 \tag{I-34}$$

$$\chi = 0: \quad u_2 = \frac{2}{\gamma - 1} M\left[(\gamma n - 1)\, a_1(t) - \gamma n\, a_1(t - \tau)\right] \tag{I-35}$$

These second order boundary conditions are in the same form as the first order boundary conditions found when p' was taken small compared with the Mach number (Equations (I-21) and (I-22)).

The cyclic requirement on u and a must still be applied. Difficulties arise in the application of this condition because of the fact that the period of the lowest order solution is not necessarily the same as the true period of oscillation. That is, if it is required that $a(t) = a(t + \mathcal{T})$ where $\mathcal{T}$ is some (undetermined) period of oscillation it is not true in general that $a_1(t) = a_1(t + \mathcal{T})$. This is because the lowest order approximation to the period in the present ordering scheme is simply the linear wave travel time. Clearly, when nonlinear wave effects and the combustion zone and nozzle are considered, the period can differ from this acoustic period by a correction of order M. In general this may be stated as follows: though $a(t + \mathcal{T}) = a(t)$, and

$$a_1(t + \mathcal{T}) + a_2(t + \mathcal{T}) + \cdots = a_1(t) + a_2(t) + \cdots$$

it may not be concluded that $a_i(t + \mathcal{T}) = a_i(t)$ since $\mathcal{T}$ depends on a_i (i an integer). This means that though, through an oscillation of one period, the lowest order solution may be a good approximation (deviation of

$O(M^2)$) to the true solution, for general position and time the prediction of the lowest order solution may differ by an amount that is of first order from the true solution because of the secular growth of the difference between the positions in x, t space of the first order solution and the higher order solutions. If the solution is discontinuous, this difference in periods is particularly unfortunate, since the lowest order solution can differ from the true solution to first order even when the difference in periods is of second order. That is, for a discontinuous solution, the lowest order solution will be in error to first order at the discontinuity just because the first order jump, which the solution experiences there, is not positioned correctly. Of course the "positioning error" will again grow in time, compounding the problem.

Similar problems occur in the study of periodic solutions of ordinary, autonomous, nonlinear differential equations.[10] A method of approaching these problems due to Poincare' has proved useful in the case of ordinary differential equations. Consequently, a technique which follows the principal ideas of that method will be employed here.

First, τ, the period, is expressed as a power series expansion in M

$$\tau = \tau_0 + \tau_1 + \tau_2 + \cdots$$
$$\tau_0 = 2\,, \quad \tau_1 = O(M)\,, \quad \tau_2 = O(M^2) \tag{I-36}$$

where τ_0 has been taken equal to the acoustic wave travel time, 2. A new independent variable, θ, is then introduced

$$t = \frac{\tau}{\tau_0}\theta = \frac{(2+\tau_1+\tau_2+\cdots)}{2}\theta \tag{I-37}$$

As Θ goes from say, Θ_1 to $\Theta_1 + 2$, t will increase from t_1 to $t_1 + T$. Thus, requiring that $a(t) = a(t+T)$ in an x, t coordinate system is equivalent to requiring that $a(\Theta) = a(\Theta + 2)$ in the x, Θ coordinate system. The periodic condition may then be written (x held constant):

$$a(\theta) = a(\theta+2)$$

a and u are then represented by power series as follows

$$a(\theta,x) = 1 + a_1(\theta,x) + a_2(\theta,x) + \cdots \tag{I-38}$$

$$u(\theta,x) = M + u_1(\theta,x) + u_2(\theta,x) + \cdots \tag{I-39}$$

The periodic condition may then be rewritten

$$a_1(\theta+2,x) + a_2(\theta+2,x) + \cdots = a_1(\theta,x) + a_2(\theta,x) + \cdots$$

$$u_1(\theta+2,x) + u_2(\theta+2,x) + \cdots = u_1(\theta,x) + u_2(\theta,x) + \cdots$$

In this case, since the period, 2, is constant it must follow that

$$a_i(\theta+2) = a_i \tag{I-40}$$

It is therefore seen that the simple transformation just made has caused solutions of all orders to have the same period of oscillation as the lowest order solution. This removes the secular terms mentioned earlier and also avoids the previously mentioned positioning error in the location of any discontinuity that may exist.

The first order equations are now written using definitions (I-38) and (I-39) with Θ and x as the independent variables and the fact

that $\frac{\partial}{\partial t} = (1 - \frac{T_1}{2} + - - - - -) \frac{\partial}{\partial \theta}$, as follows

$$\frac{\partial}{\partial \theta}\left(u_1 + \tfrac{2}{\gamma-1} a_1\right) + \frac{\partial}{\partial x}\left(u_1 + \tfrac{2}{\gamma-1} a_1\right) = 0 \qquad \text{(I-41)}$$

$$\frac{\partial}{\partial \theta}\left(u_1 - \tfrac{2}{\gamma-1} a_1\right) - \frac{\partial}{\partial x}\left(u_1 - \tfrac{2}{\gamma-1} a_1\right) = 0 \qquad \text{(I-42)}$$

These equations have the familiar solutions

$$u_1 + \tfrac{2}{\gamma-1} a_1 = 2 f_r(\theta - x) \qquad \text{(I-43)}$$

$$u_1 - \tfrac{2}{\gamma-1} a_1 = 2 f_s(\theta + x) \qquad \text{(I-44)}$$

f_r and f_s are arbitrary functions representing disturbances travelling toward the nozzle and toward the injector, respectively.

Since Equations (I-41) and (I-42) are only valid in regions not containing discontinuities, the combustion chamber will be separated into two regions as indicated in Figure 1. Only one shock wave is allowed. If no shock is present, region I and II are the same and the distinction is, of course, artificial. The first order solutions for the two regions are differentiated by the subscripts I and II. Thus

$$u_{I1} + \tfrac{2}{\gamma-1} a_{I1} = 2 f_{rI}(\theta - x) \qquad \text{(I-45)}$$

$$u_{I1} - \tfrac{2}{\gamma-1} a_{I1} = 2 f_{sI}(\theta + x) \qquad \text{(I-46)}$$

$$u_{II1} + \tfrac{2}{\gamma-1} a_{II1} = 2 f_{rII}(\theta - x) \qquad \text{(I-47)}$$

$$u_{II2} + \tfrac{2}{\gamma-1} a_{II2} = 2 f_{sII}(\theta + x) \qquad \text{(I-48)}$$

The shock relations written out to second order in the shock strength require that $u + \frac{2}{\gamma - 1} a$ be continuous across a shock moving toward the injector and $u - \frac{2}{\gamma - 1} a$ be continuous across a shock moving toward the nozzle. This implies

$$f_{rI}(\theta - x) = f_{rII}(\theta - x)$$

$$f_{sI}(\theta + x) = f_{sII}(\theta + x)$$

In other words, the distinction between the first order functions in the two regions proves unnecessary.

The homogeneous boundary condition $u_1 = 0$ applied at the nozzle, $(x = 1)$ and the injector, $x = 0$, yields the following two relations

$$f_r(\theta - 1) + f_s(\theta + 1) = 0$$

$$f_r(\theta) + f_s(\theta) = 0$$

These are combined to give the following conditions on f

$$f_r = -f_s \equiv f \tag{I-49}$$

$$f(\theta) = f(\theta + 2) \tag{I-50}$$

Equation (I-50) expresses satisfaction of the periodicity condition previously discussed and comes, of course, as no surprise, since we reasoned a priori that the lowest order solution was periodic in 2.

The first order approximations for u and a may now be written

$$u_1 + \frac{2}{\gamma - 1} a_1 = 2 f(\theta - x) \tag{I-51}$$

$$u_1 - \frac{2}{\gamma - 1} a_1 = -2 f(\theta + x) \tag{I-52}$$

or

$$u_1 = f(\theta - x) - f(\theta + x) \tag{I-53}$$

$$a_1 = \frac{\gamma-1}{2}\left[f(\theta - x) + f(\theta + x)\right] \tag{I-54}$$

Equations (I-53) and (I-54) give u_1 and a_1 in terms of the arbitrary function f. The second order analysis which will now be carried out will result in a nonlinear ordinary differential equation governing the form of f. Thus, the purpose of the second order analysis is to find the form of u_1 and a_1, the first order solutions. The second order partial differential equations written using θ, x coordinates are

$$\frac{\partial}{\partial\theta}\left(u_2 + \frac{2}{\gamma-1}a_2\right) + \frac{\partial}{\partial x}\left(u_2 + \frac{2}{\gamma-1}a_2\right) = \frac{\pi}{2}\frac{\partial}{\partial\theta}\left(u_1 + \frac{2}{\gamma-1}a_1\right) - (M + u_1 + a_1)\frac{\partial}{\partial x}\left(u_1 + \frac{2}{\gamma-1}a_1\right) \tag{I-55}$$

$$\frac{\partial}{\partial\theta}\left(u_2 - \frac{2}{\gamma-1}a_2\right) - \frac{\partial}{\partial x}\left(u_2 - \frac{2}{\gamma-1}a_2\right) = \frac{\pi}{2}\frac{\partial}{\partial\theta}\left(u_1 - \frac{2}{\gamma-1}a_1\right) - (M + u_1 - a_1)\frac{\partial}{\partial x}\left(u_1 - \frac{2}{\gamma-1}a_1\right) \tag{I-56}$$

Substituting the expressions for u_1 and a_1, given in Equations (I-53) and (I-54), the second order equations become

$$\frac{\partial}{\partial\theta}\left(u_2 + \frac{2}{\gamma-1}a_2\right) + \frac{\partial}{\partial x}\left(u_2 + \frac{2}{\gamma-1}a_2\right) = 2\left[\frac{\gamma+1}{2}f(\theta - x) + \frac{\gamma-3}{2}f(\theta + x) + M + \frac{\pi}{2}\right]\frac{\partial f(\theta - x)}{\partial\theta} \tag{I-57}$$

$$\frac{\partial}{\partial\theta}\left(u_2 - \frac{2}{\gamma-1}a_2\right) - \frac{\partial}{\partial x}\left(u_2 - \frac{2}{\gamma-1}a_2\right) = 2\left[\frac{3-\gamma}{2}f(\theta - x) - \frac{\gamma+1}{2}f(\theta + x) + M - \frac{\pi}{2}\right]\frac{\partial f(\theta + x)}{\partial\theta} \tag{I-58}$$

Particular solutions to (I-57) and (I-58) are easily found from application of the theory of solution of linear first order partial differential equations or by inspection to be

$$u_2 + \frac{2}{\gamma-1} a_2 = 2 \frac{\partial f(\theta-x)}{\partial \theta} \left[\chi \left(\frac{\gamma+1}{2} f(\theta-x) + M + \frac{\pi}{2} \right) + \frac{\gamma-3}{4} \int_{\theta-\chi}^{\theta+\chi} f(\eta)\, d\eta \right] \quad \text{(I-59)}$$

$$u_2 - \frac{2}{\gamma-1} a_2 = 2 \frac{\partial f(\theta+x)}{\partial \theta} \left[\chi \left(\frac{\gamma+1}{2} f(\theta+x) - M + \frac{\pi}{2} \right) + \frac{3-\gamma}{4} \int_{\theta+\chi}^{\theta-\chi} f(\eta)\, d\eta \right] \quad \text{(I-60)}$$

To these particular solutions, arbitrary second order functions of (θ - x) and (θ + x), respectively, must be added. At the same time the solutions should be expressed as separate solutions for the two regions, I and II. Thus

$$u_{I2} + \frac{2}{\gamma-1} a_{I2} = 2 F_{rI}(\theta-x) + 2 \frac{\partial f(\theta-x)}{\partial \theta} \left[\chi \left(\frac{\gamma+1}{2} f(\theta-x) + M + \frac{\pi}{2} \right) + \frac{\gamma-3}{4} \int_{\theta-\chi}^{\theta+\chi} f(\eta)\, d\eta \right]$$

$$u_{I2} - \frac{2}{\gamma-1} a_{I2} = 2 F_{sI}(\theta+x) + 2 \frac{\partial f(\theta+x)}{\partial \theta} \left[\chi \left(\frac{\gamma+1}{2} f(\theta+x) - M + \frac{\pi}{2} \right) + \frac{3-\gamma}{4} \int_{\theta+\chi}^{\theta-\chi} f(\eta)\, d\eta \right] \quad \text{(I-61)}$$

$$u_{II2} + \frac{2}{\gamma-1} a_{II2} = 2 F_{rII}(\theta-x) + 2 \frac{\partial f(\theta-x)}{\partial \theta} \left[\chi \left(\frac{\gamma+1}{2} f(\theta-x) + M + \frac{\pi}{2} \right) + \frac{\gamma-3}{4} \int_{\theta-\chi}^{\theta+\chi} f(\eta)\, d\eta \right] \quad \text{(I-62)}$$

$$u_{II2} \frac{2}{\gamma-1} a_{II2} = 2 F_{sII}(\theta+x) + 2 \frac{\partial f(\theta+x)}{\gamma \theta} \left[\chi \left(\frac{\gamma+1}{2} f(\theta+x) - M + \frac{\pi}{2} \right) + \frac{3-\gamma}{4} \int_{\theta+\chi}^{\theta-\chi} f(\eta)\, d\eta \right] \quad \text{(I-63)}$$

(I-64)

where $F_{rI}(\theta - x)$, $F_{rII}(\theta - x)$, $F_{sI}(\theta + x)$, $F_{sII}(\theta + x)$ are arbitrary second order functions of their arguments, and the fact that $f_I(\theta - x) = f_{II}(\theta - x)$, $f_I(\theta + x) = f_{II}(\theta + x)$ has been used.

Since $u + \frac{2}{\gamma - 1} a$ is continuous through second order across a shock moving toward the injector, and since $\int_{\theta-x}^{\theta+x} f(\eta)d\eta$ must also be continuous across such a discontinuity, then equating Equations (I-61) and (I-63) yields

$$F_{rI}(\theta - x) = F_{rII}(\theta - x) \tag{I-65}$$

Similarly, across a shock moving towards the nozzle, $u_2 - \frac{2}{\gamma - 1} a_2$ and $\int_{\theta+x}^{\theta-x} f(\eta)d\eta$ are continuous, so

$$F_{sI}(\theta + x) = F_{sII}(\theta + x) \tag{I-66}$$

Here again, as in the first order solution, distinction between the arbitrary functions in the two regions is unnecessary.

Finally, then, the second order solutions are

$$u_2 + \frac{2}{\gamma-1} a_2 = 2F_r(\theta - x) + 2\frac{\partial f(\theta-x)}{\partial \theta}\left[x\left(\frac{\gamma+1}{2} f(\theta-x) + M + \frac{\pi_1}{2}\right) - \frac{3-\gamma}{4}\int_{\theta-x}^{\theta+x} f(\eta)\, d\eta\right] \tag{I-67}$$

$$u_2 - \frac{2}{\gamma-1} a_2 = 2F_s(\theta + x) + 2\frac{\partial f(\theta+x)}{\partial \theta}\left[x\left(\frac{\gamma+1}{2} f(\theta+x) - M + \frac{\pi_1}{2}\right) + \frac{3-\gamma}{4}\int_{\theta+x}^{\theta-x} f(\eta)\, d\eta\right] \tag{I-68}$$

At the nozzle, $x = 1$, the second order boundary condition is

$$u_2 = M a_1 \tag{I-69}$$

Adding Equations (I-67) to (I-68) to find an expression for u_2, substituting $a_1 = \frac{\gamma - 1}{2}\left[f(\theta - x) + f(\theta + x)\right]$ from Equation (I-54), setting $x = 1$,

and noting that $f(\theta - 1) = f(\theta + 1)$ (since $f(\theta) = f(\theta + 2)$), yields the following expression valid at $x = 1$

$$F_r(\theta-1) + F_s(\theta+1) + \frac{df}{d\theta}\left[(\gamma+1) f(\theta-1) + T_1\right] - \frac{3-\gamma}{2}\int_0^2 f(\eta)\, d\eta = M(\gamma-1) f(\theta-1) \tag{I-70}$$

where it has been noted that, due to the periodicity of $f(\eta)$, $\int_{\theta-1}^{\theta+1} f(\eta)d\eta = \int_0^2 f(\eta)d\eta$

The injector end, or combustion zone, boundary condition, to be applied at $x = 0$, is

$$u_2(\theta) = M\frac{2}{\gamma-1}\left[(\gamma n - 1)\, a_1(\theta) - \gamma n\, a_1(\theta-\mu)\right]$$
$$\mu = \frac{2}{\pi}\tau = (1 - \frac{\pi}{2} + \ldots)\tau \tag{I-71}$$

Using Equations (I-67), (I-68) and (I-54) this becomes

$$F_r(\theta) + F_s(\theta) = 2M\left[(\gamma n - 1) f(\theta) - \gamma n\, f(\theta-\mu)\right] \tag{I-72}$$

or $$F_s(\theta) = -F_r(\theta) + 2M\left[(\gamma n - 1) f(\theta) - \gamma n\, f(\theta-\mu)\right] \tag{I-73}$$

Substitution of the expression for $F_s(\theta)$ given in (I-73) into Equation (I-70) yields

$$F(\theta) - F(\theta+2) + 2M\left[(\gamma n - 1) f(\theta) - \gamma n\, f(\theta-\mu)\right]$$
$$+\left[(\gamma+1) f(\theta) + T_1 - \frac{3-\gamma}{2}\int_0^2 f(\eta)\, d\eta\right]\frac{df(\theta)}{d\theta} = (\gamma-1) M f(\theta) \tag{I-74}$$

where the definition $F_r(\theta) \equiv F(\theta)$ has been introduced.

The cyclic condition may be applied by requiring

$$\left(u_2 + \frac{2}{\gamma-1} a_2\right)_{\theta,x} = \left(u_2 + \frac{2}{\gamma-1} a_2\right)_{\theta+2,x}$$

Using Equation (I-67) and the fact that $f(\theta)$ and $\int_{\theta-x}^{\theta+x} f(\eta)d\eta$ are periodic with period 2, the following condition on $F(\theta)$ results

$$F(\theta) = F(\theta+2) \tag{I-75}$$

Combination of equations (I-74) and (I-75) yields the following equation for $f(\theta)$

$$\left[(\gamma+1) f(\theta) + T_1 - \frac{3-\gamma}{2} \int_0^2 f(\eta)\, d\eta\right] \frac{df}{d\theta} = M\left[(\gamma+1-2\gamma n) f(\theta) + 2\gamma n f(\theta-\mu)\right]$$

(I-76)

This equation is seen to be in the form of an ordinary, nonlinear, first order differential difference equation, where the retarded variable enters the equation in the second term on the right hand side.

T_1, the first order correction to the period, is a constant (in θ) dependent upon the form and amplitude of $f(\theta)$. If a shock is present, T_1 may be evaluated in the standard manner of following the shock through one period of oscillation and calculating the change in the wave travel time. Both Sirignano[24] and Chu[25] employed this technique in their studies of one-dimensional periodic shock waves.

Another way of finding T_1 that has, perhaps, more general applicability, is based on certain extensions of some work by Cantrell and Hart[4]

who investigated stability criteria for flow in acoustic cavities.

Both methods are presented in Appendix A. The results of either calculation are the same, and are given as the following expression for T_1

$$T_1 = \frac{(3-\gamma)}{2}\int_0^2 f(\eta)\,d\eta - \frac{(\gamma+1)}{2}\left[f(0) + f(2)\right]$$

f(0) is the value of f immmediately after the shock, f(2) the value immediately before the shock. Substituting this expression for T_1 into Equation (I-76) yields a differential equation for f as function of Θ ,that is only dependent on the parameters n , μ , M and γ .

$$(\gamma+1)\left(f-\hat{k}\right)\frac{df}{d\theta} = Ma\,f + Mb\,f_\mu \qquad \text{(I-77)}$$

$$f_\mu = f(\theta-\mu),\quad \hat{k} = \tfrac{1}{2}\left(f(0)+f(2)\right),\quad a=\gamma+1-2\gamma n,\quad b=2\gamma n$$

This is easily placed in a form where M does not appear, and in which the dependent variable is of order unity,by introducing $g = (\gamma+1)\frac{f}{M}$. Then the equation becomes

$$(g-k)\frac{dg}{d\theta} = ag + b\,g_\mu \qquad \text{(I-78)}$$

$$k = \tfrac{1}{2}\left(g(0)+g(2)\right)$$

The boundary condition for this equation is, of course, g(0) + g(2) = 2k .

Integration of Equation (I-78) from zero to 2 yields the following relation

$$\tfrac{1}{2}\left[g^2(2) - g^2(0)\right] - k\left[g(2) - g(0)\right] = a\int_0^2 g(\theta')\,d\theta' + b\int_0^2 g_\mu(\theta')\,d\theta'$$

Using the definition of k and the fact that g must be periodic in 2 this becomes

$$(a + b) \int_0^2 g(\theta')\, d\theta' = 0$$

Since $a + b = \gamma + 1 \neq 0$, the above equation implies

$$\int_0^2 g(\theta')\, d\theta' = 0 \qquad \text{(I-79)}$$

Using the expression for T_1

$$T_1 = \frac{(3-\gamma)}{2} \int_0^2 f(\eta)\, d\eta - \frac{\gamma+1}{2} \left[f(2) + f(0) \right]$$

the definition of k, the fact that $g(\theta) = \frac{(\gamma+1) f(\theta)}{M}$ and Equation (I-79) the following expression for T_1 is derived

$$T_1 = -Mk$$

This implies that for $k > 0$, $T_1 < 0$, and the frequency of oscillation of g is above the acoustic frequency; for $k < 0$ the frequency is below the acoustic frequency; and for $k = 0$ the frequency is exactly the acoustic frequency of oscillation for the chamber. For obvious reasons, these three cases will be referred to, respectively, as above resonant oscillations, below resonant oscillations, and resonant oscillations.

C. Solution of the Governing Ordinary Differential Equation

a) General Properties of Solutions for Rational μ

If it is possible to find physically meaningful solutions to (I-78) that repeat themselves with period 2 and are separated by a discontinuity then shock wave solutions, correct to $O(M)$, for the problem as stated will have been found.

When μ is a rational fraction of 2 (the first order or acoustic period), such periodic solutions can be found through the use of numerical techniques for the integration of Equation (I-78). Solutions of this equation will now be sought, and the characteristics of these solutions investigated, under the restriction $\mu = 2\frac{q}{\ell}$, where q and ℓ are integers and $q < \ell$.

The range of values of μ to be investigated is $0 < \mu < 2$. This is the range of μ corresponding to the fundamental mode of oscillation in Crocco's linear analysis. The linear neutral stability curve shown in Figure 2 represents the fundamental longitudinal mode of instability, and is calculated using the linear result (with $\epsilon << M$)

$$n = \frac{\gamma + 1}{2\gamma(1 - \cos \pi\mu)} \qquad \text{(I-80)}$$

It is apparent from either consideration of Equation (I-80), or looking at Figure 2, that the n, μ linear stability curve is symmetric with respect to the line $\mu = 1$.

The solutions of Equation (I-78) are not symmetric about $\mu = 1$. However, they are related through a simple transformation when symmetric displacements of μ from $\mu = 1$, at constant n are considered, and μ is a rational fraction of 2. The analysis which follows derives this transformation.

Consider $\mu = 2\frac{q}{\ell}$, $0 < 2q \leq \ell$. The interval $0 \leq \Theta \leq 2$ is divided into ℓ sub-intervals, numbered in a progressive manner from the point $\Theta = 0$. The ℓ functions, g_i, are introduced, so that g_1 represents

g in the interval $0 \le \theta \le \frac{2}{\ell}$, g_2 represents g in the interval $\frac{2}{\ell} \le \theta \le \frac{4}{\ell}$, g_i represents g in the interval $(i-1)\frac{2}{\ell} \le \theta \le \frac{2i}{\ell}$, etc. The independent variable ξ is also introduced. ξ is defined as $\xi = \frac{\ell}{2}\theta - (i-1)$. Thus, $\xi = \frac{\ell}{2}\theta$ in sub interval 1, $\xi = \frac{\ell}{2}\theta - 1$ in sub interval 2, etc. ξ therefore varies from zero to one in each of the ℓ sub intervals. (Note that i is an integer between 0 and ℓ)

If a periodic solution for g exists, then it must be true that g in the ith interval before $\theta = 0$ must be the same as g in the ith interval before $\theta = 2$. Consequently, for $1 \le i \le q$, $g_{i\mu}(\xi) = g_{\ell-q+i}(\xi)$. For $q+1 \le i \le \ell$, $g_{i\mu}(\xi) = g_{i-q}(\xi)$. Using these expressions Equation (I-78) may then be written as the following system of ℓ equations:

$$\frac{\ell}{2}(g_i - k)\frac{dg_i}{d\xi} = a g_i + b g_{\ell-q+i} \qquad 1 \le i \le q \tag{I-81}$$

$$\frac{\ell}{2}(g_i - k)\frac{dg_i}{d\xi} = a g_i + b g_{i-q} \qquad q+1 \le i \le \ell \tag{I-82}$$

where $0 \le \xi \le 1$

The required boundary conditions are

$$g_1(0) + g_\ell(1) = 2k \tag{I-83}$$

$$g_i(1) = g_{i+1}(0) \qquad 1 \le i \le \ell - 1 \tag{I-84}$$

The second set of boundary conditions derives from the fact that continuous solutions between $\theta = 0$ and $\theta = 2$ are being sought, that is, only one shock is allowed.

Note that the system of Equations (I-85), (I-86) which replaces (I-78) is a system of ℓ first order nonlinear ordinary differential equations with no retarded variable, whereas (I-78) is a single first order nonlinear differential equation with a lagging variable.

Now consider $\mu = 2\frac{\ell - q}{\ell}$, $0 < q \leq \ell$, the time-lag displaced the same amount from the line $\mu = 1$ but in the opposite direction as is $\mu = 2\frac{q}{\ell}$. In this case a cyclic solution must satisfy the following ℓ equations

$$\frac{\ell}{2}\left(\tilde{g}_i - \tilde{k}\right)\frac{d\tilde{g}_i}{d\xi} = a\,\tilde{g}_i + b\,\tilde{g}_{i+q} \qquad 1 \leq i \leq \ell - q \tag{I-85}$$

$$\frac{\ell}{2}\left(\tilde{g}_i - \tilde{k}\right)\frac{d\tilde{g}_i}{d\xi} = a\,\tilde{g}_i + b\,\tilde{g}_{i-\ell+q} \qquad \ell - q + 1 \leq i \leq \ell \tag{I-86}$$

with the boundary conditions

$$\tilde{g}_1(0) + \tilde{g}_\ell(1) = 2\tilde{k} \tag{I-87}$$

$$\tilde{g}_i(1) = \tilde{g}_{i+1}(0) \qquad 1 \leq i \leq \ell - 1 \tag{I-88}$$

Here it has been noted that $\tilde{g}_{i\mu} = \tilde{g}_{\ell-(\ell-q)+i} = \tilde{g}_{i+q}$, $1 \leq i \leq \ell - q$, and $\tilde{g}_{i\mu} = \tilde{g}_{i-(\ell-q)} = \tilde{g}_{i-\ell+q}$, $\ell - q + 1 \leq i \leq \ell$.

The independent variable Φ is now defined as $\Phi = (1 - \xi)$ and the ℓ functions $h_i(\Phi)$ are introduced, where $\tilde{g}_i(\xi) = -h_{\ell-i+1}(\Phi)$. If these are substituted into Equations (I-85) and (I-86), the following set of equations results:

$$\frac{\ell}{2}\left(h_j - k_1\right)\frac{dh_j}{d\Phi} = a\,h_j + b\,h_{\ell-q+j} \qquad 1 \leq j \leq q \tag{I-89}$$

$$\frac{\ell}{2}\left(h_j - k_1\right)\frac{dh_j}{d\Phi} = a h_j + b h_{j-q} \qquad q+1 \le j \le \ell \tag{I-90}$$

where $j = \ell - i + 1$ and $k_1 = \dfrac{h_\ell(1) + h_1(0)}{2} = -\tilde{k}$.

The ℓ boundary conditions are

$$h_1(0) + h_\ell(1) = 2k_1 \tag{I-91}$$

$$h_j(1) = h_{j+1}(0) \qquad 1 \le j \le \ell-1 \tag{I-92}$$

Comparison of the system of equations (I-81), (I-82), (I-83), (I-84) with the system (I-89), (I-90), (I-91), (I-92) shows that as long as the value of n is the same, i.e., the a and b are the same, the equations and boundary conditions for the g_i when $\mu = 2\frac{q}{\ell}$ are the same as for the h_i when $\mu = 2\frac{\ell - q}{\ell}$. Consequently, if there is a cyclic solution for the case $\mu = \frac{2q}{\ell}$ expressed in terms of ℓ g_i for a given value of n then there is an identical cyclic solution for the case $\mu = 2\frac{\ell - q}{\ell}$ expressed in terms of the ℓ h_i for the same value of n.

Since, when $\mu = 2\frac{\ell - q}{\ell}$, $\tilde{g}_i(\xi) = -h_{\ell-i+1}(\Phi)$ then, also, when $\mu = 2\frac{\ell - q}{\ell}$, $\tilde{g}_i(\xi) = -g_{\ell-i+1}(\Phi)$. The relation between $\tilde{g}_i(\xi)$ and $g(\Theta)$ just given, $\tilde{g}_i(\xi) = g_{\ell-i+1}(\Phi)$ means that $\tilde{g}(\Theta)$ may be obtained from $g(\Theta)$ by a 180° rotation of the cyclic solution $g(\Theta)$ about the axis $\Theta = 1$, $g = 0$.

There is also a relationship between the first order period for the two cases $\mu = 2\frac{q}{\ell}$ and $\mu = 2\frac{\ell - q}{\ell}$. The fact that the equations and boundary conditions for the h_i and the g_i are the same means that

if a periodic solution is found in terms of the g_i for some value of k, then the same solution obtains for the h_i, with $k_1 = k$. The definition $k_1 \equiv -\tilde{k}$ then implies $\tilde{k} = -k$. Since $\frac{\pi_1}{M} = -k$, the first order period for a given solution when $\mu = 2\frac{q}{\ell}$ is the negative of the first order period for the corresponding solution when $\mu = 2\frac{\ell - q}{\ell}$. In other words, if a periodic solution for $\mu < 1$ is above resonant by some amount π_1, then the corresponding solution found by the simple rotation discussed above, will be below resonant by the same amount.

This transformation is most easily seen by using a concrete example. Consider $\mu = 2\cdot\frac{2}{5} = \frac{4}{5}$ and the associated μ with equal displacement from the line $\mu = 1$, $\mu = 2\cdot\frac{3}{5} = \frac{6}{5}$. In this case $q = 2$, $\ell = 5$. Figure 3A shows the interval $0 \leq \theta \leq 2$ divided into 5 sub intervals, and the assumed form of a cyclic solution for $g(\theta)$ when $\mu = \frac{4}{5}$. Figure 3B shows the solution resulting from a rotation of 180°. It is evident from comparing Figure 3A and Figure 3B that $g_1(\xi) = -g_5(1-\xi)$, $g_2(\xi) = -g_4(1-\xi)$, $g_3(\xi) = -g_3(1-\xi)$, $g_4(\xi) = -g_2(1-\xi)$ and $g_5(\xi) = -g_1(1-\xi)$, and, therefore, that the condition $g_i(\xi) = -g_{-i+1}(\xi)$ is satisfied.

Because the solutions for $\mu = 2\frac{q}{\ell}$ and $\mu = 2\frac{\ell - q}{\ell}$ are related in this simple way, it is only necessary to integrate Equation (I-78) for $\mu \leq 1$ to find all solutions of (I-78) for $0 < \mu < 2$, μ a rational fraction of 2.

b) Discontinuous Solutions for $\mu = 1$

Before proceeding to the solution of Equation (I-78) for μ a general rational fraction of unity, the special case $\mu = 1$ will be considered to gain a certain insight into the general behavior of solutions

to the governing equation.

When $\mu = 1$, then $q = 1$, $\ell = 2$, and there are only 2 sub divisions of the interval $0 \leq \Theta \leq 2$. Moreover, since $\mu = 2\frac{\ell - q}{\ell}$ is the same as $\mu = 2\frac{q}{\ell}$, the relationship between the g_i for $\mu = 1$ becomes $\tilde{g}_i(\xi) = -g_{3-i}(1-\xi) = -\tilde{g}_{3-i}(1-\xi)$, because $\tilde{g}_i = g_i$.* In other words, $g_1(\xi) = -g_2(1-\xi)$. Consequently, any periodic solution to Equation (I-78) when $\mu = 1$ must be antisymmetric with respect to the line $\Theta = 1$. This further implies that $g(0) + g(2)$ must vanish because, by the antisymmetry, $g_1(0) = -g_2(1)$. Thus, k is zero, and, by referring to the previous discussion of the relationship between π_1 and k, $\mu = 1$ is seen to represent the case of resonant oscillations. This was also a result in the linearized treatment. Of course, only one value of n ($n = \frac{\gamma + 1}{4\gamma}$) corresponded to $\mu = 1$ for neutral stability in that case. When $\mu = 1$, Equation (I-78) is decomposed into the following two equations which correspond to a special case of Equations (I-81), (I-82)

$$g_1 \frac{dg_1}{d\xi} = a g_1 + b g_2 \qquad \text{(I-93)}$$

$$g_2 \frac{dg_2}{d\xi} = a g_2 + b g_1 \qquad \text{(I-94)}$$

The boundary conditions are

$$g_1(0) + g_2(1) = 0 \qquad g_1(1) = g_2(0)$$

The second boundary condition, along with the antisymmetry requirement, implies that

$$g_1(1) = g_2(0) = 0 \qquad \text{(I-95)}$$

---

* This is strictly true if there is a unique solution for g. In all cases with $\mu = 1$, this is found (by numerical integration) to be the case. Arguments are presented later to strengthen this contention.

That is, the solution $g(\theta)$ passes through zero at $\theta = \mu = 1$. This requirement, that $g(1) = 0$, is equivalent to, and may be used in place of, the boundary condition $g(0) + g(2) = 0$, when $\mu = 1$.

Some other characteristics of the behavior of $g(\theta)$ when $\mu = 1$ are easily discerned. First, by rewriting Equation (I-93) and (I-94) in the following form

$$\frac{dg_1}{d\xi} = a + b\,\frac{g_2}{g_1} \tag{I-96}$$

$$\frac{dg_2}{d\xi} = a + b\,\frac{g_1}{g_2} \tag{I-97}$$

and using the fact that $g_1(1) = 0$ (Equation (I-95)), it is immediately seen that the slope of g at $\theta = \mu = 1$ becomes infinite as long as $g(\theta = 2)$ (i.e., g immediately before the shock) is nonzero. Whenever a discontinuity is present, this must be the case. Moreover, it can be shown that because of the antisymmetry and the requirement that the jump from $g(2)$ to $g(0)$ must be positive, g_2 is always non positive and g_1 always non negative. This implies that the slope of g at $\mu = 1$ is negative.

Using the definitions of a and b,

$$a = \gamma + 1 - 2\gamma n$$

$$b = 2\gamma n$$

it can be seen that for $n > \frac{\gamma + 1}{2\gamma}$, $\frac{dg}{d\theta}$ is always negative. This is because a is negative and $\frac{g_2}{g_1}$ is negative, while b is positive. By looking at Equations (I-96) and (I-97), it is obvious that the right hand sides of both are always negative. Consequently, $\frac{dg}{d\theta}$ must always be negative for the interval under consideration. Its value at $\theta = 0$, and $\theta = 2$ is simply $a = \gamma + 1 - 2\gamma n$ and, thus becomes more and more nega-

tive as n increases. Similarly, when $n = \frac{\gamma + 1}{2\gamma}$, $a = 0$, and $\frac{dg}{d\theta}$ must be zero at $\theta = 0$ and $\theta = 2$ and negative everywhere else.

For $n < \frac{\gamma + 1}{2\gamma}$, $a > 0$, and $\frac{dg}{d\theta}$ is positive at $\theta = 0$ and $\theta = 2$. The fact that the slope of $g(\theta)$ must still be negative at $\theta = 1$ implies that $g(\theta)$ has a maximum between $\theta = 0$ and $\theta = 1$, and a corresponding minimum between $\theta = 1$ and $\theta = 2$, for these values of n.

The case $a = b$ is of particular interest since it corresponds to the resonant point on the linear neutral stability curve. This is true because $a = b$ only when $n = \frac{\gamma + 1}{4\gamma}$, and, since $\mu = 1$, the values of n and μ are identical with those for neutrally stable resonant oscillations, obtained by linear analysis.

When $a = b$ Equation (I-96) and (I-97) become

$$\frac{dg_1}{d\xi} = a\left(1 + \frac{g_2}{g_1}\right) \tag{I-98}$$

$$\frac{dg_2}{d\xi} = a\left(1 + \frac{g_1}{g_2}\right) \tag{I-99}$$

which imply

$$\frac{dg_1}{dg_2} = \frac{g_2}{g_1} \tag{I-100}$$

Equation (I-100) is easily integrated to give $g_1^2 - g_2^2 = C_1$.
At $\xi = 0$, $g_1^2(0) - g_2^2(0) = C_1$, but $g_2(0) = 0$, hence $g_1^2(0) = C_1$.
At $\xi = 1$, $g_1^2(1) - g_2^2(1) = g_1^2(0)$, but $g_1^2(1) = 0$, hence $g_2^2(1) = -g_1^2(0)$. It is required by the antisymmetry condition that $g_2(1) = -g_1(0)$, consequently $g_1^2(0) = -g_1^2(0) = 0$, and $g_1^2 - g_2^2 = 0$,

or $g_1 = - g_2$ ($g_1 = g_2$ cannot be used because of the antisymmetry requirement). If the relation $g_1 = - g_2$ is substituted in Equations (I-98) and (I-99), one finds

$$\frac{dg_1}{d\xi} = \frac{dg_2}{d\xi} = 0$$

or, integrating, g_1 = constant, g_2 = constant. Since g must pass through zero at $\Theta = 1$, it is obvious that the constants are equal to zero. Thus, for the case $a = b$, the only solution for $g(\theta)$ is the trivial one, $g(\theta) = 0$.

The conclusions that can be drawn from this brief analytical examination of the behavior of $g(\theta)$ for the case $\mu = 1$ are:

1) $g(\theta)$ is antisymmetric with respect to $\mu = 1$.

2) $g(\theta)$ passes continuously through zero at $\Theta = \mu = 1$.

3) $\frac{dg}{d\theta} \longrightarrow - \infty$ at $\theta \longrightarrow 1$.

4) $\frac{dg}{d\theta}$ is always negative for $n > \frac{\gamma + 1}{2\gamma}$.

5) $\frac{dg}{d\theta}$ is zero at $\theta = 0$, $\theta = 2$ and negative elsewhere for $\frac{\gamma + 1}{2\gamma} = n$

6) $\frac{dg}{d\theta}$ is positive then negative for $0 \leq \theta \leq 1$, negative then positive for $1 \leq \theta \leq 2$ when $\frac{\gamma+1}{4\gamma} < n < \frac{\gamma+1}{2\gamma}$

7) The amplitude of $g(\theta)$ is zero at the linear neutral stability limit, $n = \frac{\gamma + 1}{4\gamma}$.

No analytical method for integrating the system of Equations (I-93) and (I-94) or the equivalent second order equation

$$\frac{d^2 g_1}{d\xi^2}\left[g_1 \frac{dg_1}{d\xi} - a g_1\right] + \left[\frac{dg_1}{d\xi}\right]^3 - 2a\left[\frac{dg_1}{d\xi}\right]^2 + (a^2 - ba)\frac{dg_1}{d\xi} - b^3 + a^2 b = 0$$

has been found for physically reasonable values of n. A numerical method instead has been successfully employed. This numerical technique will now be outlined.

The system of Equations (I-93), (I-94) presents two difficulties to straightforward step by step integration. The first problem is that $\frac{dg_2}{d\xi}(0)$ and $\frac{dg_1}{d\xi}(1)$ are infinite. The second is that the two boundary conditions $g_2(0) = 0$, $g_1(1) = 0$, are given at opposite ends of the range of the independent variable ξ. The first difficulty is easily overcome by introducing the dependent variable $G(\xi) = \frac{g_2^2}{2}(\xi)$. The governing system of Equations (I-93), (I-94) is then transformed into the following pair of equations for $G_1(\xi)$, $G_2(\xi)$:*

$$\frac{dG_1}{d\xi} = a\sqrt{G_1} - b\sqrt{G_2} \qquad \text{(I-101)}$$

$$\frac{dG_2}{d\xi} = a\sqrt{G_2} + b\sqrt{G_1} \qquad \text{(I-102)}$$

where the fact that g_2 is always non-positive and g_1 is always non negative has been used, and the positive value of the square root is to be taken. It is clear that $\frac{dG_1}{d\xi}(1)$ and $\frac{dG_2}{d\xi}(0)$ are not infinite as long as $g(0)$ is finite.

The second difficulty cannot be removed and forces the use of an

---

* Because the point $\theta = 1$ is a singular point of the equations there is no guarantee of finding a unique solution. However, many numerical integrations have been performed and in every case only one solution for each n could be found.

iteration scheme to integrate Equations (I-101), (I-102). This iteration proceeds as follows. A value of $G_1(0)$ is guessed. This, along with the boundary condition $G_2(0) = 0$, provide initial values for integration. The system of equations is then integrated step by step, using a standard differential equation "package" that is basically a Runge-Kutta scheme, up to $\xi = 1$. The value of $G_1(1)$ is then compared with zero. If it is zero, (actually, of course, within some arbitrarily small error) the integration of the equation is complete. If, however, G_1 is non zero, a new value of $G_1(0)$ must be selected and the process continued until $G_1(1)$ is zero. The new values of $G_1(0)$ are selected by using a form of the Newton-Raphson method for finding roots.

For most values of n the above described integration and iteration process converges rapidly. When n approaches the neutral stability value, however, the iteration converges much more slowly and the integration scheme is effectively limited to values of n that differ from $\frac{\gamma+1}{4\gamma}$ by very small amounts.

Figure 4 shows the form of the pressure waves predicted at $x = 0$ by integrations of this kind for a range of values of n. The function plotted against θ is $\frac{g(\theta)}{\gamma+1} \equiv \frac{f(\theta)}{M}$, which, by the definition of $f(\theta)$, is equal to $\frac{p'(0,\theta)}{2\gamma M}$. It is seen that, as was predicted through analytical consideration of the equations, the slope of $\frac{dg}{d\theta}$ is always negative for $n > \frac{\gamma+1}{2\gamma}$ and is zero for some value of ξ between 0 and 1 when $n \leq \frac{\gamma+1}{2\gamma}$. Also, the slope of g is seen to be negative and infinite at $\theta = 1$.

Figure 5 shows a plot of the peak to peak amplitude of $\frac{g(\theta)}{\gamma+1}$ and

of the amplitude of the shock $\frac{g(0) - g(2)}{\gamma + 1}$, as functions of displacement from the linearly stable value of n, $n = \frac{\gamma + 1}{4\gamma}$. It is seen that the growth in shock amplitude is surprisingly linear as n increases. Also, the peak to peak amplitude conincides with the shock amplitude for $n \geq \frac{\gamma + 1}{2\gamma}$, and is larger than the shock amplitude for $n < \frac{\gamma + 1}{2\gamma}$.

Figure 6 shows pressure wave shapes close to the stability limit. As this value of n is approached, the positive slope of $g(\theta)$ at $\theta = 0$ and $\theta = 2$ becomes larger and larger, and the maximum and minimum of $g(\theta)$ move closer and closer to $\theta = 1/2$ and $\theta = 3/2$, respectively. Indeed, the tendency at the stability limit seems to be toward a wave shape that has a zero amplitude shock and a slope of $\frac{\gamma + 1}{2}$ at both $\theta = 0$ and $\theta = 2$, that is symmetric about $\theta = 1/2$ in the region $0 \leq \theta \leq 1$, and that is symmetric about $\theta = 3/2$ in the region $1 \leq \theta \leq 2$. This kind of behavior is consistent with the results of the analytical examination of the governing equation at the stability limit, $n = \frac{\gamma + 1}{4\gamma}$, performed earlier.

In summary, it may be said that for the case $\mu = 1$, the following facts about periodic solutions to the governing equations are true:

1) The amplitude of the discontinuous waves is zero at the stability limit and increases in a nearly linear fashion as n is increased from its neutrally stable value.

2) All the waveforms of finite amplitude exhibit discontinuities, though, in the limit as the neutrally stable value of n is approached, the jump tends to zero, and, near the stability limit, the peak to peak amplitude of the wave is larger than the shock amplitude.

3) No periodic solutions exist for $n < \frac{\gamma + 1}{4\gamma}$. That is, the

linearly stable region for $\mu = 1$ is still predicted unconditionally stable in this nonlinear analysis.

4) The character of the decay in pressure after the shock is strongly dependent upon the value of n. For large n the decay becomes very steep and tends toward classical "sawtooth" decay. For n near $\frac{\gamma+1}{4\gamma}$ the decay is more sinusoid in nature; increasing after the shock, then decreasing, then increasing again before the shock.

c) Discontinuous Solutions for μ a Rational Fraction Less Than Unity

When $\mu = 2\frac{q}{\ell}$, $2q < \ell$, the solution of Equation (I-78) becomes more difficult. Because the region $0 \leq \Theta \leq 2$ is now to be considered as consisting of ℓ sub intervals rather than just two, the convenient antisymmetry property of the solutions found for $\mu = 1$ does not hold when $\mu < 1$. This means that $k = \frac{g(0) + g(2)}{2}$ can not be taken equal to zero, and, therefore, that π_1 will not necessarily be zero.

When $\mu = 1$, the value of Θ for which $g(\Theta)$ must pass through zero is fixed by the antisymmetry requirement to be $\Theta = \mu = 1$. For $\mu < 1$ no such simple means of determining the zero of $g(\Theta)$ (if one exists) is apparent. This deficiency is important, since the knowledge of the zero of $g(\Theta)$ was crucial in the numerical integration scheme used when $\mu = 1$. Even if a simple condition for starting the numerical integration process, analogous to the condition $g(1) = 0$, used when $\mu = 1$, were found, one would still be faced with the problem of guessing the other $(\ell - 1)$ initial conditions and then performing the $(\ell - 1)$ iterations required until a solution satisfying that condition was found. For large ℓ this would be a formidable task indeed. For this reason, when $\mu < 1$ the governing first order nonlinear equation is not broken down

into ℓ nonlinear first order equations not containing time-lags as was done when $\mu = 1$, but, instead, the integration of the original equation including the lagging variable effect is attempted directly.

Equation (I-78) may be rewritten in the following form

$$\psi \frac{d\psi}{d\theta} = a\psi + b\psi_\mu + (\gamma+1)k \tag{I-103}$$

where $\psi = (g - k)$, and the fact that $a + b = \gamma + 1$ has been used. The boundary condition $g(0) + g(2) = 2k$ becomes $\psi(0) + \psi(2) = 0$. Since the jump in g at $\theta = 2$ is positive, the jump in ψ must also be positive. This implies that $\psi(0)$ must be greater than zero and that $\psi(2)$ must be less than zero when $g(\theta)$ is discontinuous. Further, because, for any periodic discontinuous solution, $\psi(0)$ is positive and $\psi(0) + \psi(2) = 0$, it is clear that ψ must pass through zero somewhere between $\theta = 0$ and $\theta = 2$. This value of θ is designated $\tilde{\theta}$.

Equation (I-103) may be rewritten as follows

$$\frac{d\frac{\psi^2}{2}}{d\theta} = a\psi + b\psi_\mu + (\gamma+1)k \tag{I-104}$$

Then, at $\theta = \tilde{\theta}$

$$\frac{d\frac{\psi^2}{2}}{d\theta} = b\psi_\mu + (\gamma+1)k \tag{I-105}$$

The quantity on the right hand side of the above equation must be zero if ψ_μ is continuous at $\theta = \tilde{\theta}$. For, if it were positive, it would mean that at some earlier θ, $\psi^2/2$ must have been negative. This is not acceptable,

since ψ represents a physical quantity (the pressure) and can't be complex. On the other hand, if the right hand side were negative, it would mean that as θ increased from $\tilde{\theta}$, $\psi^2/2$ would become negative. This is equally unsatisfactory for the same reason. Thus, if ψ passes through zero at $\theta = \hat{\theta}$, if $\psi(\tilde{\theta} - \mu)$ is to be continuous, and if ψ is to remain real, then $\psi(\tilde{\theta} - \mu) = -\frac{k(\gamma + 1)}{b}$. In this case, then, in addition to the boundary condition $\psi(0) + \psi(2) = 0$ that any periodic discontinuous solution to (I-103) must satisfy, there is also the condition $\psi(\gamma - \mu) = -\frac{k(\gamma + 1)}{b}$ to be satisfied in order for the solution to always be real. This means that of the family of solutions satisfying Equation (I-103) for a given n(a and b) and μ with different values of k, there must be one solution, for some value of k, that in addition to satisfying the boundary condition $\psi(0) + \psi(2) = 0$ also satisfies the relationship $\psi(\tilde{\theta} - \mu) = -\frac{(\gamma + 1)k}{b}$, in order for there to be any real solution to (I-103) with $\psi(\tilde{\theta} - \mu)$ continuous. No solutions of this type have been found. In all cases investigated (numerically) it is found to be impossible to satisfy simultaneously both the boundary condition $\psi(0) + \psi(2) = 0$ and the condition for the continuity of $\psi(\gamma - \mu)$; $\psi(\tilde{\theta} - \mu) = -\frac{(\gamma + 1)k}{b}$.

Fortunately, another possibility exists. This is the possibility that $\psi(\tilde{\theta} - \mu)$ may be discontinuous. If this were the case, then $\frac{d\psi^2/2}{d\theta}$ could have a negative value as it approached $\tilde{\theta}$ in the direction of increasing θ and a positive value as θ increased away from $\theta = \tilde{\theta}$, provided the jump in $\psi_\mu(\tilde{\theta})$ were large enough (recall that these conditions with respect to the sign of $\frac{d\psi^2/2}{d\theta}$ must be satisfied if $\psi(\theta)$ is to be real). At $\theta = \tilde{\theta}$, $\frac{d\psi^2/2}{d\theta}$ might then have two values depending

upon whether $\tilde{\theta}$ were approached from the left ($\frac{d\psi^2/2}{d\theta}$ negative) or the right ($\frac{d\psi^2/2}{d\theta}$ positive). Only one discontinuity in $\psi(\theta)$ is allowed, and this is at $\theta = 0$ (or $\theta = 2$). Consequently, it is seen that $\psi(\tilde{\theta} - \mu)$ may be discontinuous only if $\tilde{\theta} = \mu$. That is, $\psi(\theta)$ must pass through zero at $\theta = \mu$ in this case. Also, if $k > 0$, $\psi_\mu(\mu) = \psi(2)$ must be less than $\frac{(\gamma+1)k}{b}$ if $\frac{d\psi^2/2}{d\theta}$ is to be negative as $\theta \longrightarrow \mu$ from the left. Of course, $\frac{d\psi^2/2}{d\theta}$ will be positive as $\theta \longrightarrow \mu$ from the right, since $\psi(0)$ and $b = 2\gamma n$ are always positive. If, on the other hand, $k < 0$ then $\frac{d\psi^2/2}{d\theta}$ is negative as $\theta \longrightarrow \mu$ from the left, simply because $k < 0$, $\psi(2) < 0$, and $b > 0$. However, as $\theta \longrightarrow \mu$ from the right, the condition $\psi(0) > \frac{(\gamma+1)k}{b}$ must be satisfied if $\frac{d\psi^2/2}{d\theta}$ is to be positive. In general, then, it is required that $|\psi(0)| > \frac{(\gamma+1)k}{b}$ for real solutions to exist with $\psi(\mu) = 0$.

The salient feature of solutions of this type (that is with $\psi(\mu) = 0$) is that $\frac{d\psi}{d\theta} \longrightarrow -\infty$ at $\theta = \mu$. This is because as $\theta \longrightarrow \mu$ from the left, $\frac{d\psi^2/2}{d\theta}$ is negative and non zero, while ψ is positive. Consequently, since $\frac{d\psi}{d\theta} = \frac{1}{\psi}\frac{d\psi^2/2}{d\theta}$, $\frac{d\psi}{d\theta} \longrightarrow -\infty$. Similarly, as $\theta \longrightarrow \mu$ from the right, $\frac{d\psi^2/2}{d\theta}$ is positive and non zero while ψ is negative, so, again, $\frac{d\psi}{d\theta} \longrightarrow -\infty$. The implication here is that for solutions to Equation (I-103) in which $\psi(\mu) = 0$, the function $\psi(\theta)$ and its first derivative are continuous at the point $\theta = \mu$ and that the slope of ψ is negative infinite at this point.

For the special case $\mu = 1$ it was found that, strictly on the basis of the antisymmetry of the solution with respect to $\theta = \mu = 1$, the function $\psi(\theta)$ went through zero at $\theta = \mu$. For this special case, then,

the only possible solutions for $\psi(\theta)$ were of the type $\psi(\mu) = 0$ rather than the type where $\psi_\mu(\tilde{\theta})$ is continuous. Consequently, one might expect that the solutions for $\mu < 1$ would exhibit the behavior $\psi(\mu) = 0$, merely for consistency of form with the solutions for $\mu = 1$.

This is indeed the case. Solutions of Equation (I-103) satisfying the boundary condition $\psi(0) + \psi(2) = 0$, and also the requirement $\psi(\mu) = 0$ that are real everywhere in the interval $0 \leq \theta \leq 2$ are readily found for a wide range of values of n and μ. The numerical integration of (I-104) which produces solutions of this type will now be discussed.

Because of the fact that Equation (I-103) exhibits a lagging variable, the value of the <u>function</u> $\psi(\theta)$ must be given in an interval μ units before the start of any step by step numerical integration scheme. This is, of course, in contrast to the usual problem of numerical integration of an ordinary differential equation of first order with no lagging variable, in which the <u>value</u> of the function only need be given at the starting point of the step by step integration process. The form of the function $\psi(\theta)$ is unknown originally for the problem under consideration, indeed, the stated purpose of the integration of Equation (I-103) is to find the form of $\psi(\theta)$. Consequently, it can be seen that one must guess the form and value of the function $\psi(\theta)$ over an interval μ units before a discontinuity in order to begin integration at the discontinuity. With this im mind, the actual method used to integrate Equation (I-103) will now be presented.

A solution of Equation (I-103) for some value of $\mu = \frac{2q}{\ell}$ and n is

desired. Consequently, the values of a and b are fixed in Equation (I-103). The value of the parameter $k = \frac{g(0) + g(2)}{2}$ is not known for the moment. It is therefore simply given some arbitrary value so that the integration may proceed. As in the integration scheme used when $\mu = 1$, the problem of the infinite slope of $\psi(\theta)$ is avoided by solving for $\frac{\psi^2(\theta)}{2} \equiv \Psi(\theta)$ instead of for $\psi(\theta)$. The integration is begun at $\theta = \mu$, where $\psi = 0$, and proceeds in the direction of decreasing θ towards $\theta = 0$. This is done so that the condition $\psi(\mu) = 0$ will be automatically satisfied by any solution found. A simple Runge-Kutta scheme is used to integrate the equation

$$\frac{d\Psi}{d\theta} = \sqrt{2}\, a \left|\sqrt{\Psi}\right| - \sqrt{2}\, b \left|\sqrt{\Psi_\mu}\right| + (\gamma+1) k \qquad \text{(I-106)}$$

as θ runs from μ to zero. There is a positive sign before the first term on the right hand side because it has been shown that $\psi(\theta)$ must be non negative between zero and μ; the negative sign before the second term reflects the fact that $\psi(\theta)$ between μ and 2 must be non positive. The second term on the right hand side contains the function $\Psi(\theta - \mu)$ which must be guessed.

After guessing $\Psi(\theta - \mu)$, integration may proceed and will result in <u>some</u> function $\Psi(\theta)$ for the interval $0 \leq \theta \leq \mu$ which passes through zero at $\theta = \mu$. Step by step integration of the equation

$$\frac{d\Psi}{d\theta} = -\sqrt{2}\, a \left|\sqrt{\Psi}\right| + \sqrt{2}\, b \left|\sqrt{\Psi_\mu}\right| + (\gamma+1) k \qquad \text{(I-107)}$$

is now carried out using the Runge-Kutta technique starting from $\theta = \mu$ and progressing in the direction of increasing θ up to $\theta = 2\mu$.

The signs on the right hand side again result because $\Psi(\theta)$ is non negative for $0 \leq \theta \leq \mu$ and is non positive for $\mu \leq \theta \leq 2$. The function $\Psi(\theta-\mu)$ is simply the function $\Psi(\theta)$ between $\theta = 0$ and $\theta = \mu$ which was just found by numerical integration. From $\theta = 2\mu$ to $\theta = 2$ the following equation must be integrated

$$\frac{d\Psi}{d\theta} = -\sqrt{2}\, a \left|\sqrt{\Psi}\right| - \sqrt{2}\, b \left|\sqrt{\Psi_\mu}\right| + (\delta+1)k \tag{I-108}$$

where the signs on the right hand side are determined as before, and $\Psi(\theta-\mu)$ is known from previous integration.

The function $\Psi(\theta), 2-\mu \leq \theta \leq 2$ is now compared with the function originally guessed for this same interval. In general, of course, they will not be the same. In this case the function just found by integration for $2-\mu \leq \theta \leq 2$ is used as a new initial function and the process is repeated with the hope that $\Psi(\theta)$ will eventually converge to some function that does not vary from one integration cycle to the next. There is no guarantee that such convergence will occur, although intuitively it seems reasonable. In fact, it turns out that the technique does converge and, moreover, that the convergence is very rapid and surprisingly insensitive to what the original guess of the function was, at least for most of the ranges of n and μ considered. That is, the technique converges to the same function in a few integration cycles regardless of what (or how bad) the initial guess for the function was. Because of this, it is possible to assume that the function in the interval $2-\mu \leq \theta \leq 2$ is simply a constant and to start the integration under this assumption. Again, convergence to the same final function occurs fairly rapidly even if the constant chosen to represent the function in the interval $2-\mu \leq \theta \leq 2$

is as much as an order of magnitude different from the mean value of the final solution in that interval.

Once a function $\psi(\theta)$ which repeats itself cyclically and passes through zero at $\theta = \mu$ is found using the above procedure, it is necessary to check and see if it satisfies the boundary condition $\psi(0) + \psi(2) = 0$. If it does not, new values of $k = \frac{g(0) + g(2)}{2}$ must be selected and the functional iteration repeated until the boundary condition is satisfied. In general, new values of k are selected through the use of a form of Newton's method for finding roots. For some values of n and μ two different values of k may produce different solutions which both converge and satisfy the boundary condition $\psi(0) + \psi(2) = 0$. In this case the solution for the lower value of k converges much more slowly than usual and is extremely sensitive to k. For these "lower branch" values of k Newton's method is often impractical and a "brute force" method is employed to find the proper value of k. In this technique k is simply changed in decreasing amounts when the value of the quantity $\psi(0) + \psi(2)$ is close to zero.

Equation (I-103) has been solved for a great many values of n and μ in the range $0 < \mu < 1$ and $.46 < n < 10$ using the numerical technique just described. The ratio of specific heats, γ has arbitarily been taken equal to 1.2 for all calculations.

Figure 2 compares the nonlinear stability limit for discontinuous solutions with the linear neutral stability curve. The nonlinear stability limit separates the regions in the n, μ plane where discontinuous, periodic pressure waves can be found, from regions in which no such solutions occur. This limit is obtained by gradually decreasing n for a fixed μ

until no solutions which are real, and at the same time satisfy the boundary condition $\psi(0) + \psi(2) = 0$ are found. Only the "upper branch" values of k are considered when two solutions occur for the same n and μ. As shown later, the "lower branch" values of k correspond to unstable periodic discontinuous oscillations. Only stable solutions are of interest, since, because of their instability, unstable solutions cannot represent the regime oscillations in the combustion chamber. The smallest value of n giving valid stable solutions is then said to be a point on the nonlinear stability curve. The linear stability curve is simply the dividing line between regions on the n, μ plane where small perturbations from steady operation will grow (inside the curve) or decay (outside the curve) and is obtained in the same manner as it has been previously.

Figure 7 shows the nonlinear stability limit again. In addition lines of constant shock amplitude have been drawn, in order to represent the overall behavior of the amplitude of the discontinuous solutions. All the curves shown (including the stability limits) are symmetric with respect to $\mu = 1$. For a given n, the largest amplitude oscillations are found when the oscillations are resonant ($\mu = 1$). The amplitude of the waves decreases as one moves away from $\mu = 1$ on a line of constant n. Near resonance, for n values of interest, the shock amplitude can be quite large. For example, when $n = 2$, shock amplitudes $\left(\frac{p'(0) - p'(2)}{2\delta M}\right)$ can be of the order of 10. (This corresponds to $\frac{\epsilon}{M} \sim 5$ or, for $M = 0.1$, $\epsilon \sim .5$)

For the most part, the region inside the nonlinear stability curve and the region inside the linear stability curve overlap. In this area of

overlap the growth of small perturbations is predicted by the linear analysis, while, at the same time, nonlinear analysis predicts the possibility of periodic discontinuous oscillations. This suggests that, in these regions of the n , μ plane, the final form that instability, started by an infinitesimal disturbance, takes, is characterized by the discontinuous periodic oscillations predicted in the present nonlinear analysis.

There are, on the contrary, regions in the n , μ plane for which the area of linear instability and the area where discontinuous periodic oscillations are possible do not overlap. These regions are of two types. The first occurs when the nonlinear stability curve lies inside the linear stability limit. On Figure 2 this situation is seen to be present for μ values between 1/3 and 4/3 . In the region between the curves, linear results again predict the growth of small perturbations, however, the final form that the instability takes cannot be that of periodic discontinuous oscillations in this case. Since Sirignano,[2] using his method of analysis, found that periodic, continuous, finite amplitude oscillations could exist close to the linear stability limit, it is natural to expect that the final form the instability takes in the region between the curves might be oscillations of this type. This will be shown to be the case shortly, using the present method of analysis.

The second area where the region of linear instability, and the region of existence of discontinuous periodic solutions do not coincide, is found outside the linear stability limit for $0 < \mu < 2/3$ and for $4/3 < \mu < 2$ as can be seen on Figure 8 . Here the linear

stability limit lies inside the nonlinear stability curve. This, then, is a region that is linearly stable while, at the same time, it is also a region where periodic discontinuous oscillations are possible. Clearly, the discontinuous oscillations cannot be the final result of the growth of infinitesimal perturbations in this case, simply because infinitesimal perturbations do not grow but rather decay to zero in this region. The only other possibility is that oscillations that are periodic and discontinuous may be triggered by finite amplitude disturbances when n , and μ have values in this area.

In Figure 9 the shock amplitude and peak to peak amplitude (they are not necessarily the same) of discontinuous period solutions are plotted as a function of normal displacement from the linear stability curve. The values of n and μ on the linear stability limit are designated by superscript zero. It is seen that for $n^{(0)} = 2.52$ and $\mu^{(0)} = .28$, an outward displacement from the linear stability curve is a displacement into a region that is linearly stable but where periodic, discontinuous oscillations are possible. Outward displacements from the linear stability curve are taken to be negative and inward displacements positive. It can be seen from the figure that, for positive normal displacements, only one periodic discontinuous solution for a given n and μ can be found. Note that an inward displacement of this type places one in the region of overlap discussed above. It can be argued that this one solution is a stable solution, in the sense that small perturbations away from the solution decay back to the solution. This has not been proved in the present work, for, indeed, the

proof of stability of such solutions seems to be considerably more difficult than the solution of the entire problem as formulated. However, the facts that small perturbations grow in the region in question, (from linear analysis) and that the finite amplitude periodic discontinuous solutions to the governing partial differential equations found in the region are the only finite amplitude periodic solutions possible, serve as a basis from which to argue that the periodic discontinuous solutions predicted, are stable. For, if a perturbation to the steady-state is applied, with amplitude between zero and the amplitude of the discontinuous periodic solution, then from the standpoint of linear theory the amplitude of this disturbance will grow without limit. However, the present analysis shows that periodic solutions can be found when nonlinearities in the wave interactions are considered, in particular, when discontinuous waveforms are allowed. One can then claim that any infinitesimal perturbation in this region grows in amplitude until nonlinear effects cause the disturbance to take the form of the periodic discontinuous solution predicted for given values of n, and μ. For disturbances with amplitudes greater than that of the periodic nonlinear solution, since there is no other periodic solution in this finite amplitude regime above the discontinuous periodic solution, (at least for the range of amplitudes of order Mach number) it is to be expected that decay in amplitude of such disturbances will occur until periodic oscillations, with the discontinuous waveforms that are predicted by the present analysis, occur. Since perturbations with amplitudes either above or below the amplitude curve for discontinuous periodic solutions eventu-

ally result in oscillations of the character predicted along the curve, then, if the reasoning presented is correct, the discontinuous periodic solutions in this overlap region of linear and nonlinear instability are, indeed, stable solutions.

For normal displacements in the outward (negative) direction, on the other hand, two discontinuous solutions are found for displacements larger than about 0.6 in absolute value. Here it seems reasonable to assume that the lower solution is unstable and that the upper solution is stable. It is known from the linear results of Crocco that infinitesimal perturbations decay to zero in this region,so, if the lower discontinuous solution is taken to be unstable, that is, perturbations away from the solution continue to grow away from the solution, then consistency with the linear prediction results, since perturbations with amplitudes less than that of the unstable solution decay toward zero. Also disturbances with amplitudes larger than that of the lower solution would grow away from the lower solution and toward the upper solution, which is consistent with the idea of the upper solution being stable. The lower solution could thus be considered as a triggering limit. That is, finite amplitude disturbances with amplitudes less than that of the lower solution would decay to zero, while disturbances with amplitudes larger than that of the lower solution, for a given n and μ, would result in instability with oscillations that were of the form of the upper solutions.

For displacements in the outward normal direction less than 0.6 in absolute value only one periodic, discontinuous solution to the governing partial differential equations can be found. By looking at Figure 9

it is apparent that this one solution is of the family of upper solutions. For the one (upper) solution to be stable it is necessary that some unstable solution to the partial differential equations exist between zero and the amplitude of the upper solution. For, if the upper solution is stable, a disturbance of any amplitude in the neighborhood of the solution amplitude should eventually take the form of the stable periodic solution. In particular, the amplitude of a small amplitude disturbance would have to grow. On the contrary, the linear analysis predicts that small amplitude disturbances will decay. Clearly, a small amplitude disturbance cannot grow and decay simultaneously. Thus, unless there is an unstable solution with an amplitude between the amplitude of the upper solution and zero, the linear and nonlinear predictions cannot co-exist harmoniously.

Here, again, recourse to the fact that Sirignano found continuous solutions near the stability limit allows expeditious solution of the dilemma. For, if guided by his results, one searches for continuous solutions in the region in question, he finds that the present analysis can predict periodic, continuous low amplitude oscillations that are the unstable solutions required.

Because of the important role that finite amplitude, continuous periodic solution play in regions of the n, μ plane close to the stability limit, and since they are necessary to have a complete picture of the amplitude dependence of nonlinear periodic solutions, further discussion of the discontinuous solutions and their waveforms will be set aside until the method of finding the required continuous solutions has been presented.

d) Continuous Solutions of Finite Amplitude

In order to find continuous periodic solutions to the problem as posed, Equation (I-76) is rewritten in terms of $g(\theta)$ as

$$\left[\frac{\bar{\bar{\tau}}}{\tau_1} + g - \frac{3-\gamma}{2(\gamma+1)}\int_0^2 g(\theta')\,d\theta'\right]\frac{dg}{d\theta} = ag + b g_\mu \qquad \text{(I-109)}$$

with $g(0) = g(2)$ as the boundary condition for continuous solutions, and where $\bar{\bar{\tau}}_1 \equiv \frac{\tau_1}{M}$. This equation has been normalized with respect to Mach number so that none of the terms becomes small as $M \longrightarrow 0$. It is to be realized that Equation (I-109), though derived with the idea of considering periodic discontinuous oscillations, is also valid for the investigation of continuous oscillations. That is, the development that resulted in Equation (I-109) (or equivalently Equation (I-76)) nowhere required that the waveform had to be discontinuous.

For the case when a shock wave is present, it is possible to determine τ_1 in terms of the value of $g(\theta)$ before and after the shock, and of the integral of $g(\theta)$ over one period. This is because deviations from steady-state operation in the chamber can be represented in terms of $g(\theta)$ to first order. Such deviations have a calculable effect on the velocity of the shock, and therefore on the period of oscillation. Because of this, the first order relationship for the dependence of the period on the form of $g(\theta)$ could be derived. When no shock is present, however, there is no way to determine τ_1 without actually integrating Equation (I-109) and finding periodic solutions. This means that Equation (I-109) can not be put in a form similar to Equation (I-78) in which τ_1 does not appear.

If Equation (I-109) is integrated over one period, the following relationship is obtained:

$$\left[\overline{\overline{T_1}} - \frac{3-\gamma}{2(\gamma+1)}\int_0^2 g(\theta')\,d\theta'\right](g(2)-g(0)) + \frac{g^2(2)}{2} - \frac{g^2(0)}{2} = (a+b)\int_0^2 g(\theta')\,d\theta' \qquad \text{(I-110)}$$

Since $g(\theta)$ is periodic in 2, and since g is now assumed continuous, then $g(2) = g(0)$, and the left hand side of the above equation vanishes. Since $a + b = \gamma + 1$, and since γ is non negative, then it must be true that $\int_0^2 g(\theta')d\theta' = 0$. Any periodic continuous solution to Equation (I-109) must satisfy this condition. A solution to the equation

$$(\overline{\overline{T_1}} + g)\frac{dg}{d\theta} = ag + bg_\mu \qquad \text{(I-111)}$$

that is periodic and continuous also satisfies the condition $\int_0^2 g(\theta')d\theta' = 0$. Consequently, any periodic (with period 2) continuous solution of Equation (I-111) is also a periodic continuous solution of Equation (I-109). The problem of finding periodic continuous solutions exhibiting a period of 2 and satisfying the governing partial differential equations is, then, equivalent to solving Equation (I-111) for $g(\theta)$ under the conditions that $g(\theta)$ be periodic in 2 and continuous.

Two methods of finding such solutions for Equation (I-111) have been developed. The first technique, direct numerical integration of the governing equation, is obvious and straightforward, but also, unfortunately, rather difficult. Since a variable, retarded by the amount μ, appears in Equation (I-111), again, as was the case for discontinuous oscillations,

an initial guess of the function must be supplied for an interval μ units before the start of the step by step integration process. However, the functional iteration technique used to find the waveforms for discontinuous oscillations fails when continuous oscillations are considered. This is because the continuous periodic solutions to the ordinary differential equation, Equation (I-111), appear to be unstable. That is, unless the correct form of the solution is guessed initially, the waveform will change in time, and the amplitude will either monotonically increase or decrease.

In order to find a periodic solution (limit cycle) for Equation (I-111) then, the following procedure is used. A waveform and amplitude is guessed for the interval μ units before the starting point for numerical integration. Step by step integration is then carred out over several cycles to see whether the solution grows or decays. If growth is predicted, the initially assumed amplitude is decreased until the growth rate decreases, becomes small, and passes through zero to become negative. If the amplitude decays, on the other hand, the initial amplitude is increased until the decay rate becomes small, and again passes through zero. In this way the dividing line between solutions that grow and decay can be approximated and the waveform and amplitude of the oscillation which changes only slowly is taken as an approximation of the limit cycle. This must be done for each assumed initial waveform. Fortunately, the limit cycle approximations that can be obtained are practically the same for any initial waveform that does, indeed, produce any approximate limit cycle. These initial guesses that result in approximate solutions that do not grow or decay rapidly in time are all close to a sine wave in form. Consequently, this waveform can

be adopted as the initial guess for the functional form of the wave.

Even if one finds a limit cycle for Equation (I-109) for given n, μ and $\bar{\bar{\pi}}_1$, the condition that the solution must be periodic in 2 must still be satisfied. The way in which this is done is to vary the value of $\bar{\bar{\pi}}_1$ to see if, indeed, a limit cycle can be found, for some value of $\bar{\bar{\pi}}_1$, that does have a period of 2. For most values of n and μ it is impossible to find any limit cycles at all, regardless of the value of $\bar{\bar{\pi}}_1$. Near the stability limit it is possible, however, not only to find periodic solutions (limit cycles) but also limit cycles that have period 2 ; in other words, solutions to Equation (I-109) of the type required. It is unfortunately, very difficult (and time consuming, even on the IBM 7094) to perform the many iterative steps required to find periodic solutions within a reasonable limit of accuracy.

Because of these difficulties that straightforward numerical integration present, it is natural to look for a simple analytical method for finding approximate solutions to Equation (I-111). Such a technique has been found and is, indeed, the second method of solution of Equation (I-111) mentioned earlier. This method will now be presented.

When the expansion parameter ϵ was first introduced, it was defined as the product of Mach number and some function of n and μ of order one or less called $H(n, \mu)$. It was also mentioned at that time that $H(n, \mu)$ should become small at values of n and μ close to the stability limit in order to be consistent with the predictions of linear analysis. Actually, from looking at Figure 9 it is seen that $H(n, \mu)$ is double valued for some values of n, and μ. Indeed, near the stability limit at $\mu^{(0)} = .28$, while the lower value of $H(n, \mu)$ must tend to zero at

the stability limit for consistency with linear analysis, the upper value clearly remains of order unity. Thus, when it is said that $H(n, \mu) \rightarrow 0$, this means the lower value of $H(n, \mu) \rightarrow 0$. The fact that $H(n, \mu) = \frac{\epsilon}{M}$ becomes small near the linear stability curve, (indeed, it must be zero on that curve) implies that the amplitude of $g(\theta) = \frac{f}{M}$ should also be small near the stability limit, and vanish at the stability limit, in order to be consistent with linear results. This suggests that a quantity related to the amplitude of $g(\theta)$ may be taken as a small parameter, which might then be used in order to find approximate solutions to Equation (I-111) valid when n and μ are close to the neutrally stable values predicted by linear analysis. This small amplitude parameter will be called δ and will be more specifically defined later.

The function $g(\theta)$ as well as the quantities n, and μ and $\bar{\bar{\Pi}}_1$ are then expanded in power series in δ

$$g = \delta g^{(1)} + \delta^2 g^{(2)} + - - - -$$

$$n = n^{(0)} + \delta n^{(1)} + \delta^2 n^{(2)} + - - - -$$

$$\mu = \mu^{(0)} + \delta \mu^{(1)} + \delta^2 \mu^{(2)} + - - - -$$

$$\bar{\bar{\Pi}}_1 = \bar{\bar{\Pi}}_1^{(0)} + \delta \bar{\bar{\Pi}}_1^{(1)} + \delta^2 \bar{\bar{\Pi}}_1^{(2)} + - - - -$$

If these expansions are substituted into Equation (I-111), then, to first order in δ, the following equation results

$$\bar{\bar{\Pi}}_1^{(0)} \frac{dg^{(1)}}{d\theta} = (\gamma + 1 - 2\gamma n^{(0)}) g^{(1)} + 2\gamma n^{(0)} g^{(1)}_{\mu^{(0)}} \qquad \text{(I-112)}$$

where $g^{(1)}_{\mu^{(0)}} = g^{(1)}(\theta - \mu^{(0)})$

By introducing the definition $d = 2\gamma n$, so that

$$d = d^{(0)} + \delta d^{(1)} + \delta^2 d^{(2)} + - - - -$$

where $d^{(0)} = 2\gamma n^{(0)}$, $d^{(1)} = 2\gamma n^{(1)}$, $d^{(2)} = 2\gamma n^{(2)}$ etc., Equation (I-112) may be written

$$\bar{\bar{T}}_1^{(0)} \frac{dg^{(1)}}{d\theta} = d^{(0)}\left(g^{(1)}_{\mu^{(0)}} - g^{(1)}\right) + (\gamma+1)\, g^{(1)} \tag{I-113}$$

Solutions of the form $g^{(1)} = A \sin \pi\theta$ (A is an arbitrary constant) satisfy Equation (I-113) provided the following relationships, obtained by equating the coefficients of $\sin \pi\theta$ and $\cos \pi\theta$ on the left and right hand sides of the equation, are satisfied

$$\bar{\bar{T}}_1^{(0)} = \frac{d^{(0)}}{\pi} \sin \pi \mu^{(0)} \tag{I-114}$$

$$d^{(0)} = \frac{\gamma+1}{1 - \cos \pi \mu^{(0)}} \tag{I-115}$$

Equations (I-114) and (I-115) give, respectively, the first order (in M) period on the linear stability limit, and the relationship between n and μ defining the linear stability limit. Both expressions are identical to the ones obtained by Crocco in his linearized treatment.[1] In the present analysis an ordinary differential equation, resulting from a nonlinear analysis, has been linearized in order to obtain the conditions at the stability limit that are given by Equations (I-114) and (I-115). In the analysis of Crocco, on the other hand, the governing partial differential equations themselves, as well as the corresponding boundary conditions, were linearized.

However, identical expressions were obtained in the end.

Before proceeding to a second order analysis, it is convenient to define δ as the amplitude of the first order solution. Then, $g^{(1)} = \sin \pi\theta$.

To second order in δ, Equation (I-111) implies the following equation for $g^{(2)}$

$$\bar{\bar{T}}_1^{(0)} \frac{dg^{(2)}}{d\theta} = d^{(0)}\left(g^{(2)}_{\mu^{(0)}} - g^{(2)}\right) + (\gamma+1) g^{(2)} - \bar{\bar{T}}_1^{(1)} \pi \cos\pi\theta$$
$$+ d^{(1)}\left(\sin\pi\theta \cos\pi\mu^{(0)} - \cos\pi t \sin\pi\mu^{(0)} - \sin\pi \right)$$
$$- \pi\mu^{(1)} d^{(0)}\left(\sin\pi\theta \sin\pi\mu^{(0)} + \cos\pi t \cos\pi\mu^{(0)}\right)$$
$$- \pi \sin\pi t \cos\pi\theta$$

(I-116)

A solution to Equation (I-116) is found by first assuming $g^{(2)} = \alpha \sin 2\pi\theta + \beta \cos 2\pi\theta$. Then, substituting this expression into Equation (I-116), and equating the coefficients of $\sin 2\pi\theta$, $\cos 2\pi\theta$, $\sin\pi\theta$, and $\cos\pi\theta$ on the left and right hand sides of the resulting equation produces the following four equations that must be satisfied

$$\bar{\bar{T}}_1^{(0)} 2\pi\alpha = -d^{(0)}\alpha \sin 2\pi\mu^{(0)} + d^{(0)}\beta\cos 2\pi\mu^{(0)} - d^{(0)}\beta + (\gamma+1)\beta$$

(I-117)

$$-\bar{\bar{T}}_1^{(0)} 2\pi\beta = d^{(0)}\alpha\cos 2\pi\mu^{(0)} - d^{(0)}\alpha + d^{(0)}\beta \sin 2\pi\mu^{(0)} + (\gamma+1)\alpha - \frac{\pi}{2}$$

(I-118)

$$d^{(1)} \sin \pi\mu^{(0)} + \pi\mu^{(1)} d^{(0)} \cos \pi\mu^{(0)} + \bar{\bar{\Pi}}_1^{(1)} \pi = 0 \tag{I-119}$$

$$d^{(1)} \cos \pi\mu^{(0)} - d^{(1)} - \pi\mu^{(1)} d^{(0)} \sin \pi\mu^{(0)} = 0 \tag{I-120}$$

Substituting the expression for $d^{(0)}$ given in Equation (I-115) into Equation (I-120) yields

$$d^{(1)} = \frac{-\mu^{(1)} \pi (\gamma+1) \sin \pi\mu^{(0)}}{(1 - \cos \pi\mu^{(0)})^2} \tag{I-121}$$

Differentiation of Equation (I-115) with respect to $\mu^{(0)}$ gives the following expression for the slope of the linear stability curve

$$\frac{d d}{d \mu} = \frac{-(\gamma+1) \pi \sin \pi\mu}{(1 - \cos \pi\mu)^2} \tag{I-122}$$

Comparison of Equations (I-121) and (I-122) shows that the predicted first order displacements from the linear stability curve on the d, μ plane are along the tangent to that curve. As such they are trivial and, without loss of generality, $d^{(1)}$ and $\mu^{(1)}$ may be taken to be zero. If $d^{(1)}$ and $\mu^{(1)}$ are zero, then also, by Equation (I-119), $\bar{\bar{\Pi}}_1^{(1)} = 0$.

Equations (I-117) and (I-118) together form a system of two linear relations for α and β. This system is easily solved to give α and β in terms of $d^{(1)}$, $\mu^{(0)}$, and $\bar{\bar{\Pi}}_1^{(0)}$.

$$\alpha = \frac{\pi}{2(\gamma+1)}\left(1-\cos\pi\mu^{(0)}\right)\left\{\frac{\cos 2\pi\mu^{(0)} - \cos\pi\mu^{(0)}}{\left[\cos\pi\mu^{(0)} - \cos 2\pi\mu^{(0)}\right]^2 + \left[\sin 2\pi\mu^{(0)} - 2\sin\pi\mu^{(0)}\right]^2}\right\}$$

(I-123)

$$\beta = \frac{\pi}{2(\gamma+1)}\left\{\frac{\left(1-\cos\pi\mu^{(0)}\right)\left(\sin 2\pi\mu^{(0)} - 2\sin\pi\mu^{(0)}\right)}{\left[\cos 2\pi\mu^{(0)} - \cos\pi\mu^{(0)}\right]^2 + \left[\sin 2\pi\mu^{(0)} - 2\sin\pi\mu^{(0)}\right]^2}\right\}$$

(I-124)

To second order, then, second harmonic components are added to the first order, first harmonic solution , while no displacement from the n , μ linear stability curve in the n , μ plane is predicted.

The third order equation for $g^{(3)}$ is

$$\bar{\bar{T}}_1^{(0)}\frac{dg^{(3)}}{d\theta} = d^{(0)}\left(g^{(3)}_{\mu^{(0)}} - g^{(3)}\right) + (\gamma+1)g^{(3)} - \bar{\bar{T}}_1^{(2)}\pi\cos\pi t$$

$$- \pi\left[\frac{3}{2}\alpha\sin 3\pi t + \frac{3}{2}\beta\cos 3\pi t - \frac{\alpha}{2}\sin\pi t - \frac{\beta}{2}\cos\pi t\right]$$

$$+ d^{(2)}\left[\sin\pi t\cos\pi\mu^{(0)} - \cos\pi t\sin\pi\mu^{(0)} - \sin\pi t\right]$$

$$- d^{(0)}\pi\mu^{(2)}\left[\sin\pi t\sin\pi\mu^{(0)} + \cos\pi t\cos\pi\mu^{(0)}\right]$$

(I-125)

The function $g^{(3)}$ is assumed to have the form $g^{(3)} = C \sin 3\pi\theta + D \cos 3\pi\theta$. The coefficients of $\sin 3\pi\theta$ and $\cos 3\pi\theta$ on the left and right hand sides of the equation obtained by substituting this form for $g^{(3)}$ into Equation (I-125) are then equated, and the coefficients of $\sin \pi\theta$ and $\cos \pi\theta$ on the right hand side are set equal to zero. This results in four expressions

$$C\left[3\pi \bar{\bar{T}}_1^{(0)} + \alpha^{(0)} \sin 3\pi\mu^{(0)}\right] + D\left[\alpha^{(0)}(1-\cos 3\pi\mu^{(0)}) - (\gamma+1)\right] + \frac{3\pi\beta}{2} = 0 \tag{I-126}$$

$$C\left[\alpha^{(0)} - \cos 3\pi\mu^{(0)} - (\gamma+1)\right] - D\left[3\pi \bar{\bar{T}}_1^{(0)} - \sin 3\pi\mu^{(0)}\right] + \frac{3\pi\alpha}{2} = 0 \tag{I-127}$$

$$-\pi \bar{\bar{T}}_1^{(2)} + \frac{\pi\beta}{2} - \alpha^{(2)} \sin\pi\mu^{(0)} - \alpha^{(0)}\pi\mu^{(2)} \cos\pi\mu^{(0)} = 0 \tag{I-128}$$

$$\frac{\pi\alpha}{2} + \alpha^{(2)}(\cos\pi\mu^{(0)} - 1) - \pi\alpha^{(0)}\mu^{(2)} \sin\pi\mu^{(0)} = 0 \tag{I-129}$$

The linear stability curve is generated by Equation (I-115), which may be rewritten

$$(1-\cos\pi\mu)2\gamma n - (\gamma+1) \equiv G(n,\mu) = 0 \tag{I-130}$$

Noting that

$$\frac{\partial G}{\partial n} = (1-\cos\pi\mu)2\gamma \quad , \quad \frac{\partial G}{\partial \mu} = 2\gamma n \pi \sin\pi\mu$$

Equation (I-129) may be written

$$n^{(2)}\left(\frac{\partial G}{\partial n}\right)_{G=0} + \mu^{(2)}\left(\frac{\partial G}{\partial \mu}\right)_{G=0} = \frac{\pi\alpha}{2} \tag{I-131}$$

Both sides of (I-131) are now divided by $\sqrt{\left(\frac{\partial G}{\partial n}\right)^2 + \left(\frac{\partial G}{\partial \mu}\right)^2}$. If, further, $\hat{i}$ and $\hat{j}$ are defined respectively as unit vectors along the μ axis and the n axis, then Equation (I-131) becomes

$$\left(n^{(2)}\hat{j} + \mu^{(2)}\hat{i}\right)\cdot\left(\frac{\vec{\nabla}G}{|\vec{\nabla}G|}\right)_{G=0} = \frac{\pi\alpha}{\left(|\vec{\nabla}G|\right)_{G=0}} \tag{I-132}$$

where

$$\vec{\nabla}G = \frac{\partial G}{\partial n}\hat{j} + \frac{\partial G}{\partial \mu}\hat{i}$$

and

$$|\vec{\nabla}G| = \sqrt{\left(\frac{\partial G}{\partial n}\right)^2 + \left(\frac{\partial G}{\partial \mu}\right)^2}$$

$\frac{\vec{\nabla}G}{|\vec{\nabla}G|}$ represents the unit normal to the curve $G = 0$ in the direction of increasing G . From the way in which G has been defined this vector always points inside the curve $G = 0$. The right hand side of Equation (I-132) is therefore the inward normal displacement to the linear stability curve predicted by the third order analysis just carried out. It is only dependent on quantities at a given point on the linear stability curve $(n^{(0)}, \mu^{(0)})$. For convenience, $\mathcal{D}$, the normal displacement divided by δ^2 , is defined

$$\mathcal{D} = \frac{\pi\alpha}{2\left[\left|\vec{\nabla}G\right|\right]_{G=0}} = \frac{\pi\alpha}{4\gamma\sqrt{(1-\cos\pi\mu^{(0)})^2 + \pi^2 n^{2(0)}\sin^2\pi\mu^{(0)}}} \tag{I-133}$$

When $\mathcal{D}$ is positive, an inward normal displacement is indicated, when $\mathcal{D}$ is negative, the displacement is in the outward normal direction. For $n^{(2)}$ and $\mu^{(2)}$ to be on the normal to the curve $G = 0$ at a given point, the following relationship must hold

$$\frac{n^{(2)}}{\mu^{(2)}} = \frac{\left(\frac{\partial G}{\partial n}\right)_{G=0}}{\left(\frac{\partial G}{\partial \mu}\right)_{G=0}} = \frac{1-\cos\pi\mu^{(0)}}{n^{(0)}\pi\sin\pi\mu^{(0)}} \tag{I-134}$$

If Equation (I-134) is combined with Equation (I-128) and (I-129) the following expression, which gives the second order correction to $\overline{\overline{T}}_1^{(0)}$ for the normal displacement given in Equation (I-133), results

$$\overline{\overline{T}}_1^{(2)} = \frac{\beta}{2} - \frac{\alpha}{2}\left[\frac{4\gamma^2(1-\cos\pi\mu^{(0)})\sin\pi\mu^{(0)} + d^{2(0)}\pi^2\sin\pi\mu^{(0)}\cos\pi\mu^{(0)}}{\pi^2 d^{2(0)}\sin^2\pi\mu^{(0)} + 4\gamma^2(1-\cos\pi\mu^{(0)})^2}\right] \tag{I-135}$$

The constants C and D multiplying the third harmonic terms are found, by simultaneously solving Equations (I-126) and (I-127), to be

$$C = \frac{3\pi}{2}\left\{\frac{\alpha\left[d^{(0)}(\cos 3\pi\mu^{(0)} - 1) + (\gamma+1)\right] + \beta\left[\overline{\overline{T}}_1^{(0)}3\pi + d^{(0)}\sin 3\pi\mu^{(0)}\right]}{\left[d^{(0)}(\cos 3\pi\mu^{(0)} - 1) + (\gamma+1)\right]^2 + \left[\overline{\overline{T}}_1^{(0)}3\pi + d^{(0)}\sin 3\pi\mu^{(0)}\right]^2}\right. \tag{I-136}$$

$$D = \frac{C\left(\bar{\bar{\pi}}_1^{(0)} 3\pi + d^{(0)} \sin 3\pi\mu^{(0)}\right) + \frac{3\pi\beta}{2}}{d^{(0)}\left(\cos 3\pi\mu^{(0)} - 1\right) + \gamma + 1}$$

(I-137)

The analysis just carried out to third order in δ predicts that finite amplitude, continuous, periodic solutions can be found, for a given point on the linear stability curve, at a point displaced $\delta^2 \mathcal{D}$ units away from the curve in the inward normal direction. The waveform of the solution is given through the constants α, β, C and D which multiply the second and third harmonic components. The period of the oscillation is the sum of $\bar{\bar{\pi}}_1^{(0)}$ and $\bar{\bar{\pi}}_1^{(2)}$, the latter given in Equation (I-135). Thus, for any point on the neutral stability curve it is possible to find finite amplitude periodic continuous waves in regions very close to the curve, where the condition that δ is a small quantity is satisfied.

Sirignano[2] used a similar technique to find finite amplitude continuous waves near the linear stability limit for the first longitudinal mode of instability. In his analysis, however, it was the governing partial differential equations that were solved rather than a single ordinary differential equation derived from those equations. Consequently, the manipulations he had to perform were about an order of magnitude more voluminous than those required for the analysis just presented. On the other hand, an advantage of solving the partial differential equations directly, rather than first manipulating the partial differential equations into an ordinary

differential equation, is that the stability of the solutions that are obtained can be found directly.[2] Sirignano found that displacements into the region of linear stability led to stable finite amplitude periodic solutions, while displacements into regions of linear stability produced solutions that were unstable.

Since, to obtain the ordinary differential equation that has just been solved it was necessary to impose a periodicity requirement, it is not possible to easily ascertain whether the solutions to that ordinary differential equation (Equation (I-111)) are stable solutions of the governing partial differential equations. Instead, recourse is made to the results of Sirignano, and normal inward displacements from the linear stability curve are assumed to produce stable periodic continuous solutions, while outward displacements are taken to indicate unstable periodic solutions.

Periodic continuous solutions to Equation (I-111) have been found, using the expansion technique just presented, for all values of n and μ of interest along the linear stability curve for fundamental mode longitudinal oscillations. Because of the similarity of form of Equations (I-111) and (I-78), the relationship between solutions of the equation for μ values displaced symmetrically from the line $\mu = 1$ that was found earlier when discontinuous waveforms were being considered, holds as well in the case of continuous waveforms. That is, if a continuous periodic solution to Equation (I-111) is found for some μ that is a rational fraction of 2 less than unity, call it μ_1, then, at the same value for n, a solution for a μ value of $2 - \mu_1$ exists, and is found simply by rotating the solution for $\mu = \mu_1$ 180°. As

before, if the solution for μ_1 is below resonant, then the solution for $2 - \mu_1$ will be above resonant and vice versa. In particular, for $\mu = 1$ continuous solutions must be resonant, that is, their period must be 2 .

Figure 10 shows a plot of $\mathcal{D}$, the normal displacement coefficient, as a function of μ . The curve is obviously symmetric with respect to the line $\mu = 1$, as it must be according to the preceding discussion. $\mathcal{D}$ is positive for $2/3 < \mu < 4/3$, indicating inward normal displacements.* Stable periodic continuous solutions to Equation (I-111) close to the linear stability curve for these values of μ are therefore predicted. On the other hand, when $0 < \mu < 2/3$ and $4/3 < \mu < 2$ $\mathcal{D}$ is negative. For these values of μ the displacements are in the outward normal direction, and the periodic continuous solutions to Equation (I-111) that exist near the stability limit are unstable solutions.

It must be remembered that the solutions that have been found using a power series expansion to represent $g(\theta)$ are valid only as long as δ, the expansion parameter, is small. If Δ is defined as the normal displacement from the linear stability curve at a given point, then, using the third order results (in δ) just obtained, the following relationship between δ , Δ , and $\mathcal{D}$ holds

$$\delta = \sqrt{\frac{\Delta}{\mathcal{D}}} \qquad \text{(I-138)}$$

Extensive numerical integration of Equation (I-111) has shown that for each point on the linear stability curve there is a value of Δ beyond which no continuous periodic solutions can be found. This value of the normal displacement from the linear stability curve at which continuous solutions

* The fact that the sign of $\mathcal{D}$ changes at $\mu^{(0)} = 2/3$ and $\mu^{(0)} = 4/3$ is a consequence of the sign change in α at these points. The changing sign of α can be seen in Equation (I-123).

are no longer possible will be called $\tilde{\Delta}$. $\tilde{\Delta}$ is a very small number when the nonlinear stability limit for discontinuous solutions is inside the linear stability limit. In this region of the n , μ plane σ is also small, but enough larger than $\tilde{\Delta}$ so that δ at $\tilde{\Delta}$ (call it $\tilde{\delta}$) is a small number, say of the order of 0.2 . For example, when $\mu^{(0)} = .8$, $\tilde{\Delta}$ takes its maximum value in the region $.67 < \mu^{(0)} < 1$, $\tilde{\Delta} = .0043$. At the same value of $\mu^{(0)}$, σ has a value of .08 . Using Equation (I-138) this gives a value of $\tilde{\delta}$ of .23 . For $.67 < \mu < 1.33$, then, it is to be expected that the continuous periodic oscillations in the region between $\tilde{\Delta}$ and the linear stability limit are sufficiently well approximated using a power series expansion technique which includes terms through $O(\delta^3)$ in order to solve Equation (I-111). Indeed, the numerical solutions to Equation (I-111) that have been found in this region verify this, as long as Δ is not too close to $\tilde{\Delta}$.

When $\mu < .67$ or $\mu > 1.33$, on the other hand, though $\tilde{\Delta}$ and σ are both still small numbers, the ratio $\frac{\Delta}{\sigma}$ can be O(1) or larger. Consequently, by looking at Equation (I-138) it is seen that $\tilde{\delta}$ also must be of order unity. When δ is this large it is not likely that a power series approximation to $g(\bullet)$ gives a good representation of $g(\bullet)$, especially when only three terms in the power series are used. Therefore, numerical integration of Equation (I-111) must be relied upon to find continuous periodic solutions near $\Delta = \tilde{\Delta}$ in this case. (see Figure 11)

e) The Matching of Discontinuous and Continuous Periodic Solutions

Numerical integration of the ordinary differential equation governing the form of the pressure oscillations, Equation (I-76), has shown that for normal displacements from the linear neutral stability curve on the n , μ

plane less than a certain value, $\tilde{\Delta}$, only continuous solutions can be found, while for normal displacements greater than $\tilde{\Delta}$ only discontinuous solutions can be found. Therefore, at $\Delta = \tilde{\Delta}$ a transition from continuous to discontinuous oscillations is predicted and the normal displacement $\tilde{\Delta}$ can be considered as a kind of matching point for the two families of waveforms. It is of interest to investigate the character of the governing equation, and the solutions to that equation, as $\Delta \longrightarrow \tilde{\Delta}$.

In the investigation of discontinuous solutions presented earlier, the governing equation, Equation (I-76) was rewritten in the form

$$\psi \frac{d\psi}{d\theta} = a\psi + b\psi_{\mu} + (\gamma+1)k \tag{I-103}$$

where $\psi = (g - k)$, and the boundary condition on ψ is $\psi(0) + \psi(2) = 0$. In order for a periodic discontinuous solution to Equation (I-103) to satisfy the boundary condition $\psi(0) + \psi(2) = 0$, it is necessary that ψ pass through zero somewhere in the interval $0 \leq \theta \leq 2$. In other words $g(\theta) = k$ for some value of θ . The value of θ for which this occurs has been shown earlier to be $\theta = \mu$. At this point $\frac{d\psi}{d\theta}$ is infinite. For $|\Delta| > |\tilde{\Delta}|$ it is found that periodic discontinuous solutions to Equation (I-103) can be found with the amplitude of $g(\theta)$ sufficiently large compared with k so that ψ passes through zero at $\theta = \mu$. As $|\Delta|$ decreases toward $|\tilde{\Delta}|$, however, the amplitude of g decreases, while $|k|$ increases, until, at $|\Delta| \longrightarrow |\tilde{\Delta}|$, the amplitude of g tends asymptotically to $|k|$. Also, as $|\Delta| \longrightarrow |\tilde{\Delta}|$, the shock amplitude of the discontinuous oscillations decreases faster and faster relative to the rate of decrease of the peak

to peak amplitude of the oscillation. The indication seems to be that as $|\Delta| \longrightarrow |\tilde{\Delta}|$ the shock amplitude tends to zero. For $|\Delta| < |\tilde{\Delta}|$ ψ is always positive or always negative and it is impossible to satisfy the condition $\psi(0) + \psi(2) = 0$. Thus, it is seen that the point where $\Delta = \tilde{\Delta}$ apparently corresponds to the point where the amplitude of g is equal to $|k|$. It is to be recalled that $k = -\frac{T_1}{M} = -\bar{\bar{T}}_1$. This means that at $\Delta \longrightarrow \tilde{\Delta}$ the amplitude of g tends asymptotically to $|\bar{\bar{T}}_1|$.

For $|\Delta| < |\tilde{\Delta}|$ the continuous periodic oscillations that are found are characterized by the fact that the amplitude of $g(\theta)$ is less than $|\bar{\bar{T}}_1|$. The governing equation for continuous oscillations, Equation (I-111), derived earlier, is

$$(g + \bar{\bar{T}}_1)\frac{dg}{d\theta} = ag + bg_\mu \qquad \text{(I-111)}$$

with the boundary condition $g(0) = g(2)$. It is clear that if the amplitude of $g(\theta)$ is less than $|\bar{\bar{T}}_1|$, it is impossible for $\frac{dg}{d\theta}$ ever to be infinite unless $|\bar{\bar{T}}_1|$ is infinite. This is the case for all periodic continuous solutions with $|\Delta| < |\tilde{\Delta}|$, that is, for all possible continuous solutions. This is in contrast with the result for discontinuous oscillations. There all solutions to the governing equation exhibit an infinite slope at $\theta = \mu$. As $|\Delta|$ increases toward $|\tilde{\Delta}|$ it is found that the continuous periodic oscillations grow in amplitude, while at the same time $|\bar{\bar{T}}_1|$ decreases. Indeed, as $|\Delta| \longrightarrow |\tilde{\Delta}|$ the minimum value of $|g + \bar{\bar{T}}_1|$ in the interval $0 \leq \theta \leq 2$ for the periodic continuous solutions approaches zero. As $|\Delta| \longrightarrow |\tilde{\Delta}|$, then, the possibility that $\frac{dg}{d\theta}$ may become large exists, and also the amplitude of

$g(\theta)$ approaches $|\bar{\bar{T}}_1|$ for continuous periodic solutions. The changing character of the continuous waveforms as $|\Delta| \longrightarrow |\tilde{\Delta}|$ may be seen in Figure 12 . Normal displacements are measured from the point on the linear stability limit where $\mu^{(0)} = .28$. The waveforms are seen to have steep positive peaks followed by a longer, shallower negative peak. The first (positive) peak becomes larger and the slope of the curve preceding the peak steeper as $|\Delta|$ is increased. Finally, when $|\Delta| \longrightarrow |\tilde{\Delta}|$, $g \longrightarrow -\bar{\bar{T}}_1$ for a certain value of θ , and, as is seen in Figure 12 , the slope of g tends to become infinite. It is interesting to note that Sirignano observed a similar blow up of the steeper peak in the pressure wave as displacement from the linear stability curve increased, even though his analysis treated the governing partial differential directly, and no equation similar to Equation (I-111) was involved. This blow up of the solution was taken by him to mean that only shock-type solutions existed at large displacements. Since this "blow up" occurs at $\Delta = \tilde{\Delta}$, and since discontinuous periodic oscillations have been found for $|\Delta| > |\tilde{\Delta}|$, the present work verifies his surmise.

From the preceding discussion it is concluded that at a normal displacement from the linear stability limit of $\tilde{\Delta}$, the amplitudes of either discontinuous or continuous periodic oscillations are asymptotically equal to the corresponding first order correction to the absolute value of the period of oscillation divided by the Mach number.

This has particular significance for periodic solutions along the line $\mu = 1$. When $\mu = 1$ it has been shown that $\bar{\bar{T}}_1 = 0$. This means that $\tilde{\Delta} = \tilde{\delta} = 0$. In other words, no periodic, continuous solu-

tions of finite amplitude are possible when $\mu = 1$. This is in agreement with the numerical and analytical results obtained previously when discontinuous waveforms were considered. There it was concluded that discontinuous solutions exist right up to the linear stability limit. The impossibility of finding finite amplitude continuous solutions when $\mu^{(0)} = 1$ is also reflected in the fact that C and D , the third harmonic coefficients in the representation of g as a power series in δ., become infinite at this point (as may be seen in expression (I-136) and (I-137). The conclusion must be drawn that when $\mu = 1$ the only possible continuous periodic solutions to Equation (I-111) are zero amplitude oscillations on the linear stability limit.

Though, for either discontinuous or continuous oscillations it is true that the amplitude is equal to $|\bar{\bar{T}}_1|$ at $\Delta = \tilde{\Delta}$, it has not yet been shown that $\bar{\bar{T}}_1$ is the same for both continuous and discontinuous solutions. That is, the actual matching of the two families of waveforms at $\Delta = \tilde{\Delta}$ has yet to be shown. In order to indicate the kind of matching that does occur, the amplitude, first order correction to the period, and the waveforms for both continuous and discontinuous periodic oscillations will now be presented as functions of Δ , for normal displacements from two points on the linear stability limit. The two points chosen, $\mu^{(0)} = .80$ and $\mu^{(0)} = .28$, are selected as being representative,respectively,of regions where $\tilde{\Delta}$ is positive (normal displacements into regions of linear instability) and $\tilde{\Delta}$ is negative (normal displacements into regions of linear stability).

Figure 13 shows a plot of the amplitude of $f(\theta)/M$ (equivalently $\frac{p'}{2\gamma M}$ at $x = 0$) as a function of inward normal displacement from the

point on the neutral stability curve where $\mu^{(0)} = .8$. Stable, periodic, continuous solutions can be found only for displacements less than $\Delta = .0042$. The curve of peak to peak amplitude as a function of normal displacement, Δ , is seen to have the parabolic character predicted when the method of power series expansion in δ is used to find continuous solutions to the governing equation, Equation (I-111). For normal displacements somewhat larger than $\Delta = .0042$, discontinuous periodic solutions are readily found and the curve of peak to peak amplitude as a function of Δ can be drawn as in Figure 13 . As one approaches values of close to .0042 , however, the numerical technique presented earlier that is used to integrate Equation (I-78) becomes badly behaved and the number of iterations required to converge on an acceptable discontinuous waveform increases greatly. Indeed, because of this, between $\Delta = .0042$ and $\Delta = .01$ no solutions of this type were generated. The curve of the peak to peak amplitude of discontinuous solutions is therefore arbitrarily continued in a reasonable, if hypothetical, manner in this interval. This continuation is indicated by the dashed lines in Figure 13 . It is seen that the curve of peak to peak amplitude for discontinuous solutions seems to agree with, and blend into the corresponding curve for continuous solutions very well, even if the dashed portion of the curve is not considered. Also shown in Figure 13 is a curve of the shock amplitude of the discontinuous solutions. The end of the curve, for displacments close to $\tilde{\Delta}$, is hypothetical, and has been drawn making use of the fact that at $\Delta = \tilde{\Delta}$ the shock amplitude must be zero.

Figure 14 is a graph of $-T_1/M$ as a function of Δ . Again the curve is composed of two parts; one part for $\Delta < \tilde{\Delta} = .0042$ which

represents T_1 for stable periodic continuous oscillations, and the second part for $\Delta > \tilde{\Delta}$, which represents T_1 for stable discontinuous periodic oscillations. As was the case for the plot of amplitude against Δ , the two portions of the curve seem to blend into one another very well, even though near $\tilde{\Delta}$ there is a gap (represented again by dashed lines) where the numerical method employed could not easily be used to produce the anticipated discontinuous solutions. It is to be noted that, even though the oscillations change from continuous waves to discontinuous waves, the period of oscillation seems to change in a continuous manner through this transition. Moreover, the period of oscillation appears to decrease in a nearly linear fashion as Δ increases.

Figure 15 shows f/M as a function of θ for two values of Δ at $\mu^{(0)} = .80$.* By Equation (I-54), f/M is equivalent to $\frac{p'}{2\gamma M}$ at $x = 0$. Though the waveforms are similar in that they both show infinite slopes when $\theta = \mu$, they both are discontinuous, and for both $\int_0^2 f(\eta)\, d\eta = 0$, it is seen that for the larger value of Δ , f is always decreasing between the discontinuities, while for the smaller value of Δ , f decreases, reaches a minimum and increases again. This seems to indicate that as Δ and the amplitude of the shock increase the waveform tends toward a sawtooth form and away from a form with a more sinusoidal shape. It is also apparent in the figure that the shock amplitude and peak to peak amplitude coincide for the larger Δ , while the peak to peak amplitude exceeds the shock amplitude for the smaller Δ .

Two continuous waveforms at normal displacements of $\Delta = .001$ and $\Delta = .004$ for the same $\mu^{(0)}$ are shown in Figure 16 . The waveforms

* Note that because μ changes with Δ , two different values of are associated with the two different values of Δ .

show the sharp positive peak and the shallower smoother negative peak that were seen to be the case for normal displacements at $\mu^{(0)} = .28$. Here again as Δ increases the positive peak becomes larger and sharper, as may be seen by comparing the two waveforms.

The dependence of the peak to peak amplitude for both continuous and discontinuous periodic solutions to Equation (I-76), on the outward normal displacement, Δ , and the dependence of the shock amplitude for discontinuous solutions on Δ , are shown in Figure 9 for the point on the linear stability limit where $\mu^{(0)} = .28$. The curve of peak to peak amplitude for unstable periodic solutions, (the lower curve) is seen to be composed of two parts representing discontinuous and continuous periodic solutions. The two curves match well where $\Delta = \tilde{\Delta} = .042$, even though numerical integration for discontinuous solutions was not continued right up to $\Delta = \tilde{\Delta}$. The interval where no discontinuous solutions were found is a small fraction of Δ in this case. Here again, dashed lines represent hypothetical continuation of the curve for discontinuous solutions. The curve of shock amplitude as a function of Δ shows that the shock amplitude of unstable discontinuous solutions decreases as $\tilde{\Delta}$ is approached. The dashed line continuation of this curve is drawn subject to the condition that the shock amplitude at $\Delta = \tilde{\Delta}$ is zero.

Figure 17 shows $-T_1/M$ as a function of Δ for the same point on the linear neutral stability curve, $\mu^{(0)} = .28$. As was the case for $\mu^{(0)} = .80$, the two portions of the curve representing continuous and discontinuous solutions match well. Here, however, the behavior of T_1 is very nonlinear as $|\Delta|$ increases. For the case of stable

discontinuous solutions (the upper curve) it can be seen by comparing Figures 9 and 17 that as the amplitude increases the oscillations become more off-resonant. This was also found to be the case for the stable solutions at $\mu^{(0)} = .80$. The unstable periodic solutions, on the other hand, become less off resonant as $|\Delta|$ is increased, independent of whether the amplitude is increasing or decreasing.

Figure 18 shows two discontinuous waveforms predicted at a normal displacement of -.11 from the point on the linear neutral stability curve $\mu^{(0)} = .28$. Two waveforms occur because both a stable discontinuous periodic solution and an unstable discontinuous solution are found for this value of Δ . The larger amplitude waveform is the stable solution. It is seen that the shock amplitude is a larger fraction of the peak to peak amplitude for the stable solution. The decay in f following the shock is quite different for the two waveforms. The unstable solution behaves in an almost sinusoidal manner after the shock. In fact the amplitude of this "secondary oscillation" is almost 55% of the peak to peak amplitude of the total waveform. The decay in pressure after the shock for the stable solution is less wild; the "secondary oscillation" represents only about 14% of the overall peak to peak amplitude. It should be noted here that waveforms for unstable oscillations have very little practical meaning since, due to their instability, they cannot exist for any finite period of time and could never be observed.

Continuous waveforms for normal displacements at $\mu^{(0)} = .28$ have been discussed earlier. They appear in Figure 12 . Here again the comment with respect to the meaning of unstable waveforms made above applies.

All the waveforms that have been presented so far are representative

of pressure oscillations at the injector face, $x = 0$. (Note that because the expression for p' is the same at $x = 0$, and $x = 1$, the waveforms at the injector and nozzle are identical.) It is of some interest to see the pressure waveform at an intermediate value of x , and also to see the pressure wave shape in space at a fixed value of time. These waveforms are presented in Figures 19 and 20 respectively.

f) Relaxation of the Restriction of μ to Rational Fractions of Two for Discontinuous Periodic Solutions

All discontinuous periodic solutions to Equation (I-78) that have been presented so far have been obtained under the restriction that μ must be a rational fraction of two. It will be recalled that this restriction allowed a simple relationship between solutions to Equation (I-78) for μ values symmetrically displaced from $\mu = 1$ to be derived. Also, when μ is a rational fraction of two, numerical integration of Equation (I-78) was somewhat easier. It is not true, however, that the restriction of μ to rational values of two is applied merely for the sake of simplicity and convenience. It can be shown, in fact, that there is no basic characteristic in the governing equation, Equation (I-78), which restricts μ to rational fractions of two when $f(\theta)$ is discontinuous. Equation (I-78) is written

$$(g-k)\frac{dg}{d\theta} = ag + bg_{\mu} \qquad \text{(I-78)}$$

where

$$g = \frac{(\gamma+1)f}{M}$$

If g is discontinuous at some θ, for convenience say $\theta = 0$, it has been shown that, at $\theta = \mu$, $(g - k)$ must pass through zero and $\frac{dg}{d\theta}$ must be infinite if periodic solutions are to be found. Even when μ is irrational one can integrate Equation (I-78) numerically, subject to this restriction and the boundary condition $g(0) + g(2) = 2k$, and find solutions that are apparently periodic in two, as required. However, the function $f(\theta)$ thus obtained turns out to be very peculiar indeed. This can be seen through the argument which follows.

Since $\frac{dg}{d\theta}$ is infinite at $\theta = \mu$, then at $\theta = 2\mu$, $\frac{d^2g}{d\theta^2}$ is infinite, at $\theta = 3\mu$, $\frac{d^3g}{d\theta^2}$ is infinite, and, in general, at $\theta = j\mu$ (j an integer) $\frac{d^jg}{d\theta^j}$ is infinite. The function $g(\theta)$ (and therefore $f(\theta)$) is not analytic at any of these points. If μ is a rational fraction of 2, say $\frac{2p}{q}$, p, q integers, then if the region $0 \leq \theta \leq 2$ is divided into q sub intervals; $0 < \theta < \frac{2}{q}$, $\frac{2}{q} < \theta < \frac{4}{q}$, - - - - $\frac{2(i-1)}{q} < \theta < \frac{2i}{q}$, i an integer less than or equal to q, the function $g(\theta)$ will be non analytic only at the q points separating the intervals, (i.e. at $\theta = 0$, $\theta = \frac{2}{q}$, $\theta = \frac{4}{q}$ - - - - $\theta = 2$) and will be a well behaved analytic function over each of the open sub intervals. Moreover, these non analytic points are repeated cyclically. That is, if, at $\theta = i\mu$, the jth order derivative of g is infinite, then also at $\theta = i\mu + 2$ the jth order derivative will be infinite. For example, when $\mu = \frac{4}{5}$, then at $\theta = \frac{2}{5}$ the third derivative of g is infinite, at $\theta = \frac{4}{5}$ the first derivative is infinite, at $\theta = \frac{6}{5}$ the fourth derivative is infinite, at $\theta = \frac{8}{5}$ the second derivative is infinite, and at $\theta = 0$ and $\theta = 2$ the function is discontinuous. If one examines the following cycle, $2 \leq \theta \leq 4$, he finds

that the infinite second derivative at $\theta = \frac{8}{5}$ causes an infinite 3rd derivative at $\theta = 2\frac{2}{5}$, that the discontinuity in the function causes the first derivative to be infinite at $\theta = 2\frac{4}{5}$, that the infinite third derivative at $\theta = 2\frac{2}{5}$, causes an infinite fourth derivative at $\theta = 2\frac{6}{5}$ and that the infinite first derivative at $\theta = 2\frac{4}{5}$ cases at infinite second derivative at $\theta = 2\frac{8}{5}$. It is clear that the infinity in the 3rd derivative of $g(\theta)$ at $\theta = \frac{2}{5}$, is also present at $\theta = 2 + \frac{2}{5}$; and that the same is true for all the non analytic points, that is, they are all periodic in 2 .

When μ is irrational, on the other hand, the number of points at which $g(\theta)$ is non analytic in the interval $0 \leq \theta \leq 2$ becomes infinite because the original discontinuity is propagated in intervals that are irrational fractions of the total interval. In other words, the effects of the original discontinuity will never be felt exactly at the θ value at which a later discontinuity occurs. In this case, though g and its first derivative appear to be continuous and periodic, g is non analytic at an infinite number of points in a given cycle, because higher derivatives are infinite and, moreover, the character of these points where g is non analytic varies from cycle to cycle (note that as θ becomes very large the difference between succeeding cycles resides only in the very high order derivatives of g) . In the limit as $\theta \longrightarrow \infty$, however, it is clear that a limit cycle with period 2 must exist.*

Since $\mu = \frac{2}{\pi}\tau$, the statement that μ must be a rational fraction of two in order for periodic discontinuous solutions to exist is equivalent to the statement that μ must be a rational fraction of the

---

* This follows from the fact that solutions for f that are continuous in f and its first derivative can in principle be found using the numerical methods described previously.

period. τ is physically related to injector design, propellants used, etc., and there seems to be no reason why it should be restricted to values such that μ is a rational fraction of 2 . Thus, if μ is restricted to rational values, one is led to the conclusion that for some values of μ that are physically realistic, no really periodic discontinuous solutions exist, even at points on the n , μ plane that are in a region of nonlinear instability as defined earlier. This does not seem reasonable on a physical basis, and thus gives credence to the idea that periodic solutions exist also when μ is irrational.

Moreover, any irrational μ can be approximated with arbitrary accuracy by a μ that is a rational fraction of 2 . It is unreasonable to expect that periodic solutions to the governing equation exist for values of μ that are arbitrarily close to irrational values, but not at the irrational values themselves. Such behavior would, indeed, produce regions on the n , μ plane such that along a line of constant n , there would be, at the same time, an infinite number of points where discontinuous periodic oscillations were possible and an infinite number of points where none could occur. This is in contradiction to the natural expectation that a continuous change in the combustion parameters should produce a continuous change in the type of pressure oscillation possible. Consequently, one is once again led to the conclusion that periodic solutions should exist for irrational μ as well as μ that are rational and that the restriction of μ to rational fractions of 2 is merely a convenient artifice useful in the symmetry proof presented earlier.

In summary, there seems to be no reason why periodic solutions should be found only when μ is a rational fraction of 2, while there are strong

mathematical and physical reasons for expecting periodic solutions also to be found for irrational μ . Consequently it is to be expected that periodic solutions do exist when μ is irrational and that their form can be approximated with arbitrary accuracy by integrating the governing equation at a rational μ value arbitrarily close to the irrational μ in question. Because of this it is possible to speak of regions of nonlinear instability in the n , μ plane with no restrictions on μ . Also the curves of amplitude against normal displacement, and first order period against normal displacement, can be interpreted as truly continuous curves and not as curves with an infinite number of "holes" in them occurring where μ takes irrational values.

g) Stability Limits in the n , τ Plane

All results that have been presented so far are given in terms of n and μ . It is of interest to see how these results might look expressed, instead, in terms of n and τ .

μ , the stretched time-lag, enters the analysis just presented in the second order boundary condition at $x = 0$. It appears in the term $M\gamma n\, f(\theta - \mu)$. Since f is O(M) and M is O(M) , the term as a whole is $O(M^2)$. On the other hand $\mu = \frac{2}{T}\tau = (1 - \frac{T_1}{2} + - - - -)\tau$, where T_1 is O(M). At first glance then, the difference between $nM\gamma f(\theta - \mu)$ and $\gamma nM\, f(\theta - \tau)$ seems to be of third order. This is indeed the case as long as $f(\theta)$ is continuous. When $f(\theta)$ exhibits a discontinuity or shock of O(M) , however, then $nM\gamma f(\theta - \mu)$ and $nM\gamma f(\theta - \tau)$ can differ by an amount of $O(M^2)$ in the neighborhood of the discontinuity. Therefore, to second order in M , μ and τ are not simply interchangeable and must be related through the expression

$\tau = \frac{\Gamma}{2}\mu$, at least when discontinuous waveforms are possible.

Because Γ_1 may be represented as $\Gamma_1 = M\bar{\bar{\Gamma}}_1(n, \mu)$, where $\bar{\bar{\Gamma}}_1$ depends only on n and μ (and on whether one is considering stable or unstable oscillations, when both are present), Γ_1 will increase as M increases and will be different for every M at a given n and μ. Since $\tau = (1 + \frac{\Gamma_1}{2})\mu$ to the order under consideration, it is also apparent that τ is proportional to the Mach number and is different for every Mach number at a given n and μ. Thus, from a single curve in the n, μ plane, an infinite number of curves may be drawn on the n, τ plane, depending on the value of M chosen.

In order to give an idea of how the stability limits change as one transforms from the n, μ plane to the n, τ plane, a Mach number of 0.3 has been selected for the transformation. A Mach number of 0.3 is relatively large and should emphasize the changes in shape that occur. Figure 21 shows the nonlinear stability limit for discontinuous oscillations and the linear stability limit on the n, τ plane for this value of the Mach number. The curves that appear in Figure 21 are the transformed form of the curves in Figure 2. It can be seen that the stability limits in the n, τ plane are no longer symmetric with respect to the line $\tau = \mu = 1$. The asymmetry is evidenced in the greater degree of spreading of the stability limits for $\tau > 1$. Comparison of Figure 21 with Figure 2 shows that in general the stability limits are wider in n, τ space than in n, μ space. It is seen that the linear stability limit as well as the nonlinear stability limit is distorted by the transformation. This is because, even along the linear neutral stability curve, Γ_1 is nonzero except at $\mu = 1$.

The difference between the stability limits on the n , τ plane and on the n , μ plane is not too large even for $M = 0.3$, the maximum difference being about 20% for $n < \approx 3.5$. As M gets smaller, the difference between the curves on the n , τ plane and the n , μ plane also becomes smaller, and, in the limit as $M \longrightarrow 0$ they must be identical.

CHAPTER II
DISTRIBUTED COMBUSTION

A. Presentation of the Model and the Governing Equations

In this chapter the concentrated combustion assumption will be relaxed and an analysis will be presented that allows the consideration of more general axial distributions of combustion. The types of combustion distribution to be considered will be restricted to those that are sufficiently spread along the axial dimension of the combustion chamber so that the derivative of the mean gas velocity in steady operation is of the same order of magnitude as the mean gas velocity. Most of the other assumptions used in the first chapter will also be employed here. These are:

1) The short nozzle condition is employed. That is, the Mach number at the entrance of the nozzle is taken to be constant.

2) The chamber is assumed to have a constant cross sectional area.

3) The flow is taken to be one dimensional.

4) The chamber gas is assumed to be homocompositional and calorically perfect.

The homoentropic assumption used in the first chapter is relaxed here. However, though entropy variations will be taken into account, entropy waves excited by such mechanisms as mixture ratio variations will not be considered.

Using the above approximations and assumptions, partial differential equations describing the flow in the chamber may be set down for all regions of the chamber not containing discontinuities. These equations represent the physical requirements that mass, momentum and energy be conserved.

Conservation of Mass

$$\frac{\partial \rho^*}{\partial t^*} + \frac{\partial(\rho^* u^*)}{\partial x^*} = \frac{\partial w^*}{\partial x^*} = -\frac{\partial \rho_\ell^*}{\partial t^*} - \frac{\partial \rho_\ell^* u_\ell^*}{\partial x^*} \tag{II-1}$$

where $w^* \equiv \int_0^x \dot{W}^*_{(x',t)} dx'$, $\dot{W}^*$ is the rate of production of gas per unit volume, u_ℓ^* represents the velocity of the liquid propellant elements and ρ_ℓ^* is the mass of liquid droplets per unit volume of gas.

Conservation of Momentum

$$\rho^* \frac{\partial u^*}{\partial t^*} + \rho^* u^* \frac{\partial u^*}{\partial x^*} = -\frac{\partial p^*}{\partial x^*} + \frac{\partial w^*}{\partial x^*}(u_\ell^* - u^*) - \rho_\ell^* \frac{\partial u_\ell^*}{\partial t^*} \tag{II-2}$$

where $\frac{\partial u_\ell^*}{\partial t^*} = \frac{\partial u_\ell^*}{\partial t^*} + u_\ell^* \frac{\partial u_\ell^*}{\partial x^*}$ represents the rate of acceleration a liquid propellant element experiences.

Conservation of Energy

$$\frac{\partial}{\partial t^*}(\rho^* h_s^* - p^*) + \frac{\partial}{\partial x^*}(\rho^* u^* h_s^*) = h_{\ell s}^* \frac{\partial w^*}{\partial x^*} - \rho_\ell^* \frac{\partial h_{\ell s}^*}{\partial t^*} \tag{II-3}$$

where $h_{\ell s}^* = h_\ell^* + \frac{1}{2} u^{*2}$ represents the specific total energy of the liquid propellant, including chemical energy, and $\frac{\partial h_{\ell s}^*}{\partial t^*}$ represents the rate of change of this energy in a frame of reference moving with the liquid droplets.

Two more assumptions will now be introduced in order to uncouple the equations of the gaseous motion from those of the liquid propellant

elements. The first of these, previously used by Crocco and Cheng[1] in their linear analysis of distributed combustion, assumes that $h^*_{\ell s}$ is a constant. The second assumption requires that u^*_ℓ be constant. In order for these assumptions to be valid, the extent of droplet heat up must be small and the drag forces on the droplet should also be small. Since both droplet heat up and drag effects on the droplets remove energy from the gasdynamic field, both effects are stabilizing. Moreover, Crocco[5] has shown that these effects are small compared with the effects of combustion and nozzle admittance. Consequently, by ignoring these effects the stability situation investigated is slightly worse than might be expected if they were included and, therefore, the results of the present analysis must be considered as being slightly pessimistic.

Two additional equations are still required in order to have Equations (II-1), (II-2), (II-3) represent a system of 3 equations in the dependent variables ρ, u and p. The first of these equations is simply the equation of state for a perfect gas

$$p^* = \rho^* R^* T^* \tag{II-4}$$

The second equation expresses $\frac{\partial w^*}{\partial x^*}$ in terms of the pressure p^*, by using the time-lag postulate. This equation will be introduced later.

Using the equation of state and the fact that the gas considered is calorically perfect, Equation (II-3) may be rewritten in a form in which only p^*, u^*, ρ^*, $h^*_{\ell s}$ and $\frac{\partial w^*}{\partial x^*}$ appear

$$\frac{1}{\gamma-1}\frac{\partial p^*}{\partial t^*} + \frac{\partial}{\partial t^*}\left(\tfrac{1}{2}\rho^* u^{*2}\right) + \frac{\gamma}{\gamma-1}\frac{\partial}{\partial x^*}(p^* u^*) + \frac{\partial}{\partial x^*}\left(\tfrac{1}{2}\rho^* u^{*3}\right) = h^*_{\ell s}\frac{\partial w^*}{\partial x^*} \tag{II-5}$$

All variables will now be made non-dimensional by using the following definitions

$$p = \frac{p^*}{p_R^*} \qquad \rho = \frac{\rho^*}{\rho_R^*} \qquad h = \frac{h^*}{h_R^*} \qquad u = \frac{u^*}{a_R^*}$$

$$t = t^* \cdot \frac{a_R^*}{L^*} \qquad x = \frac{x^*}{L^*} \qquad w = \frac{w^*}{\rho_R^* a_R^*} \qquad u_\ell = \frac{u_\ell^*}{a_R^*}$$

The subscript R indicates conditions at $x^* = 0$ under steady operation, and L^* is the length of the chamber.

Using these new variables Equations (II-1), (II-2) and (II-5) become

$$\frac{\partial \rho}{\partial t} + \frac{\partial(\rho u)}{\partial x} = \frac{\partial w}{\partial x} \tag{II-6}$$

$$\rho \frac{\partial u}{\partial t} + \rho u \frac{\partial u}{\partial x} = -\frac{1}{\gamma} \frac{\partial p}{\partial x} + \frac{\partial w}{\partial x}(u_\ell - u) \tag{II-7}$$

$$\frac{1}{\gamma} \frac{\partial p}{\partial t} + \frac{\gamma-1}{2} \frac{\partial(\rho u^2)}{\partial t} + \frac{\partial}{\partial x}(pu) + \frac{\gamma-1}{2} \frac{\partial(\rho u^3)}{\partial x} = h_{\ell s} \frac{\partial w}{\partial x} \tag{II-8}$$

B. Solution of the Governing Partial Differential Equations

The dependent variables p , ρ , u , and w are separated into steady-state parts, indicated by superposed bars, and time variant parts indicated by primes.

Thus

$$p = \bar{p} + p', \quad \rho = \bar{\rho} + \rho', \quad u = \bar{u} + u', \quad w = \bar{w} + w' \tag{II-9}$$

The primed quantities are then represented by power series expansions in terms of the Mach number at the entrance to the nozzle, M_E . Thus

$$u' = u_1 + u_2 + u_3 + - - - -$$

$$p' = p_1 + p_2 + p_3 + - - - - \qquad \text{(II-10)}$$

$$w' = w_1 + w_2 + w_3 + - - - -$$

$$\rho' = \rho_1 + \rho_2 + \rho_3 \quad - - - -$$

where $u_1 = O(M_E)$, $u_2 = O(M_E^2)$, etc.*

The expansion parameter used here is similar to the one used in the study of concentrated combustion in that both are proportional to the mean level of combustion in steady-state operation. In the present analysis, however, the requirement that the unsteady parts of the dependent variables must vanish along the linear stability limit in the n , τ plane will not be carried explicitly in the expansion parameter. That is, no function like $H(n, \tau)$ multiplies the Mach number as was the case for concentrated combustion. Of course, it makes no difference in the final result whether such a function is included or not.

If the time derivatives are suppressed in Equations (II-6), (II-7) and (II-8) the following steady-state equations result

$$\frac{d(\bar{\rho}\bar{u})}{dx} = \frac{d\bar{w}}{dx} \qquad \text{(II-11)}$$

$$\bar{\rho}\bar{u}\frac{d\bar{u}}{dx} = -\frac{d\bar{p}}{dx} + (u_g - \bar{u})\frac{d\bar{w}}{dx} \qquad \text{(II-12)}$$

* It is also assumed that the nth order term in any power series expansion has derivatives with respect to both x and Θ that are of nth order. This can be shown to be valid as long as $\frac{d\bar{u}}{dx} = O(M_E)$.

$$\frac{d(\bar{\rho}\bar{u})}{dx} + \frac{\gamma-1}{2}\frac{d(\bar{\rho}\bar{u}^3)}{dx} = h_{\ell s}\frac{d\bar{w}}{dx} \qquad \text{(II-13)}$$

The last equation may be written in the equivalent form

$$\bar{\rho}\,\bar{u}\,\frac{d\bar{h}_s}{dx} = (h_{\ell s} - \bar{h}_s)\frac{d\bar{w}}{dx} \qquad \text{(II-14)}$$

where the fact that $\bar{h}_s = \frac{\bar{p}}{\bar{\rho}} + \frac{\gamma - 1}{2}\bar{u}^2$ has been used. A solution to Equation (II-14) is $\bar{h}_s = h_{\ell s} = 1$. If this relationship is substituted into Equation (II-13) and the resulting equation solved simultaneously along with Equations (II-11) and (II-12), then the following relationships are found

$$\bar{p} = \bar{\rho} = \bar{T} = 1 + O(M_E^2) \qquad \text{(II-15)}$$

$$\bar{w} = \bar{u} + O(M_E^3) \qquad \text{(II-16)}$$

where it has been noted that $\bar{u} \leq M \leq M_E$. Also, u_ℓ has been taken to be of the same order of magnitude as M_E . Essentially, this means that the injection velocity must be smaller than or equal to the nozzle entrance velocity. For rocket engine designs of interest, this is usually the case. In any event as $M_E \longrightarrow 0$, u_ℓ must also $\longrightarrow 0$ if a true steady-state situation is to occur.

Equation (I-16) indicates that giving the steady-state velocity profile is equivalent, at least to $O(M_E^2)$, to giving the steady-state

mass source distribution in the chamber. Also, since $w(x)$ represents the total rate of mass introduction in the chamber between $x = 0$ and x, then M_E represents the total rate of mass production in the entire chamber in the steady-state. Moreover, since $h_s = 1$, M_E also represents the total rate of energy added to the chamber by combustion in the steady-state. The condition requiring that the combustion be sufficiently distributed axially can now be stated simply as $\frac{d\bar{u}}{dx} = O(\bar{u}) = O(M_E)$.

Before proceeding to solve the system of equations, Equations (II-6), (II-7), (II-8), t, the time coordinate will be stretched following the procedure used in the first chapter. The independent variable Θ is therefore introduced, where

$$t = \frac{\tau}{2}\Theta, \qquad = (1 + \tau_1 + \tau_2 + - - - -),$$

and τ_1 is $O(M_E)$, τ_2 is $O(M_E^2)$, etc. This transformation will cause periodic solutions of the equations for p, u and ρ to have periods of 2 to all orders of approximation, as long as a solution to the problem exists that is periodic in t with a period τ differing from 2 by an amount of $O(M_E)$.

The term $\frac{\partial w}{\partial x}$ appears in all three of the governing partial differential equations for ρ, u, and p. Consequently, it must be expressed in terms of these quantities before solution of the equations for these three quantities is possible. This is accomplished through the use of the Crocco time-lag postulate. The expression for the burning rate in the case of distributed combustion, using the time-lag model, was originally derived by Crocco and Cheng.[1] This development resulted in the following relationship for w'

$$w' = - \int_0^x \frac{d\tau}{dt} \frac{\partial \bar{w}}{\partial x'} dx' + O(M_E^3) \qquad \text{(II-17)}$$

where τ is the sensitive time-lag. To first order $\frac{d\tau}{dt}$ may be related to the pressure as it was in the first chapter. Thus

$$\frac{d\tau}{dt} = - n(p_1(t) - p_1(t - \tau)) + O(M_E^2)$$

In the above expression time is measured following a given liquid propellant element. In a coordinate system fixed with respect to the combustion chamber the equation can be written

$$\frac{d\tau}{dt} = -n \left(p_1(t,x) - p_1(t-\tau, x - u_\ell \tau) \right) \qquad \text{(II-18)}$$

where the fact that u_ℓ is a constant has been used and $u_\ell \tau$ is the "space lag", in other words, the distance before the station of interest at which the propellant element first becomes sensitive to the chamber conditions. Using Equation (II-18) to substitute for $\frac{d\tau}{dt}$ in Equation (II-17), the following expression for w' results

$$w' = n \int_0^x \left[p_1(t,x') - p_1(t-\tau, x' - u_\ell \tau) \right] \frac{d\bar{u}}{dx'} dx' + O(M_E^3)$$

where it has been noted that $\frac{d\bar{w}}{dx} = \frac{d\bar{u}}{dx} + O(M_E^3)$. Since u_ℓ is $O(M_E)$, then, if τ is restricted to values of order unity, it is clear that

$$\int_0^x p_1(t-\tau, x' - u_\ell \tau) \frac{d\bar{u}}{dx'} dx' = \int_0^x p_1(t-\tau, x') \frac{d\bar{u}}{dx'} dx' + O(M_E^3)$$

Consequently

$$w' = n \int_0^x \left[p_1(t,x) - p_1(t-\tau, x) \right] \frac{d\bar{u}}{dx'} dx' \quad + O(M_E^3)$$

(II-18)

Differentiation of Equation (II-19) with respect to x yields

$$\frac{\partial w'}{\partial x} = n \frac{d\bar{u}}{dx} \left[p_1(t,x) - p_1(t-\tau, x) \right] + O(M_E^3)$$

(II-19)

If the stretched time-lag, μ , is now introduced, where $\mu = \frac{2}{T} \tau$, then Equation (II-19) becomes the following expression in θ , x coordinates

$$\frac{\partial w'}{\partial x'} = n \frac{d\bar{u}}{dx} \left[p_1(\theta, x) - p_1(\theta - \mu, x) \right] + O(M_E^3)$$

(II-20)

Note that this expression is $O(M_E^2)$, so that $w_1 = 0$.

It will prove useful shortly to have an equation which governs explicitly the behavior of the entropy of the gas in the chamber. If $s \equiv \frac{s^*}{c_p^*}$, then, by the combination of the first and second laws of thermodynamics

$$T ds = dh - \frac{\gamma - 1}{\gamma} \frac{dp}{\rho}$$

(II-21)

This expression may be combined with the equations for conservation of mass, momentum, and energy, Equations (II-6), (II-7) and (II-8) in order to yield an entropy equation

$$\rho T \frac{\partial s}{\partial t} = \frac{\partial w}{\partial x} \left(h_{ls} - h + \frac{\gamma - 1}{2} u^2 - (\gamma - 1) u u_l \right)$$

(II-22)

In the steady-state the above equation can be written

$$\frac{d\bar{s}}{dx} = (\gamma-1)(\bar{u}-u_\ell)\frac{d\bar{u}}{dx} \tag{II-23}$$

If, for convenience, $\bar{s}$ $(x = 0)$ is taken to be zero, then $\bar{s} = (\gamma - 1)(\frac{\bar{u}^2}{2} - u_\ell \bar{u}) = O(M_E^2)$. Since $(\gamma - 1)$ is a small number, the steady-state entropy variation is seen to be very small indeed.

Equations (II-7) and (II-8) are now written down, correct to first order in M_E, as

$$\frac{\partial u_1}{\partial \theta} = -\frac{1}{\gamma}\frac{\partial p_1}{\partial x} \tag{II-24}$$

$$\frac{1}{\gamma}\frac{\partial p_1}{\partial \theta} + \frac{\partial u_1}{\partial x} = 0 \tag{II-25}$$

where the corresponding steady-state equations have been subtracted off. If the second equation is added and then subtracted from the first equation the following pair of equations is obtained

$$\frac{\partial}{\partial \theta}\left(u_1 + \frac{p_1}{\gamma}\right) + \frac{\partial}{\partial x}\left(u_1 + \frac{p_1}{\gamma}\right) = 0 \tag{II-26}$$

$$\frac{\partial}{\partial \theta}\left(u_1 - \frac{p_1}{\gamma}\right) - \frac{\partial}{\partial x}\left(u_1 - \frac{p_1}{\gamma}\right) = 0 \tag{II-27}$$

These equations would correspond exactly to the first order equations presented in Chapter I if the entropy were constant.

Equations (II-26) and (II-27) have the simple solutions

$$u_1 + \frac{p_1}{\gamma} = 2f_r(\theta - x) \tag{II-28}$$

$$u_1 - \frac{p_1}{\gamma} = 2 f_S (\theta + x) \tag{II-29}$$

Since Equations (II-26) and (II-27) are valid only in regions free from shocks, it is in principle necessary to separate the chamber into two shock free regions as was done in the case of concentrated combustion, and to consider solutions in the two regions separately. The separation of the chamber into two regions, regions I and II, is illustrated in Figure I. In region I

$$\left(u_1 + \frac{p_1}{\gamma}\right)_I = 2 f_{rI} (\theta - x) \tag{II-28A}$$

$$\left(u_1 - \frac{p_1}{\gamma}\right)_I = 2 f_{sI} (\theta + x) \tag{II-29A}$$

while in region II

$$\left(u_1 + \frac{p_1}{\gamma}\right)_{II} = 2 f_{rII} (\theta - x) \tag{II-28B}$$

$$\left(u_1 - \frac{p_1}{\gamma}\right)_{II} = 2 f_{sII} (\theta + x) \tag{II-29B}$$

The functions in the different regions can be related by using the fact that $u_1 + \frac{2}{\gamma - 1} a_1$ is continuous through a shock moving toward the injector, and that $u_1 - \frac{2}{\gamma - 1} a_1$ is continuous through a shock moving toward the nozzle. In order to make use of this, $u_1 + \frac{p_1}{\gamma}$ must be related to $u_1 + \frac{2}{\gamma - 1} a_1$, and $u_1 - \frac{p_1}{\gamma}$ must be related to $u_1 - \frac{2}{\gamma - 1} a_1$.

Integration of the equation

$$ds = \frac{dT}{T} - \frac{\gamma - 1}{\gamma} \frac{dp}{p} \tag{II-30}$$

representing a combination of the first and second laws of thermodynamics, yields the following relationship between p, s, and a

$$p = a^{\frac{2\gamma}{\gamma-1}} e^{\frac{-\gamma}{\gamma-1} s} \tag{II-31}$$

where it is to be noted that $s = 0$ at $x = 0$ under steady-state conditions. To first order in M_E, Equation (II-31) may be written

$$\frac{p_1}{\gamma} = \frac{2}{\gamma-1} a_1 - \frac{1}{\gamma-1} s_1 \tag{II-32}$$

where it is assumed that s is expandable in a power series in M_E, so that $s = (s_1 + s_2 + - - - -)$ and s_1 is $O(M_E)$, s_2 is $O(M_E^2)$, etc. The quantity $u_1 + \frac{2}{\gamma - 1} a_1$ can then be expressed as $u_1 + \frac{p_1}{\gamma} + \frac{s_1}{\gamma - 1}$. Since $u_1 + \frac{2}{\gamma - 1} a_1$ is continuous through a shock moving toward the injector, it must be true that $u_1 + \frac{p_1}{\gamma} + \frac{s_1}{\gamma - 1}$ is also continuous across the shock. Because of the fact that the entropy jump across a shock with amplitude of $O(M_E)$ is of $O(M_E^3)$, the continuity of $u_1 + \frac{p_1}{\gamma} + \frac{s_1}{\gamma - 1}$ through a left moving shock, that is, a shock moving toward the injector, implies that $u_1 + \frac{p_1}{\gamma}$ is also continuous through the shock. This means that $f_r(\theta - x)$ is the same on both sides of a left moving shock and, in fact, that any distinction between $f_{rI}(\theta - \lambda)$ and $f_{rII}(\theta - x)$ is unnecessary. Similar reasoning, applied to the case of right moving shocks and the quantity $u_1 - \frac{2}{\gamma - 1} a_1 = u_1 - \frac{p_1}{\gamma} - \frac{s_1}{\gamma - 1}$, yields the conclusions that $f_s(\theta + x)$ is continuous across right moving shocks and that it is unnecessary to distinquish between $f_s(\theta + x)$ in regions I and II. Consequently, Equations (II-28) and (II-29) are correct as they stand for all regions of the combustion chamber.

Two boundary conditions which all solutions to the governing

partial differential equations must satisfy are the solid wall condition at $x = 0$, $u(x = 0) = 0$; and the short nozzle boundary condition at $x = 1$, $(\frac{u}{a})_{x=1} = M_E$. To first order in M_E these reduce to solid wall conditions at both ends of the chamber. That is, $u_1(x = 0) = u_1(x = 1) = 0$. Applying these boundary conditions to Equations (II-28) and (II-29) yields the following solutions for u_1 and p_1 in terms of an arbitrary function, f

$$u_1 + \frac{p_1}{\gamma} = 2f(\theta - x) \tag{II-33}$$

$$u_1 - \frac{p_1}{\gamma} = -2f(\theta + x) \tag{II-34}$$

where $f \equiv f_r = -f_s$ and $f(\theta) = f(\theta + 2)$.

As was the case in the study of concentrated combustion, it is necessary to perform a second order analysis in order to find the function $f(\theta)$. To second order in M_E , Equations (II-7) and (II-8) become

$$\frac{\partial u_2}{\partial \theta} + \frac{1}{\gamma}\frac{\partial p_2}{\partial x} = \frac{\gamma_1}{2}\frac{\partial u_1}{\partial \theta} - 2u_1\frac{\partial u_1}{\partial x} - 2u_1\frac{d\bar{u}}{dx} - \rho_1\frac{\partial u_1}{\partial t} \tag{II-35}$$

$$\frac{1}{\gamma}\frac{\partial p_2}{\partial \theta} + \frac{\partial u_2}{\partial x} = \frac{\gamma_1}{2\gamma}\frac{\partial p_1}{\partial \theta} - (\gamma - 1)\bar{u}\frac{\partial u_1}{\partial \theta} - \frac{\gamma - 1}{2}\frac{\partial u_1^2}{\partial \theta} - \bar{u}\frac{\partial p_1}{\partial x}$$

$$- p_1\frac{d\bar{u}}{dx} - p_1\frac{\partial u_1}{\partial x} + \frac{\partial w_2}{\partial x} \tag{II-36}$$

where the fact that $\frac{d\bar{u}}{dx} = O(M_E)$ has been used. First adding, then

subtracting the second equation to the first produces the following two equations with their left hand sides in the same form as Equations (II-26) and (II-27)

$$\frac{\partial}{\partial\theta}\left(u_2+\tfrac{1}{\gamma}p_2\right)+\frac{\partial}{\partial x}\left(u_2+\tfrac{1}{\gamma}p_2\right)=\frac{\pi}{2}\frac{\partial}{\partial\theta}\left(u_1+\tfrac{1}{\gamma}p_1\right)-(\gamma-1)(\bar{u}+u_1)\frac{\partial u_1}{\partial\theta}$$

$$-(u_1+\bar{u})\frac{\partial p_1}{\partial x}-p_1\frac{\partial}{\partial x}(\bar{u}+u_1)-\rho_1\frac{\partial u_1}{\partial\theta}-(\bar{u}+u_1)\frac{\partial u_1}{\partial x}-2u_1\frac{d\bar{u}}{dx}+\frac{d\bar{u}}{dx}n\left[p_1-p_{1\mu}\right] \tag{II-37}$$

$$\frac{\partial}{\partial\theta}\left(u_2-\tfrac{1}{\gamma}p_2\right)-\frac{\partial}{\partial x}\left(u_2-\tfrac{1}{\gamma}p_2\right)=\frac{\pi}{2}\frac{\partial}{\partial\theta}\left(u_1-\tfrac{1}{\gamma}p_1\right)+(u_1+\bar{u})\frac{\partial p_1}{\partial\theta}$$

$$+(\gamma-1)(\bar{u}+u_1)\frac{\partial u_1}{\partial\theta}+p_1\frac{\partial}{\partial x}(\bar{u}+u_1)-\rho_1\frac{\partial u_1}{\partial\theta}-(\bar{u}+u_1)\frac{\partial u_1}{\partial x}-2u_1\frac{d\bar{u}}{dx}-\frac{d\bar{u}}{dx}n\left[p_1-p_{1\mu}\right] \tag{II-38}$$

where Equation (II-20) has been used to substitute for $\frac{\partial w_2}{\partial x}$, and $p_{1\mu} = p_1(\theta-\mu)$.

The right hand sides of both Equation (II-37) and (II-38) contain only terms involving u_1 and p_1 and their derivatives, with the exception of the term $\rho_1\frac{\partial u_1}{\partial\theta}$ which appears in the same way in both equations. The quantity ρ_1 can be expressed in terms of p_1 and s_1 as $\rho_1 = \frac{p_1}{\gamma} - s_1$. The entropy equation, Equation (II-22) must, therefore, be solved for s_1 before Equations (II-37) and (II-38) can be solved for u_2 and p_2. To first order Equation (II-22) may be written

$$\frac{\partial s_1}{\partial\theta} = 0 \tag{II-39}$$

This equation has the obvious solution $s_1 = s_1(x)$. To second order in

M_E the entropy equation is

$$\frac{\partial s_2}{\partial \theta} + \bar{u}\frac{ds_1}{dx} + u_1\frac{ds_1}{dx} = -\left(s_1 + \frac{\gamma-1}{\gamma}p_1\right)\frac{d\bar{u}}{dx} \qquad \text{(II-40)}$$

where the fact that $\frac{d\bar{s}}{dx} = O(M_E^2)$ has been used. Since we are interested only in periodic solutions for the physical quantities, we now require that $s(2,x) = s(0,x)$. This can be expressed in the equivalent form $\frac{1}{2}\int_0^2 \frac{\partial s_2}{\partial \theta'}\, d\theta' = 0$, where it is understood that the integration is carried out with x fixed. Integrating Equation (II-40) from zero to two and dividing by two then produces the following expression

$$\bar{u}\frac{ds_1}{dx} + \frac{1}{2}\frac{ds_1}{dx}\int_0^2 u_1\, d\theta' + s_1\frac{d\bar{u}}{dx} + \frac{\gamma-1}{\gamma}\frac{d\bar{u}}{dx}\frac{1}{2}\int_0^2 p_1\, d\theta' = 0 \qquad \text{(II-41)}$$

From Equations (II-23) and (II-24) it can be seen that $u_1 = f(\theta - x) - f(\theta + x)$ and $p_1 = \gamma\left[f(\theta - x) + f(\theta + x)\right]$. Moreover, because f is periodic in two, $\int_0^2 f(\theta' - x)d\theta' = \int_0^2 f(\theta' + x)d\theta'$. Thus $\int_0^2 u_1 d\theta' = 0$ and $\int_0^2 p_1 d\theta' = 2\gamma\int_0^2 f(\eta)d\eta$. Using these results in Equation (II-41) gives the following equation

$$\frac{d}{dx}\left[\bar{u}s_1 + (\gamma-1)\bar{u}\int_0^2 f(\eta)\, d\eta\right] = 0 \qquad \text{(II-42)}$$

or, integrating

$$\bar{u}s_1 + (\gamma-1)\bar{u}\int_0^2 f(\eta)\, d\eta = \text{const.} \qquad \text{(II-43)}$$

Since $\bar{u}\ (x=0) = 0$, the constant on the right hand side of Equation (II-43) is zero and, finally

$$S_1 = -(\gamma-1)\int_0^2 f(\eta)\,d\eta \qquad \text{(II-44)}$$

This means that s_1 is a constant, independent of θ and x , that is dependent on the first order wave form. Since $(\gamma - 1)$ is in general a small number for most combustion products, it is seen that, to first order, the (constant) deviation from the steady-state entropy profile in the chamber is small.

The first order results $u_1 = f(\theta - x) - f(\theta + x)$, $p_1 = \gamma\left[f(\theta - x) + f(\theta + x)\right]$ are used to substitute for u_1 and p_1 in the inhomogeneous parts of Equations (II-37) and (II-38). The right hand side of Equation (II-37), call it R_A , can then be written

$$R_A = \left[\frac{\partial}{\partial\theta} f(\theta-x)\right]\left\{T_1 + (\gamma+1)f(\theta-x) + (\gamma-3)f(\theta+x) + 2\bar{u} + S_1\right\}$$

$$+\left[\frac{\partial}{\partial\theta} f(\theta+x)\right]\left\{(\gamma+1)f(\theta+x) + (\gamma+1)f(\theta-x) - S_1\right\}$$

$$+\frac{d\bar{u}}{dx}\left\{(\gamma n-(\gamma-2))f(\theta+x) + (\gamma n-(\gamma+2))f(\theta-x) - n\gamma\left[f(\theta-x-\mu)+f(\theta+x-\mu)\right]\right\}$$

(II-45)

Similarly, the right hand side of Equation (II-38), R_B, becomes

$$R_B = \left[\frac{\partial}{\partial\theta} f(\theta+x)\right]\left\{(3-\gamma)f(\theta-x) - (\gamma+1)f(\theta+x) + 2\bar{u} - S_1 - T_1\right\}$$

$$- \left[\frac{\partial}{\partial\theta} f(\theta-x)\right]\left\{(\gamma+1)f(\theta-x) + (\gamma+1)f(\theta+x) - S_1\right\}$$

$$- \frac{d\bar{u}}{dx}\left\{(n\gamma-(\gamma-2))f(\theta-x) + (n\gamma-(\gamma+2))f(\theta+x) - \gamma n\left[f(\theta-x-\mu) + f(\theta+x-\mu)\right]\right\} \quad \text{(II-46)}$$

A particular solution to Equation (II-37) which produces R_A when operated upon by $\frac{\partial}{\partial\theta} + \frac{\partial}{\partial x}$ is found by inspection to be

$$P_r = \left[\frac{\partial}{\partial\theta} f(\theta-x)\right]\left\{(\gamma+1)x f(\theta-x) + \frac{\gamma-3}{2}\int_{\theta-x}^{\theta+x} f(\eta)\,d\eta + 2\int_0^x \bar{u}\,dx' + T_1 x + S_1 x\right\}$$

$$+ \bar{u}\left[(\gamma n-(\gamma+2))f(\theta-x) - \gamma n f(\theta-\mu-x)\right] + \frac{\gamma+1}{4} f^2(\theta+x) + \frac{\gamma+1}{2} f(\theta-x) f(\theta+x)$$

$$- \frac{S_1}{2} f(\theta+x) + \frac{(\gamma n-(\gamma-2))}{2}\int_{\theta-x}^{\theta+x} \frac{d\bar{u}}{dx}\left(\eta-(\theta-x)\right) f(\eta)\,d\eta - \frac{\gamma n}{2}\int_{\theta-x-\mu}^{\theta+x-\mu} \frac{d\bar{u}}{dx}\left(\eta-(\theta-x-\mu)\right) f(\eta)\,d\eta$$

(II-47)

Similarly, a particular solution to (II-38) is

$$P_s = \left[\frac{\partial}{\partial\theta} f(\theta+x)\right]\left\{(\gamma+1)x\,f(\theta+x) + \frac{3-\gamma}{2}\int_{\theta+x}^{\theta-x} f(\eta)\,d\eta - 2\int_0^x \bar{u}\,dx' + S_1 x + T_1 x\right\}$$

$$+\bar{u}\left[(\gamma n-(\gamma+2))\,f(\theta+x) - \gamma n\, f(\theta+x-\mu)\right] - \frac{\gamma+1}{4} f^2(\theta-x) - \frac{\gamma+1}{2} f(\theta+x) f(\theta-x)$$

$$+\frac{S_1}{2} f(\theta-x) - \frac{(\gamma n-(\gamma-2))}{2}\int_{\theta+x}^{\theta-x} \frac{d\bar{u}}{dx}\left(\frac{\theta+x-\eta}{2}\right) f(\eta)\,d\eta + \frac{\gamma n}{2}\int_{\theta+x-\mu}^{\theta-x-\mu} \frac{d\sigma}{dx}\left(\frac{\theta+x-\mu-\eta}{2}\right) f\eta\,d\eta \qquad \text{(II-48)}$$

The complete solution to Equation (II-37) is given by adding to P_r an arbitrary second order function of $\theta - x$, $2F_r(\theta - x)$. The complete solution to Equation (II-38) is formed in a similar manner by adding the arbitrary second order function $2F_s(\theta + x)$ to P_s. Thus

$$u_2 + \frac{p_2}{\gamma} = 2F_r(\theta-x) + P_r \qquad \text{(II-49)}$$

$$u_2 - \frac{p_2}{\gamma} = 2F_s(\theta+x) + P_s \qquad \text{(II-50)}$$

Because Equations (II-37) and (II-38) are only valid in shock free regions, the chamber is again considered to be separated into two regions, regions I and II, as shown in Figure I. Then, for region I

$$\left(u_2 + \frac{p_2}{\gamma}\right)_I = F_{rI}(\theta - x) + P_{rI} \tag{II-51}$$

$$\left(u_2 - \frac{p_2}{\gamma}\right)_I = F_{sI}(\theta + x) + P_{sI} \tag{II-52}$$

and for region II

$$\left(u_2 + \frac{p_2}{\gamma}\right)_{II} = F_{rII}(\theta - x) + P_{rII} \tag{II-53}$$

$$\left(u_2 - \frac{p_2}{\gamma}\right)_{II} = F_{sII}(\theta + x) + P_{sII} \tag{II-54}$$

The relationship between F_{rI} and F_{rII}, F_{sI} and F_{sII}, P_{rI} and P_{rII} and P_{sI} and P_{sII} must be determined. This is done as has been done previously, by using the fact that $u_2 + \frac{2}{\gamma - 1} a_2$ is continuous through shocks moving to the left (toward the injector) and $u_2 - \frac{2}{\gamma - 1} a_2$ is continuous through the shocks moving to the right (toward the nozzle). To $O(M_E^2)$ Equation (II-31) becomes

$$p_1 + p_2 = -\frac{\gamma}{\gamma-1} s_1 + \frac{2\gamma}{\gamma-1} a_1 - \frac{\gamma}{\gamma-1} s_2 + \frac{2\gamma}{\gamma-1} a_2 + \frac{\gamma^2}{2(\gamma-1)^2} s_1^2$$

$$- \frac{2\gamma^2}{(\gamma-1)^2} a_1 s_1 + \frac{\gamma(\gamma+1)}{(\gamma-1)^2} a_1^2 \tag{II-55}$$

Using the first order result (Equation (II-32))

$$\frac{p_1}{\gamma} = \frac{2}{\gamma-1} a_1 - \frac{1}{\gamma-1} s_1$$

and solving (II-55) for $\frac{2}{\gamma - 1} a_2$, yields

$$\frac{2}{\gamma-1} a_2 = \frac{1}{\gamma} p_2 + \frac{s_2}{\gamma-1} + \frac{1}{4(\gamma-1)} s_1^2 + \frac{p_1 s_1}{2\gamma} - \frac{\gamma+1}{4\gamma^2} p_1^2 \tag{II-56}$$

Across a left moving shock it is true that $(u_2 + \frac{2}{\gamma - 1} a_2)_I = (u_2 + \frac{2}{\gamma - 1} a_2)_{II}$. Using Equation (II-56) this equality may be written

$$\left(u_2 + \frac{p_2}{\gamma}\right)_I + \frac{s_{2I}}{\gamma-1} + \frac{1}{4(\gamma-1)} s_{1I}^2 + \frac{s_{1I}}{2} \frac{p_{1I}}{\gamma} - \frac{\gamma+1}{4} \frac{p_{1I}^2}{\gamma^2}$$

$$= \left(u_2 + \frac{p_2}{\gamma}\right)_{II} + \frac{s_{2II}}{\gamma-1} + \frac{1}{4(\gamma-1)} s_{1II}^2 + \frac{s_{1II}}{2} \frac{p_{1II}}{\gamma} - \frac{\gamma+1}{4} \frac{p_{1II}^2}{\gamma^2} \tag{II-57}$$

Noting that s_1 is a constant, independent of whether one is in region I or II, and that s_2 is continuous through shocks to $O(M_E^2)$ the above equation reduces to

$$\left(u_2 + \frac{p_2}{\gamma}\right)_I = \left(u_2 + \frac{p_2}{\gamma}\right)_{II} + \frac{s_1}{2}\left(\frac{p_{1II}}{\gamma} - \frac{p_{1I}}{\gamma}\right) - \frac{\gamma+1}{4}\left(\frac{p_{1II}^2}{\gamma^2} - \frac{p_{1I}^2}{\gamma^2}\right) \tag{II-58}$$

The quantity $(p_{1,II} - p_{1,I})$ is simply the jump in pressure across the shock wave. Using Equations (II-33) and (II-34) this quantity is found to have the following value

$$p_{1,II} - p_{1,I} = \gamma \left(f(0) - f(2) \right)$$

(II-59)

where $f(0)$ is the value of f immediately after a shock and $f(2)$ is the value immediately before. The quantity $(p_{1,II}^2 - p_{1,I}^2)$ is simply equal to $\gamma (f(0) - f(2)) (p_{1,II} + p_{1,I})$, or again employing the first order expression for p_1,

$$p_{1,II}^2 - p_{1,I}^2 = \gamma^2 \left[f_{(0)}^2 - f_{(2)}^2 + 2 f_{(0-x)} \left(f_{(0)} - f_{(2)} \right) \right]$$

(II-60)

Equation (II-58) then takes the form

$$\left(u_2 + \frac{p_2}{\gamma} \right)_I = \left(u_2 + \frac{p_2}{\gamma} \right)_{II} + \frac{s_1}{2} \left(f_{(0)} - f_{(2)} \right) - \frac{\gamma+1}{4} \left[2 f_{(0-x)} \left(f_{(0)} - f_{(2)} \right) + f_{(0)}^2 - f_{(2)}^2 \right]$$

(II-61)

Across a right moving shock the quantity $u_2 - \frac{2}{\gamma - 1} a_2$ is continuous. This condition may be written $(u_2 - \frac{2}{\gamma - 1} a_2)_I = (u_2 - \frac{2}{\gamma - 1} a_2)_{II}$ at the shock. Using Equations (II-56), (II-33) and (II-34), this requirement can be expressed as the following condition on $u_2 - \frac{1}{\gamma} p_2$ at the shock, analogous to Equation (II-61)

$$\left(u_2 - \frac{p_2}{\gamma} \right)_I = \left(u_2 - \frac{p_2}{\gamma} \right)_{II} + \frac{s_1}{2} \left(f_{(0)} - f_{(2)} \right) - \frac{\gamma+1}{4} \left[2 f_{(0+x)} \left(f_{(0)} - f_{(2)} \right) + f_{(0)}^2 - f_{(2)}^2 \right]$$

(II-62)

The particular solution to Equation (II-37), P_r, may be written as the sum of two parts

$$P_r = \Psi_r + \Phi_r \tag{II-63}$$

where

$$\Psi_r \equiv \left[\frac{\partial}{\partial\theta} f(\theta-x)\right]\left\{(\gamma+1)x\, f(\theta-x) + \frac{\gamma-3}{2}\int_{\theta-x}^{\theta+x} f(\eta)\,d\eta + 2\int_0^x \bar{u}\,dx' + T_1 x + S_1 x\right\}$$

$$+ \bar{u}\left[(\gamma n - (\gamma+2))\, f(\theta-x) - \gamma n\, f(\theta-x-\mu)\right]$$

$$+ \frac{\gamma n - (\gamma-2)}{2}\int_{\theta-x}^{\theta+x} \frac{d\bar{u}}{dx}\left(\eta - (\theta-x)\right) f(\eta)\,d\eta - \frac{\gamma n}{2}\int_{\theta-x-\mu}^{\theta+x-\mu} \frac{d\bar{u}}{dx}\left(\eta - (\theta-x-\mu)\right) f(\eta)\,d\eta \tag{II-64}$$

and

$$\Phi_r \equiv \frac{\gamma+1}{4} f^2(\theta+x) + \frac{\gamma+1}{2} f(\theta-x) f(\theta+x) - \frac{S_1}{2} f(\theta-x) \tag{II-65}$$

Because $f(\theta - x)$ is continuous across left running shock waves, Ψ_r is also continuous across such waves to the order of approximation considered. Φ_r, on the other hand, need not be continuous across left moving shocks because of its dependence upon $f(\theta + x)$. The quantity $u_2 + \frac{1}{\gamma} p_2$, can be written in terms of $F_r(\theta - x)$, Ψ_r, and Φ_r as

$$u_2 + \frac{1}{\gamma} p_2 = 2F_r(\theta - x) + \psi_r + \Phi_r \tag{II-66}$$

Using this expression, Equation (II-61) becomes

$$2F_{rI} + \psi_{rI} + \Phi_{rI} = 2F_{rII} + \psi_{rII} + \Phi_{rII} + \frac{S_1}{2}\left(f(0) - f(2)\right) - \frac{\gamma+1}{4}\left(2f(\theta - x)\left(f(0) - f(2)\right) + f^2(0) - f^2(2)\right) \tag{II-67}$$

which is valid at a left running shock. Noting that, as mentioned above, $\psi_{rI} = \psi_{rII}$ across the shock and that, at the shock

$$\Phi_{rI} = \frac{\gamma+1}{4} f^2(2) + \frac{\gamma+1}{2} f(2) f(\theta - x) - \frac{S_1}{2} f(2) \tag{II-68}$$

and

$$\Phi_{rII} = \frac{\gamma+1}{4} f^2(0) + \frac{\gamma+1}{2} f(0) f(\theta - x) - \frac{S_1}{2} f(0) \tag{II-69}$$

Equation (II-67) becomes, simply

$$F_{rI}(\theta - x) = F_{rII}(\theta - x) \tag{II-70}$$

The particular solution to Equation (II-38), P_s may be rewritten

$$P_s = \psi_s + \Phi_s \tag{II-71}$$

where

$$\psi_s \equiv \left[\frac{\partial f(\theta+x)}{\partial \theta}\right]\left\{(\gamma+1)x\, f(\theta+x) - 2\int_0^x \bar{u}\, dx' + \frac{3-\gamma}{2}\int_{\theta+x}^{\theta-x} f(\eta)\, d\eta + S_1 x + T_1 x\right\}$$

$$+ \bar{u}\left[(\gamma n - (\gamma+2))\, f(\theta+x) - \gamma n\, f(\theta+x-\mu)\right]$$

$$- \frac{\gamma n - (\gamma-2)}{2}\int_{\theta+x}^{\theta-x} \frac{d\bar{u}}{dx}\left(\frac{\theta+x-\eta}{2}\right) f(\eta)\, d\eta + \frac{\gamma n}{2}\int_{\theta+x-\mu}^{\theta-x-\mu} \frac{d\bar{u}}{dx}\left(\frac{\theta+x-\mu-\eta}{2}\right) f(\eta)\, d\eta$$

(II-72)

and

$$\Phi_s = \frac{\gamma+1}{4} f^2(\theta-x) - \frac{\gamma+1}{2} f(\theta+x) f(\theta-x) + \frac{S_1}{2} f(\theta-x)$$

(II-73)

Here ψ_s is continuous through right moving shock waves, while Φ_s need not be. $u_2 - \frac{1}{\gamma} p_2$ can now be expressed in terms of $F_s(\theta + x)$, ψ_s and Φ_s as

$$u_2 + \frac{1}{\gamma} p_2 = 2 F_s(\theta+x) + \psi_s + \Phi_s$$

(II-74)

Equation (II-64) can be written as follows, at a right moving shock wave

$$2 F_{sI}(\theta+x) + \psi_{sI} + \Phi_{sI} = 2 F_{sII}(\theta+x) + \psi_{sII} + \Phi_{sII}$$

$$+ \frac{S_1}{2}\left(f(0) - f(2)\right) - \frac{\gamma+1}{4}\left[2 f(\theta+x)\left(f(0) - f(2)\right) + f^2(0) - f^2(2)\right]$$

(II-75)

Since $\Psi_{sI} = \Psi_{sII}$, and, also

$$\Phi_{sI} = -\frac{(\gamma+1)}{4} f^2(0) - \frac{(\gamma+1)}{2} F(0) f(\theta+x) + \frac{S_1}{2} f(0)$$

(II-76)

while

$$\Phi_{sII} = -\frac{\gamma+1}{4} f^2(2) - \frac{(\gamma+1)}{2} f(2) f(\theta+x) + \frac{S_1}{2} f(2)$$

(II-77)

Equation (II-75) reduces to

$$F_{sI}(\theta+x) = F_{sII}(\theta+x)$$

(II-78)

Equation (II-70) states that $F_r(\theta - x)$ is continuous across left moving shocks, while Equation (II-78) expresses the fact that $F_s(\theta + x)$ is continuous across right moving shocks. It will be recalled that the first order functions $f_r(\theta - x)$ and $f_s(\theta + x)$ exhibit this same property with respect to shock waves moving in the appropriate direction. Therefore, as was the case for the first order functions f_r and f_s , it is superfluous to distinguish between F_r and F_s in regions I and II.

Having shown the relationship between the arbitrary second order functions in regions I and II, it is now possible to apply the boundary conditions at the two ends of the chamber in a simple way. At the injector end, $x = 0$, the boundary condition is simply the solid wall condition, $u_2 = 0$. An expression for u_2 is found by combining Equations (II-49) and (II-50) to be

$$u_2 = F_r(\theta - x) + F_s(\theta + x) + \frac{P_r}{2} + \frac{P_s}{2}$$

(II-79)

Examination of the definitions of P_r and P_s, Equations (II-47) and (II-48), shows that at $x = 0$ these functions reduce to

$$P_r(x=0) = \frac{3(\gamma+1)}{4} f^2(\theta) - \frac{s_1}{2} f(\theta) \tag{II-80}$$

$$P_s(x=0) = -\frac{3(\gamma+1)}{4} f^2(\theta) + \frac{s_1}{2} f(\theta) \tag{II-81}$$

when the fact that $\bar{u}(x = 0) = 0$ is used. Equations (II-80) and (II-81) show that $P_r(x = 0) + (P_s(x = 0) = 0$, consequently $u_2(x = 0)$ becomes

$$u_2(x=0) = F_r(\theta) + F_s(\theta) \tag{II-82}$$

Since the boundary condition at $x = 0$ requires that $u_2 = 0$ there, Equation (II-82) implies the following relationship between the second order functions

$$F_r(\theta) = -F_s(\theta) \tag{II-83}$$

The boundary condition at the nozzle end of the chamber requires that the Mach number at the entrance to the nozzle, that is, at $x = 1$, be equal to M_E. To second order this means

$$u_2 = M_E a_1 \tag{II-84}$$

Using the first order expression for a_1 in terms of p_1 and s_1, Equation (II-32), this becomes

$$u_2 = M_E \frac{\gamma-1}{2\gamma} p_1 + M_E \frac{s_1}{2} \tag{II-85}$$

or, implying the first order expression for p_1 in terms of f

$$u_2(x=1) = M_E(\gamma-1)f(\theta-1) + M_E\frac{S_1}{2}$$

(II-86)

The particular solution P_r, evaluated at $x = 1$, can be written

$$P_r = \left[\frac{\partial}{\partial\theta}f(\theta-1)\right]\left\{(\gamma+1)f(\theta-1) + \frac{\gamma-3}{2}\int_0^2 f(\eta)\,d\eta + 2\int_0^1 \bar{u}\,dx' + T_1 + S_1\right\}$$

$$+ M_E\left[(\gamma n-(\gamma+2))f(\theta-1) - \gamma n f(\theta-1-\mu)\right] + \frac{3(\gamma+1)}{4}f^2(\theta-1)$$

$$- \frac{S_1}{2}f(\theta-1) + \frac{\gamma n-(\gamma-2)}{2}\int_{\theta-1}^{\theta+1}\frac{d\bar{u}}{dx}\left(\frac{\eta-(\theta-1)}{2}\right)f(\eta)\,d\eta$$

$$- \frac{\gamma n}{2}\int_{\theta-1-\mu}^{\theta+1-\mu}\frac{d\bar{u}}{dx}\left(\frac{\eta-\theta+1+\mu}{2}\right)f(\eta)\,d\eta$$

(II-87)

where, because of the periodicity of f, $\int_{\theta-1}^{\theta+1} f(\eta)d\eta = \int_0^2 f(\eta)d\eta$ and $f(\theta-1) = f(\theta+1)$. Also, the fact that $\bar{u}(x=1) = M_E + O(M_E^3)$ has been used. Similarly, P_s at $x = 1$ may be expressed as

$$P_s = \left[\frac{\partial}{\partial\theta} f(\theta-1)\right]\left\{(\gamma+1) f(\theta-1) - \frac{3-\gamma}{2}\int_0^2 f(\eta)\,d\eta - 2\int_0^1 \bar{u}\,dx' + T_1' + S_1\right\}$$

$$+ M_E\left[(\gamma n - (\gamma+2)) f(\theta-1) - \gamma n\, f(\theta-1-\mu)\right] - \frac{3(\gamma+1)}{4} f^2(\theta-1) + \frac{S_1}{2} f(\theta-1)$$

$$- \frac{(\gamma n - (\gamma-2))}{2}\int_{\theta+1}^{\theta-1} \frac{d\bar{u}}{dx}\left(\frac{\theta+1-\eta}{2}\right) f(\eta)\,d\eta + \frac{\gamma n}{2}\int_{\theta+1-\mu}^{\theta-1-\mu} \frac{d\bar{u}}{dx}\left(\frac{\theta+1-\mu-\eta}{2}\right) f(\eta)\,d\eta$$

(II-88)

Combining Equations (II-87), (II-88) and (II-79) in order to find the proper expressions for u_2 at $x = 1$ and then substituting this into Equation (II-86), representing the boundary condition at $x = 1$, yields

$$F_r(\theta-1) + F_s(\theta+1) + \frac{\partial}{\partial\theta} f(\theta-1)\left\{(\gamma+1) f(\theta-1) - \frac{3-\gamma}{2}\int_0^2 f(\eta)\,d\eta + T_1' + S_1\right\}$$

$$+ M_E\left[(\gamma n - (\gamma+2)) f(\theta-1) - \gamma n\, f(\theta-1-\mu)\right]$$

$$+ \frac{(\gamma n - (\gamma-2))}{4}\int_{\theta-1}^{\theta+1}\left[\frac{d\bar{u}}{dx}\left(\frac{\eta-(\theta-1)}{2}\right) + \frac{d\bar{u}}{dx}\left(\frac{\theta+1-\eta}{2}\right)\right] f(\eta)\,d\eta$$

$$- \frac{\gamma n}{4}\int_{\theta-1-\mu}^{\theta+1-\mu}\left[\frac{d\bar{u}}{dx}\left(\frac{\eta-\theta+1+\mu}{2}\right) + \frac{d\bar{u}}{dx}\left(\frac{\theta+1-\mu-\eta}{2}\right)\right] f(\eta)\,d\eta = M_E\left[(\gamma-1) f(\theta-1) + \frac{S_1}{2}\right]$$

(II-89)

By Equation (II-83), $F_s(\theta + 1) = - F_r(\theta + 1)$. Also, since we require periodicity in 2 , $F_r(\theta + 1) = F_r(\theta - 1)$. Consequently, the first two terms on the left hand side of Equation (II-89) add to zero and the equation becomes an equation determining the form of f , the arbitrary first order function. T_1 , the first order correction to the period is evaluated in Appendix A. The final result of that calculation is

$$T_1 = - \frac{\gamma+1}{2} \left(f(0) + f(2) \right) + \frac{3-\gamma}{2} \int_0^2 f(\eta)\, d\eta - S_1 \tag{II-90}$$

Substituting this relation in Equation (II-89) and rearranging, one gets

$$\left[(\gamma+1) f - (\gamma+1) C_1 \right] \frac{df}{d\theta} = A f + B f_\mu + M_E \frac{S_1}{2} + I_A + I_B \tag{II-91}$$

where

$$C_1 = \frac{f(0) + f(2)}{2}, \quad A = M_E (2\gamma + 1 - \gamma n), \quad B = M_E \gamma n$$

$$I_A = - \frac{(\gamma n - (\gamma - 2))}{4} \int_{\theta-1}^{\theta+1} \left[\frac{d\bar{u}}{dx} \left(\frac{\eta - (\theta - 1)}{2} \right) + \frac{d\sigma}{dx} \left(\frac{\theta + 1 - \eta}{2} \right) \right] f(\eta)\, d\eta, \quad I_B = \frac{\gamma n}{4} \int_{\theta-1-\mu}^{\theta+1-\mu} \left[\frac{d\bar{u}}{dx} \left(\frac{\eta - \theta + 1 - \mu}{2} \right) + \frac{d\bar{u}}{dx} \left(\frac{\theta + 1 - \mu - \eta}{2} \right) \right] f(\eta)\, d\eta$$

C. Solution of the Equation Governing the First Order Function f(θ)

Equation (II-91) is an ordinary nonlinear, differential-integral equation with a retarded variable. As such it is considerably more complicated, and more difficult to solve for the function f(θ) , than was the corresponding equation, Equation (I-76), found for the case of concentrated

combustion. Even so, there appears to be no reason, in principle, why this equation cannot be integrated numerically. However, attention should be called to the fact that, because of the integral terms, it is not sufficient to guess the function μ units before the starting point of a step by step integration process, as was the case with Equation (I-76). Instead the function must be guessed over the whole interval $0 \leq \theta \leq 2$. This might render the functional iteration technique used to solve Equation (I-76) somewhat less effective in the solution of Equation (II-91).

In the present investigation the integration of Equation (II-91) has been attempted for only one steady-state velocity distribution. The distribution chosen is simply a constant slope ramp function along the axial chamber dimension. In other words, $\bar{u}(x) = u_E x = M_E x + O(M_E^3)$. It can be seen that this implies that $\frac{d\bar{u}}{dx} = M_E$. With this kind of velocity profile the two integral terms in Equation (II-91) become

$$I_A = \frac{\gamma - 2 - \gamma\eta}{2} M_E \int_{\theta-1}^{\theta+1} f(\eta)\, d\eta \tag{II-92}$$

and

$$I_B = \frac{\gamma\eta}{2} M_E \int_{\theta-1-\mu}^{\theta+1-\mu} f(\eta)\, d\eta \tag{II-93}$$

Because $f(\theta)$ is periodic these may be rewritten

$$I_A = \frac{\gamma - 2 - \gamma\eta}{2} M_E \int_{0}^{2} f(\eta)\, d\eta \tag{II-94}$$

and

$$I_B = \frac{\gamma\eta}{2} M_E \int_0^2 f(\eta)\, d\eta \qquad \text{(II-95)}$$

Using the expression derived earlier for s_1, $s_1 = -(\gamma - 1) \int_0^2 f(\eta)d\eta$, Equation (II-91) for the velocity profile $\frac{d\bar{u}}{dx} = M_E$, becomes

$$\left[(\gamma+1)f - (\gamma+1)C_1\right] \frac{df}{d\theta} = Af + Bf_\mu - \frac{M_E}{2} \int_0^2 f(\eta)\, d\eta \qquad \text{(II-96)}$$

In this equation the dependence on the integral quantities I_A and I_B is not present. Consequently, the equation is simply a nonlinear differential equation with a retarded variable, similar in form to the governing differential equation in the case of concentrated combustion. If Equation (II-96) is integrated with respect to θ from $\theta = 0$ to $\theta = 2$, one obtains the following condition that any periodic solution to Equation (II-96) must satisfy

$$(A + B - M_E) \int_0^2 f(\eta)\, d\eta = 0 \qquad \text{(II-97)}$$

where the left hand side is found to be zero by using the definition of C1. Because of the fact that $A + B = (2\gamma + 1) M_E$, it can be seen that Equation (II-97) can be satisfied for real gases ($\gamma > 0$) , and $M_E > 0$, only if $\int_0^2 f(\eta)d\eta = 0$. Therefore, any periodic solution (with period two) to the equation

$$(\gamma+1)(f - C_1)\frac{df}{d\theta} = Af + Bf_\mu \qquad \text{(II-98)}$$

is also a periodic solution (with period two) to Equation (II-96) and the problem is reduced to finding periodic solutions to Equation (II-98). It should be noted that the requirement that $\int_0^2 f(\eta)d\eta = 0$ means that the first order entropy variation, s_1, is zero. Thus, the mean pressure variation and the first order entropy variation both vanish when the combustion is distributed so that $\frac{d\bar{u}}{dx} = M_E$. Equation (II-98) can be put in the same form as Equation (I-78) by introducing the definitions

$$g = \frac{(\gamma + 1)}{M_E} f \quad \text{and} \quad k = \frac{g(0) + g(2)}{2}, \quad C = \frac{A}{M_E}, \quad \text{and} \quad D = \frac{B}{M_E}.$$

Then

$$(g-k)\frac{dg}{d\theta} = Cg + D g_\mu \tag{II-99}$$

If $C = a$ and $D = b$, Equations (II-99) and (I-78) are identical. The boundary condition on Equation (II-99) is, of course, the same as the one on Equation (I-78), that is

$$g(0) + g(2) = 2k$$

Equation (II-99) can be put in exactly the same form as Equation (I-78) through a simple transformation of g and n. The function $h = \alpha g$ and $m = n + \lambda$ are introduced, where, as yet, α and λ are undetermined constants. Equation (II-99), written in terms of h and m, is

$$(h-\hat{k})\frac{dh}{d\theta} = \alpha(2\gamma+1 - \gamma(m-\lambda)h + \alpha\gamma(m-\lambda)h_\mu \tag{II-100}$$

where $\hat{k} = \frac{h(0) + h(2)}{2}$

If the following two relationships are satisfied

$$\alpha\left(2\gamma+1-\gamma(m-\lambda)\right)=\gamma+1-2\gamma m \tag{II-101}$$

and

$$\alpha\gamma(m-\lambda)=2\gamma m \tag{II-102}$$

then Equation (II-100) will be exactly the same as Equation (II-78) with h in place of g and m in place of n. Equations (II-101) and (II-102) are easily solved simultaneously to give the following expressions for λ and α

$$\lambda=-\frac{3\gamma+1}{\gamma+1}m \tag{II-103}$$

$$\alpha=\frac{\gamma+1}{2\gamma+1} \tag{II-104}$$

These imply that

$$n=\frac{4\gamma+2}{\gamma+1}m \tag{II-105}$$

$$g=h\,\frac{2\gamma+1}{\gamma+1} \tag{II-106}$$

Because of the transformation just presented, the results already obtained for g and n for the case of concentrated combustion can be considered as results for h and m for the case of distributed combustion $\left(\frac{d\bar{u}}{dx}=M_E\right)$. In order to put the results for distributed combustion (under the restriction $\frac{d\bar{u}}{dx}=M_E$) in terms of g and n, the simple relationships given in Equations (II-105) and (II-106) need only be applied.

Since, to change from the concentrated combustion results to the distributed combustion results only requires multiplying the values of g and n by constants, it is clear that the nonlinear and linear stability limits will simply be shifted upward on the n, μ plane. The nature of this upward shifting will be such that for every value of μ, n at the stability limit for distributed combustion with $\frac{d\bar{u}}{dx} = M_E$ will be exactly $(\frac{4\gamma + 2}{\gamma + 1})$ times as large as the value of n on the stability limit for concentrated combustion. This shifting is shown in Figure 22. Also shown in the figure are the linear stability limit for the combustion distribution chosen and the linear stability limit for concentrated combustion, drawn in for the sake of comparison. The linear stability limit for the combustion distribution with $\frac{d\bar{u}}{dx} = M_E$ may also be found by substituting this steady-state velocity profile directly into the results of Crocco's linear analysis for distributed combustion.[5] Either method produces precisely the same result.

The waveform of a discontinuous solution along the line $\mu = 1$ in the case of a combustion distribution with $\frac{d\bar{u}}{dx} = M_E$ is shown in Figure 23. It is, of course, of the same form as the solutions found for the case of concentrated combustion.

It should be emphasized that, though the form of the first order function f and the dependence of that form on the combustion parameters n, and μ, has only been investigated for the simple velocity profile (combustion distribution) $\frac{d\bar{u}}{dx} = M_E$, an equation has been derived (Equation II-91) that in principle can determine f and its dependence on n, and μ for any velocity profile as long as $\frac{d\bar{u}}{dx} = O(M_E)$. It should be noted that a combustion distribution with the velocity profile $\frac{d\bar{u}}{dx} = 2 M_E$, $0 \leq x \leq \frac{1}{2}$,

produces exactly the same stability results as does the velocity profile $\frac{d\bar{u}}{dx} = M_E$. This can be seen by examining I_A and I_B . For the two velocity profiles just mentioned these integrals are identical and, consequently the governing equation for $f(\theta)$ is also the same.

In conclusion, then, it is felt that the velocity profile $\frac{d\bar{u}}{dx} = M_E$ is a convenient opposite extreme to the case of concentrated combustion, and thus that the results for this particular profile characterize the influence of distributing the combustion.

Before proceeding to a summary of the results of this thesis, it is appropriate to note that the analysis for distributed combustion as well as that for concentrated combustion has been restricted to the case where only one shock is present. (Equivalently to the fundamental longitudinal mode corresponding to a linear analysis.) It is possible to consider higher modes of oscillation, that is, more than one shock being present in the chamber without great additional difficulty. In fact it can be shown that for the case of concentrated combustion or for distributed combustion with $\frac{d\bar{u}}{dx} = M_E$ it is possible to transform the equations governing the higher modes of oscillation into an equation identical to Equation (I-78).

CHAPTER III

SUMMARY AND DISCUSSION

A. General Considerations

In summary, the present investigation has succeeded in developing an analytical method for predicting whether periodic finite amplitude axial oscillations may exist in a given liquid rocket combustion chamber if the combustion processes occurring there can be represented using Crocco's time-lag postulate. Both discontinuous (shock-type) periodic waveforms and continuous periodic waveforms for the oscillations have been found. The dependence of the amplitude and the waveform of these periodic oscillations on n and τ, the combustion parameters, has been investigated. Two particular combustion distributions have been considered; the first being the limiting case of concentrated combustion, the second being the case where combustion is distributed throughout the chamber so that the steady-state velocity profile satisfies the equation $\frac{d\bar{u}}{dx} = O(M_E)$. In general, it may be said that, in contrast to earlier expectations,[5,2] the possibility of supporting both continuous and discontinuous finite amplitude pressure oscillations using a combustion model with a characteristic time that is of the order of the period of oscillation has been demonstrated.

B. Analytical Techniques and Results

It is appropriate at this point to review in a more specific way some of the analytical methods used, and some of the results found, in the first two chapters.

Critical to the successful analysis of the problem was the

selection of an expansion parameter proportional to, and of the same order as, the Mach number at the entrance to the supercritical nozzle. If a different expansion parameter, based on the difference between energy input and withdrawal from the chamber, was employed, it was found that discontinuous periodic oscillations could not be predicted when the combustion processes were represented by the time-lag model. It is to be noted that this latter kind of expansion parameter was used in all previous linear and nonlinear work which employed the time-lag postulate.

The Mach number at the entrance to the nozzle serves as a measure of the total amount of combustion occurring in the chamber in the steady-state and also as a measure of the mean flow out of the nozzle under steady conditions. It can therefore be thought of as a measure of the deviation of the flow field in the chamber from a simple acoustic field with no mean flow. Picking the expansion parameter to be proportional to, and of the same order as, the Mach number in this analysis therefore caused the governing partial differential equations for the flow field to take the form of simple acoustic equations to lowest order. No energy or mass addition needed to be considered to this lowest order. The combustion (driving) terms and the nozzle (damping) term appeared only in the second order equations and boundary conditions. Because of this, standard techniques could be employed in order to relate the first order thermodynamic and gasdynamic dependent variables to an arbitrary function of order M. Application of the solid wall boundary conditions then showed that this first order function was periodic with period equal to the acoustic period for the fundamental mode of oscillation. A second order analysis then had to be pursued in order to find the form that the

arbitrary first order function must take. The second order nozzle and combustion terms were found to appear only in the boundary conditions, (concentrated combustion) or in the partial differential equations and the boundary condition (distributed combustion). In either case it was these terms, combined with the nonlinear wave propagation terms, that determined the form of the arbitrary first order function.

The second order partial differential equations that included the combustion terms and nonlinear effects were solved with relative ease, particularly in the case of concentrated combustion. However, the integration of the equations introduced two arbitrary second order functions. Thus, three arbitrary functions appeared in the second order expressions for the dependent variables. Three conditions therefore needed to be applied in order to find an equation determining the first order function. The three conditions available were the boundary conditions at $x = 0$ and $x = 1$, and the periodicity requirement. The boundary conditions were rather easily applied, though the fact that Riemann invariants are continuous to second order in shock strength through shocks of the proper family had to be used in order to apply the boundary conditions correctly when discontinuous oscillations were considered. The application of the periodic condition, on the other hand, presented some difficulties because, in general, the period of the assumed oscillation had to be considered different from the period of the first order function. In other words, the period could not be taken a priori to be equal to the acoustic period but, rather, was taken to have a value within a correction of order M of it. The difficulties occurring because of this difference

in periods were overcome by introducing a stretched time coordinate, Θ, to replace the physical time coordinate, t. This insured that to all orders of approximation the period of oscillation in the stretched time variable would be equal to the acoustic period. When this transformation was made, the periodic condition was implicitly applied and, therefore, the application of the boundary conditions to the second order solutions in Θ, x space produced a nonlinear equation determining if periodic solutions for the arbitrary first order function, f, were possible and, if so, what their form and dependence upon n and μ was. (μ is the stretched time-lag that enters when the time coordinate is stretched.) Also, the equation determined whether the periodic solutions were continuous or discontinuous.

For the case of concentrated combustion the equation determining the form of f was a nonlinear, first order ordinary differential equation with a retarded variable. For the general case of distributed combustion the equation was a nonlinear differential-integral equation with a retarded variable. However, for the special combustion distribution with $\frac{d\bar{u}}{dx} = M_E$, the governing equation could be transformed into the same equation as the one governing f for the case of concentrated combustion.

Only a little information on the behavior of the ordinary differential equation for the case of concentrated combustion could be found analytically, however these findings were of some importance in setting up the numerical procedure for the integration of the equation. The most important result of the analytical examination of the equation was probably the discovery that discontinuous solutions to the equation with the same n value, but with μ values displaced symmetrically from the line $\mu = 1$,

could be related by a simple 180^{o} rotation. Because of the way the effect of the discontinuity was propagated in time, this simple symmetry relationship could only be applied in a strictly correct mathematical sense when μ was a rational fraction of the acoustic period. Several arguments were employed that indicated that the property should also hold for irrational μ. Because of the relationship between solutions symmetrically displaced from $\mu = 1$, curves of amplitude as functions of n and μ were found to be symmetric with respect to the line $\mu = 1$. This meant also that the nonlinear stability limit had to be symmetric with respect to the line $\mu = 1$. The periods of the oscillations that were solutions to the governing equation, on the other hand, were found to be antisymmetric with respect to $\mu = 1$. In particular, solutions along the line $\mu = 1$ had to be resonant oscillations, solutions with $\mu > 1$ below resonant oscillations and solutions with $\mu < 1$ above resonant oscillations. These symmetry characteristics of the equation meant that numerical integration of the nonlinear ordinary differential equation only had to be carried out for $\mu \leq 1$ in order to find all solutions in the interval $0 < \mu < 2$. This interval corresponds to the range of interest for the fundamental longitudinal mode of oscillation.

In addition to the symmetry properties of the solutions to the equation governing f for concentrated combustion (or distributed combustion with $\frac{d\bar{u}}{dx} = M_E$), two additional analytical findings are of interest. The first of these is the requirement that the integral of f over one period of oscillation is zero. This means that the deviation of the mean pressure from the steady-state value must be zero to first order, even when discontinuous pressure waves are present. Moreover, for the case of distri-

buted combustion with $\frac{d\bar{u}}{dx} = M_E$, it implies that the value of the first order entropy variation is equal to zero, since this quantity is proportional to the mean pressure. It should be noted that the comments just made with respect to the mean pressure and first order entropy need not necessarily be true for general combustion distributions with $\frac{d\bar{u}}{dx} = O(M_E)$. However, it is likely that, because of the spreading of the combustion, the deviation in the entropy from its steady value should be small, and, since the two quantities are proportional, the mean pressure change should also be small.

The second additional analytical result was the finding that discontinuous solutions existed right up to the stability limit when $\mu = 1$. This agrees with a result of the analysis performed by Sirignano using a combustion model that did not consider phasing effects.* He also found discontinuous solutions right up to the linear stability limit. Since the line $\mu = 1$ represents the line along which energy is added in phase with the pressure oscillations in the present analysis, the agreement between the two investigations is obvious. Moreover, it was found that, as one moved along the line $\mu = 1$, away from the linear stability limit, the amplitude of the shocks increased linearly with the distance from the linear limit. The same result was found by Sirignano using his different combustion model.

As far as the actual numerical integration of the ordinary nonlinear differential equation resulting from the study of concentrated combustion is concerned, little need be said at this point other than repeating the fact that the method of functional iteration that had to be employed because of the appearance of retarded variable, μ , in the equation, con-

* In other words the response of the combustion zone to the pressure oscillations was instantaneous in Sirignano's model.

verged rapidly to the proper periodic solution, if one existed at all, for the n and μ values considered. This numerical technique was used to find both continuous and discontinuous solutions. However, a convenient method of finding approximate continuous solutions valid close to the linear stability limit was also developed. In order to find these approximate solutions the governing ordinary differential equation was treated by a Fourier analysis technique in which the quantity f/M (or f/M_E) was taken to be a small quantity that vanished at the stability limit, in agreement with earlier linear analyses. The agreement between the approximate solutions and the numerical solutions for continuous oscillations close enough to the linear stability limit was found to be very good. However, at larger distances from the stability limit, considerable divergence between the two methods of solution was observed.

Numerical integration of the equation in question for a wide range of values of n and μ permitted the construction of a nonlinear stability limit for discontinuous solutions. Inside this curve it was possible to find stable, periodic discontinuous solutions. Outside the curve no periodic discontinuous solutions at all could be found. Comparison of the nonlinear stability limit with the linear stability limit showed that three regions with different stability characteristics existed. The largest region was the region where the area inside the linear stability limit was also inside the nonlinear stability limit. Since, by linear analysis, the growth of small perturbations was predicted here, while, at the same time, discontinuous periodic pressure waves were also predicted by the present nonlinear analysis, the conclusion was reached that the predicted discontinuous oscillations in this region were the final form

that pressure oscillations would take in a rocket engine that was intrinsically unstable because of its n and μ values being in this region of linear instability. In other words, the discontinuous periodic oscillations were taken to be the regime form of instability in this region. It should be noted that much of this region is far from the linear stability limit, in regions where f/M can be quite large. However, the analysis is still asymptotically valid for small enough M, even when this is the case. In contrast to this, the validity of the nonlinear work of Sirignano[2], which predicted only continuous finite amplitude oscillations using the time-lag model, was restricted to regions very close to the linear stability limit.

The second region of interest was found to be the region that was inside the linear stability limit but outside the nonlinear stability limit for discontinuous oscillations. The situation here was found to be really quite similar to the one just mentioned, except that the final form that intrinsic instability takes in this region was found to be characterized by periodic continuous oscillations of finite amplitude, rather than by periodic discontinuous oscillations.

The final region of interest was the area that was outside the linear stability limit (in a region of linear stability) but inside the nonlinear stability limit. It was argued that this was a region where the possibility of triggering discontinuous periodic pressure oscillations existed. This was because, for a given n and μ in this region, two periodic solutions were found, a large amplitude discontinuous solution and a smaller amplitude solution that was either discontinuous or continuous, depending on the normal displacement of the n, μ point under

consideration from the linear stability limit. The smaller amplitude solutions were interpreted as being unstable solutions and thus as representing a triggering limit, in the sense that a disturbance with an amplitude smaller than that of the small amplitude solution at a given n and μ would decay to zero, in agreement with the predictions of linear analysis, while a disturbance with an amplitude greater than that of the small amplitude solution would grow in time and have the large amplitude discontinuous solution as its limit cycle. In other words, though combustors with n and μ in this region should be intrinsically stable, it should be possible to trigger a discontinuous periodic oscillation by the introduction of a disturbance with large enough pressure amplitude. Note that the final form that triggered instability takes is predicted in the present analysis. Earlier work by Sirignano[2] predicted that triggering was possible, but, because of the restriction of his analysis to continuous waveforms, the final form and amplitude of the oscillations so triggered could not be predicted.

In the last two regions of the n, μ plane considered, continuous periodic oscillations were found. In the region where no triggering was possible, but where linear instability was predicted, the continuous oscillations were found to be stable. In the other region, where triggering was possible, the oscillations were taken to be unstable. In both cases the question of how well the continuous solutions matched with the discontinuous solutions arose. In the former situation the matching occurred at the boundary of the region, in the latter it occurred inside the region under investigation. The correspondence between the amplitude and period of the continuous and discontinuous periodic oscillations was found to be very good

in both cases. Also, in both cases the matching point occurred at the normal displacement from the linear stability limit where the amplitude of g became asymptotically equal to $|T_i|$. This corresponds to the point where the nonlinear ordinary differential equation passes from a region where singular behavior is possible to one in which no such behavior is possible. The former is true for amplitudes of g greater than $|T_1|$, the latter for amplitudes less than $|T_1|$. Therefore, it was found that a natural transition from discontinuous to continuous waveforms was inherent in the governing ordinary differential equation.

The wave shapes themselves were found to be strongly dependent on the parameters n and μ. This was true for both continuous and discontinuous oscillations. The continuous oscillations exhibited pressure waveforms, generally of a sinusoid nature, with a steep, sharp positive peak followed by a shallower negative peak. The sharpness and steepness of the positive peak was observed to increase (as well as the amplitude of the oscillation) as the normal displacement from the linear stability limit was increased. The wave had an arbitrarily steep slope arbitrarily close to the value of the normal displacement where the amplitude of g became equal to $|T_1|$.

The salient feature of all the discontinuous waveforms that were found was the negative infinite slope at μ time units after the shock. This reflects the fact that a discontinuity in pressure occurring at a given instant has an effect on the mass release and therefore on the waveform exactly μ time units later. Because the combustion term, or mass generation term, is one order of magnitude smaller ($O(M^2)$ vs. $O(M)$) than the shock itself, the delayed effect is not felt as a discontinuity in f

but rather as an infinitely rapid continuous change in f.

Another characteristic of the discontinuous waveforms was their change in shape as the normal displacement from the linear stability limit was varied. In general, as the displacement from the linear stability limit was increased, the waveforms tended toward the classical "sawtooth" form found in one dimensional cavities with no combustion.[18] As the distance from the linear stability limit became small, on the contrary, the wave shapes tended to have a more sinusoid nature (except, of course, for the infinite slope at μ time units after the shock), similar to those predicted by Chester for driven oscillations near resonance.[3]

The analytical technique that has been presented in this thesis, with the specific purpose of finding periodic continuous or discontinuous oscillations driven by a particular combustion model is, in reality, quite general. That is, other combustion models could easily be substituted for the time-lag model in the equations and boundary conditions. Indeed, a model predicting instantaneous response, such as the one used by Sirignano in his study of shock wave instability would be far simpler to consider than was the time-lag model. Models considering the droplet vaporization rate as the controlling mechanism in the combustion process might also, in principle, be considered. It should be noted, however, that any combustion model that is to be employed in the method of analysis presented here must satisfy the condition that its strength can be measured by the steady-state Mach number. In other words, the interaction between the combustion mechanism and the pressure oscillations must be of second order or smaller so that acoustic equations describe the flow field to lowest order. In particular, it is not clear that it would be possible to consider a

postulated nonlinear combustion mechanism such as droplet shattering using the present approach.

Some suggestions for the extension of the analytical work performed in this thesis present themselves. The first extension that might be attempted is the integration of the differential-integral equation determining the form of the arbitrary first order function for the case of distributed combustion, for several different velocity profiles. This would give a more precise idea of the effect that distributing the combustion zone has on the stability behavior of a combustor. This extension would in essence be a problem in numerical integration. A somewhat more difficult modification of the theory that would be of interest is the relaxation of the condition that $\frac{d\bar{u}}{dx} = O(M_E)$, which was used here in the treatment of distributed combustion. Difficulties would develop in such an analysis due to the fact that material, or entropy waves would have to be considered. Finally, pursuant to the comments made in the preceding paragraph, it should be of interest to perform analyses, similar to the one presented here, using different models of combustion.

C. Comparison With Experiment

Because of the tenuous way that the time-lag model is related to the physico-chemical combustion processes that actually occur in a liquid propellant rocket engine, it is not possible to be very optimistic about finding any real correspondence between the predictions of the present analytical work and the experimentally observed behavior of rocket engines exhibiting longitudinal mode instability. Nonetheless, because the existence of a characteristic time, which is the main feature of the time-lag model, has been verified experimentally in a series of experiments

by Crocco, Grey and Harrje,[7] it is reasonable to hope that some kind of at least qualitative agreement might occur when fully developed nonlinear oscillations are considered.

In the experiments of Crocco, Grey and Harrje just mentioned, which were performed in order to check the validity of the linear stability theory based on the time-lag model, it was observed that, near the stability limits, the regime oscillations observed were often continuous in form, while farther from the stability limit they assumed discontinuous shock-type forms.[7] This is in agreement with the results of the present work. For, it will be recalled that, according to the analytical results presented, the nonlinear stability limit passes inside the linear stability limit for certain regions of the n, μ plane, thus forming regions where stable, continuous oscillations are possible. The regions where such continuous oscillations are possible are always predicted to be very close to the linear stability limit. If the displacement from the linear stability limit is increased, a point is reached where the nonlinear stability limit for discontinuous solutions is reached and then passed, so that at displacements greater than this only discontinuous oscillations can be predicted. In other words, only close to the stability limit are continuous solutions predicted; at greater displacements only discontinuous oscillations are possible according to the present theory.

Other general qualitative agreements between theory and experiment can be cited, such as the fact that triggering of first longitudinal mode instability is possible in regions of linear stability (Reference 21), and the fact that the form that the triggered oscillations take are discontinuous in nature (Reference 22). The fact that τ, the time-lag,

is fixed according to the theory, at least for discontinuous oscillations, by the interval after the discontinuity at which the slope of the pressure waveform becomes negative infinite, and that, for a given time-lag, the value of n is determined by the shock amplitude (see Figure 7), suggests that, if one makes the somewhat chauvinistic assumption that the combustion processes are represented in some reasonable, if gross, way by the time-lag model, then, by observing the waveforms and amplitudes of discontinuous axial oscillations in an experimental rocket engine, it should be possible to assign n and τ values to that given rocket configuration and thus to locate the particular combustor on the theoretical n, τ plane. The above procedure is, of course, contingent on the observation of discontinuous waveforms that do, indeed, exhibit infinite negative slopes (or a reasonable indication of such behavior) at some point. Unfortunately, it is not clear whether, when this behavior is not observed, the absence of the expected phenomena is due to the inability of the present pressure sensing and recording devices to always record the rapid decrease in pressure, or to the fact that the predicted behavior simply does not occur. In the future, improved pressure recording equipment is to be installed at Princeton which should be capable of answering the question just posed. For the present, the author feels it is of some interest, if only of speculative interest, to present a correlation of the type described above for a particular pressure waveform that was observed in the Princeton square rocket motor which clearly exhibited a pressure decay that approximates a negative infinite slope at two points in time. The reason for the two points of infinite slope is the fact that the pressure pickup was located downstream of the injector so that both an incident and a reflected shock would be observed (see Figure 19). The square motor in question was 68 5/8 inches

long in the configuration from which the pressure trace was taken. Since the length of the nozzle from its entrance to its throat is only 1.5 inches and the combustion zone is estimated to extend from 6 to 8 inches from the injector, it is seen that the assumptions of short nozzle and concentrated combustion are not too bad for the rocket under consideration.

Simply by measuring the distance between the shock and the point of (nearly) infinite slope, and then dividing by the total observed length of the period, a value for the ratio of the assumed time-lag, $\hat{\tau}$, to the period was determined. Because of the definition of the nondimensional quantity μ, the ratio of the physical time-lag to the real period had to be equal to $\hat{\mu}/2$, where $\hat{\mu}$ is the value of μ for the particular combustion configuration considered. This value of $\mu = \hat{\mu}$ determined a line on the theoretical n, μ plane, (Figure 7). Using the experimentally determined value of the shock amplitude one then looked along the line of constant μ, $\mu = \hat{\mu}$ until a match between the theoretical and experimental shock amplitude occurred. This point where the amplitudes matched then determined the value of n, $\hat{n}$, for the particular combustor configuration under consideration.

The values of $\hat{n}$ and $\hat{\mu}$ for this one attempted correlation were $\hat{n} = 1.42$, $\hat{\mu} = .38$. By looking at Figure 2 this point on the n, μ plane is seen to be in a region where triggering is possible and where linear stability is predicted. It is somewhat surprising that this is, indeed, precisely the observed behavior of the rocket engine tested. That is, the configuration is intrinsically stable but can be pulsed into stable oscillations that are nearly periodic and are discontinuous in form.

Figure 24 shows a comparison between the theoretical and experimental waveforms for the values of n and μ under consideration. The agreement is not astonishingly good, but this is to be expected due to the roughness of the time-lag model. However, the points where the slopes become negative infinite (or approximately so) on the experimental trace are clearly seen to correspond with the theoretical predictions in a reasonable way.

Since the results just presented are for one run of one rocket configuration,it is, of course, possible that the agreement indicated is simply fortuitous. However, the evidence does seem sufficient to warrant a comprehensive comparison of theory and experiment in the future. In particular, the effect of changing the length of the experimental motor on the observed time-lag should be compared with the corresponding change predicted by theory. In such an experiment the configuration of the injector and the mixture ratio of the propellants would remain fixed so that the "physical" n and τ^* would be constant. Another experiment that might be performed would be to vary the size of the pulses used to trigger the instability to see if agreement between theory and experiment on the value of the limiting triggering amplitude exists. In this experiment the rocket configuration would not be varied. It should be emphasized that the anticipated improvements in pressure recording equipment make an experimental program of this type feasible.

Finally, it should be said that though an excellent agreement between theory and experiment is not likely, efforts of the kind mentioned above seem worthwhile,because, even if a moderately successful correlation results, the combustion parameters n , and τ for a given unstable (in

the nonlinear sense) rocket configuration will be able to be determined simply by looking at a pressure record made during the unstable operation of the given motor. In the end, the results of many such correlations could be combined to relate the heuristic combustion parameters n and τ to such relevant rocket engine design parameters as injector design and mixture ratio.

REFERENCES

1. Crocco, L. and Cheng, S.I., Theory of Combustion Instability in Liquid Propellant Rocket Motors, AGARD Monograph No. 8, Butterworths Scientific Pub., Ltd. London, 1956.

2. Sirignano, W.A., "A Theoretical Study of Nonlinear Combustion Instability: Longitudinal Mode", Technical Report No. 677, Department of Aerospace and Mechanical Sciences, Princeton University, March 1964 (Ph.D. Thesis).

3. Chester, W., "Resonant Oscillations in Closed Tubes", Journal of Fluid Mechanics, 18 (1964).

4. Cantrell, R.H., Hart, R.W., "Interaction Between Sound and Flow in Acoustic Cavities: Mass, Momentum and Energy Considerations", The Journal of the Acoustical Society of America, Volume 36, Number 4, April 1964.

5. Crocco, L., "Theoretical Studies on Liquid Propellant Rocket Instability", 10th Symposium (International) on Combustion, Combustion Institute, Pittsburgh, Penn., June 1965.

6. Crocco, L. Aerotecnica 33, 46 (1953)

7. Crocco, L., Grey, J., Harrje, D.T., "Theory of Liquid Propellant Rocket Combustion Instability and its Experimental Verification", ARS Journal, Vol. 30, No. 2, February 1960

8. Crocco, L., Harrje, D.T., and Reardon, F.H., "Transverse Combustion Instability in Liquid Propellant Rocket Motors", Journal American Rocket Society, 32 (1962) 3.

9. Crocco, L., and Sirignano, W.A., "Behavior of Supercritical Nozzles Under Three Dimensional Oscillatory Conditions" Princeton University Department of Aerospace and Mechanical Sciences Technical Report No. 790 (to be published as an AGARDograph).

10. Minorsky, N., Nonlinear Oscillations, D. Van Nostrand Co., Inc. 1962.

11. Courant, R., and Friedrichs, K.O., Supersonic Flow and Shock Waves, Interscience Publishers, Inc., 1948.

12. Shapiro, A.H., The Dynamics and Thermodynamics of Compressible Fluid Flow, The Ronald Press Co., 1953.

13. Tsien, H.S., "The Transfer Functions of Rocket Nozzles", ARS Journal, 22 (1952) 139, 162.

14. Reardon, F.H., "An Investigation of Transverse Mode Combustion Instability in Liquid Propellant Rocket Motors", Princeton University Aeronautical Engineering Report 550, June 1, 1961, (Ph.D. Thesis).

15. Scala, S.M., Transverse Wave and Entropy Wave Combustion Instability in Liquid Propellant Rockets, Princeton University Aeronautical Engineering Report No. 380, April 1957, (Ph.D. Thesis).

16. Zinn, B.T., "A Theoretical Study of Nonlinear Transverse Combustion Instability in Liquid Propellant Rocket Motors", Princeton University Department of Aerospace and Mechanical Sciences Technical Report No. 732. (Ph.D. Thesis)

17. Lin, C.C., "On a Perturbation Theory Based on the Method of Characteristics", Journal of Math and Physics, Vol. 33, No. 2, July 1954.

18. Chu, B.T., "Analysis of a Self-Sustained Nonlinear Vibration in a Pipe Containing a Heater", AFOSR-TN-1755, September 1961.

19. Fox, P.A., "On the Use of Coordinate Perturbations in the Solution of Physical Problems", MIT Project DIC-6915 Technical Report No. 1, November 1953.

20. Bowman, C.T., "Experimental Investigation of High-Frequency Longitudinal Combustion Instability In Gaseous Propellant Rocket Motors", Princeton University Department of Aerospace and Mechanical Sciences Technical Report No. 784. (Ph.D. Thesis)

21. Crocco, L., Harrje, D.T. et al, "Nonlinear Aspects of Combustion Instability in Liquid Propellant Rocket Motors", (Fourth Yearly Progress Report), Department of Aerospace and Mechanical Sciences Report 553-d, June 1, 1964.

22. Crocco, L., Harrje, D.T., et al, "Nonlinear Aspects of Combustion Instability in Liquid Propellant Rocket Motors", (Fifth Yearly Progress Report), Department of Aerospace and Mechanical Sciences Report 553-e, June 1, 1965.

23. Crocco, L., Private Communication, March 1965.

24. Sirignano, W.A., and Crocco, L., "A Shock Wave Model of Unstable Rocket Combustors", AIAA Journal, Vol. 2, No. 7, July 1964

25. Chu, B.T., and Ying, S.J., "Thermally Driven Nonlinear Oscillations in a Pipe with Travelling Shock Waves", Physics of Fluids, Vol. 6, No. 11 Nov. 1963.

Schematic representation of regions I and II

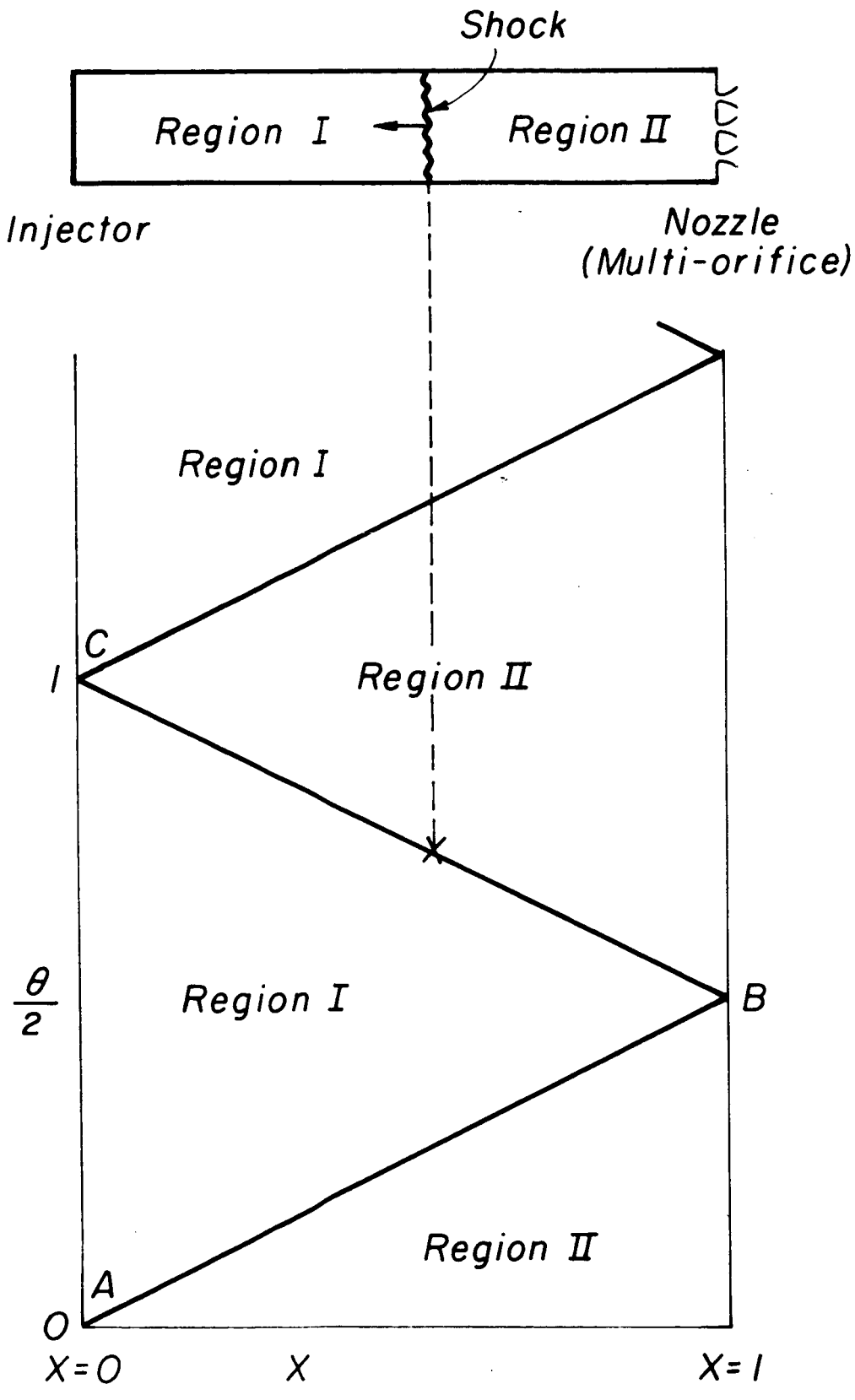

Figure I

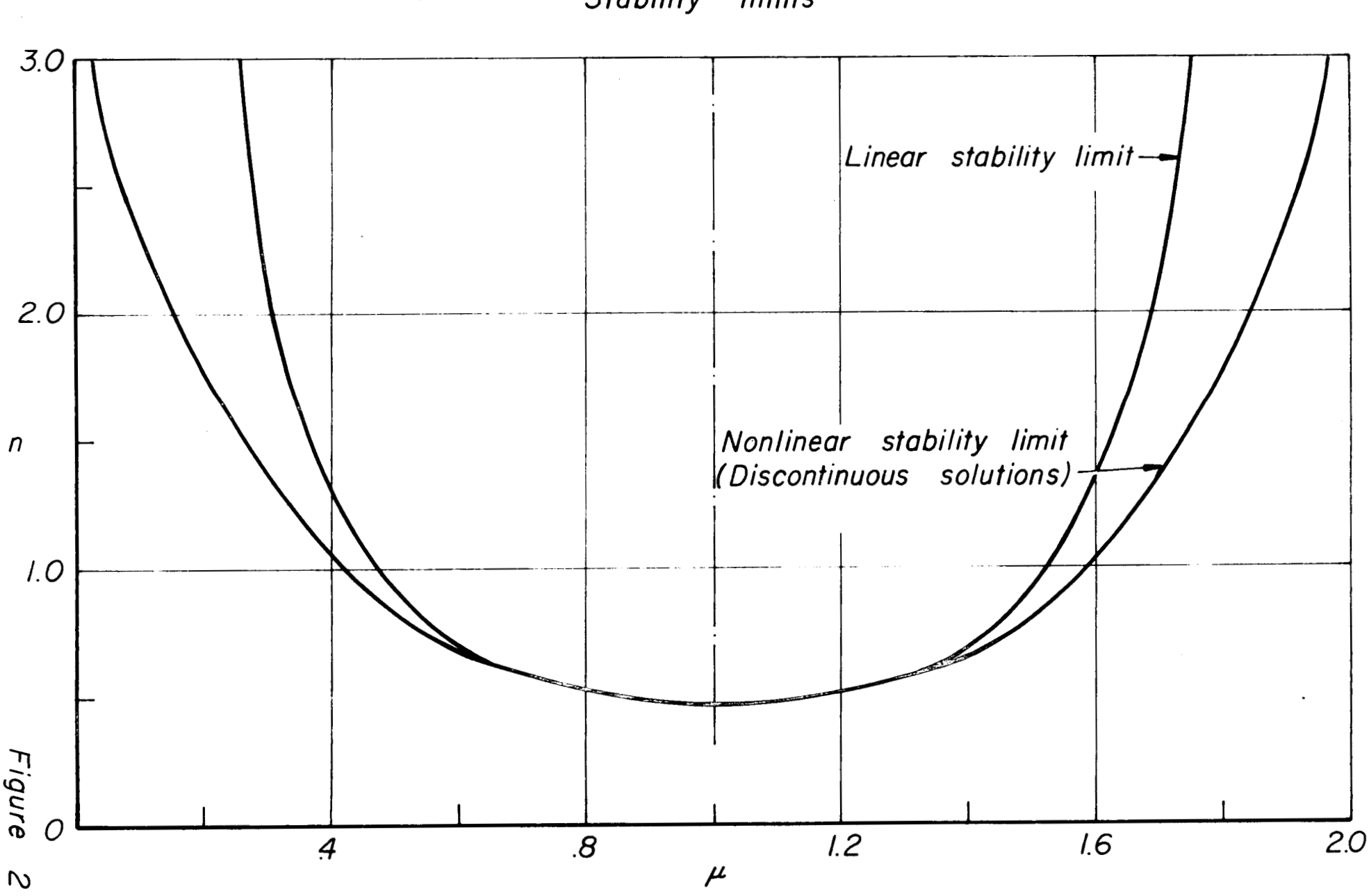
Stability limits
3.0
2.0
1.0
0
n
.4
.8
1.2
1.6
2.0
μ
Linear stability limit
Nonlinear stability limit
(Discontinuous solutions)

Figure 2

Relation of solutions for μ values symmetrically displaced from unity

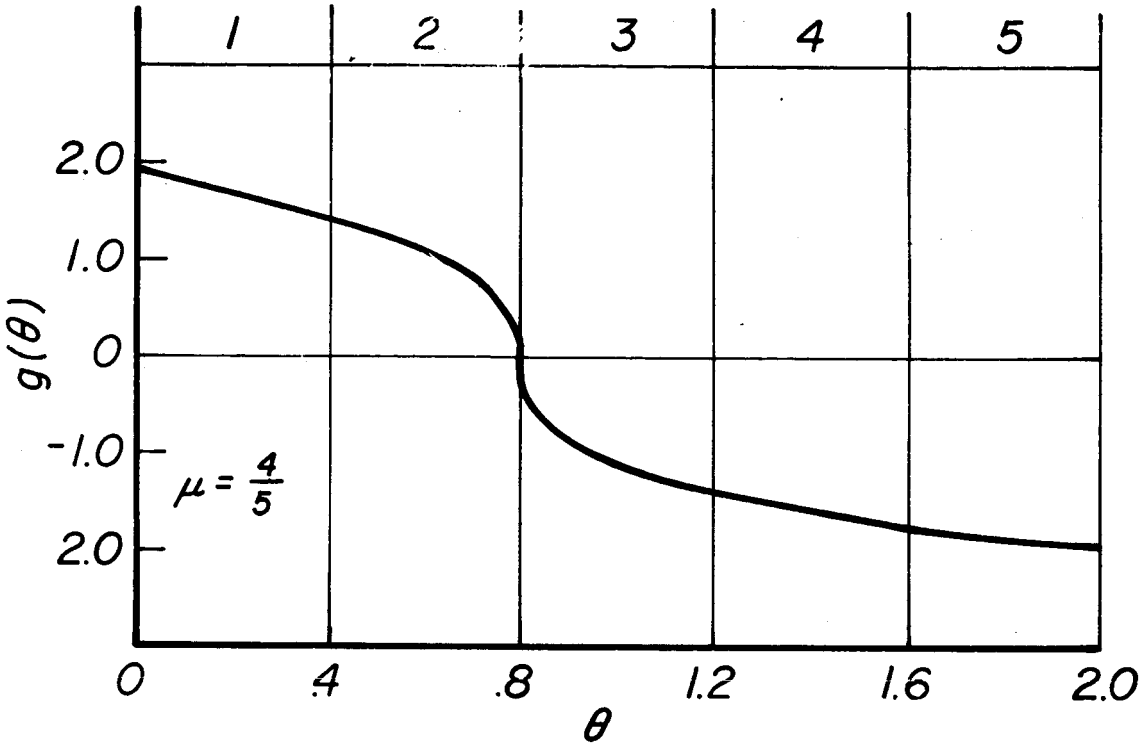

Figure 3A

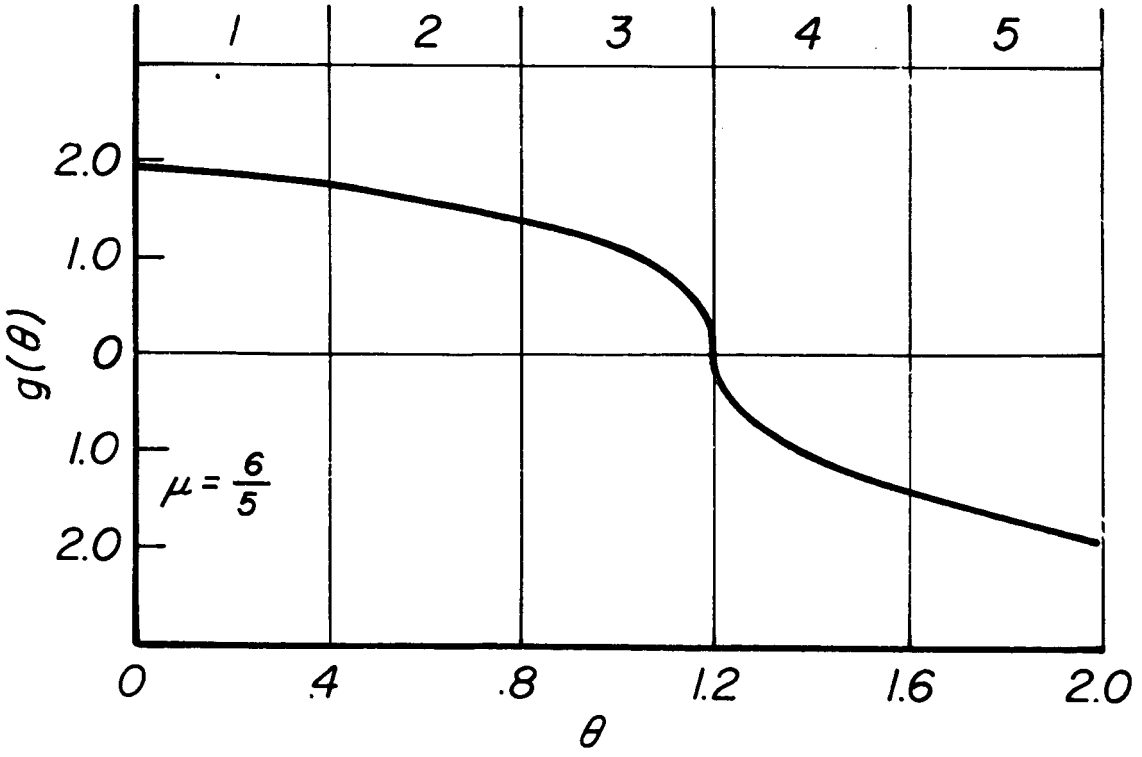

Figure 3B

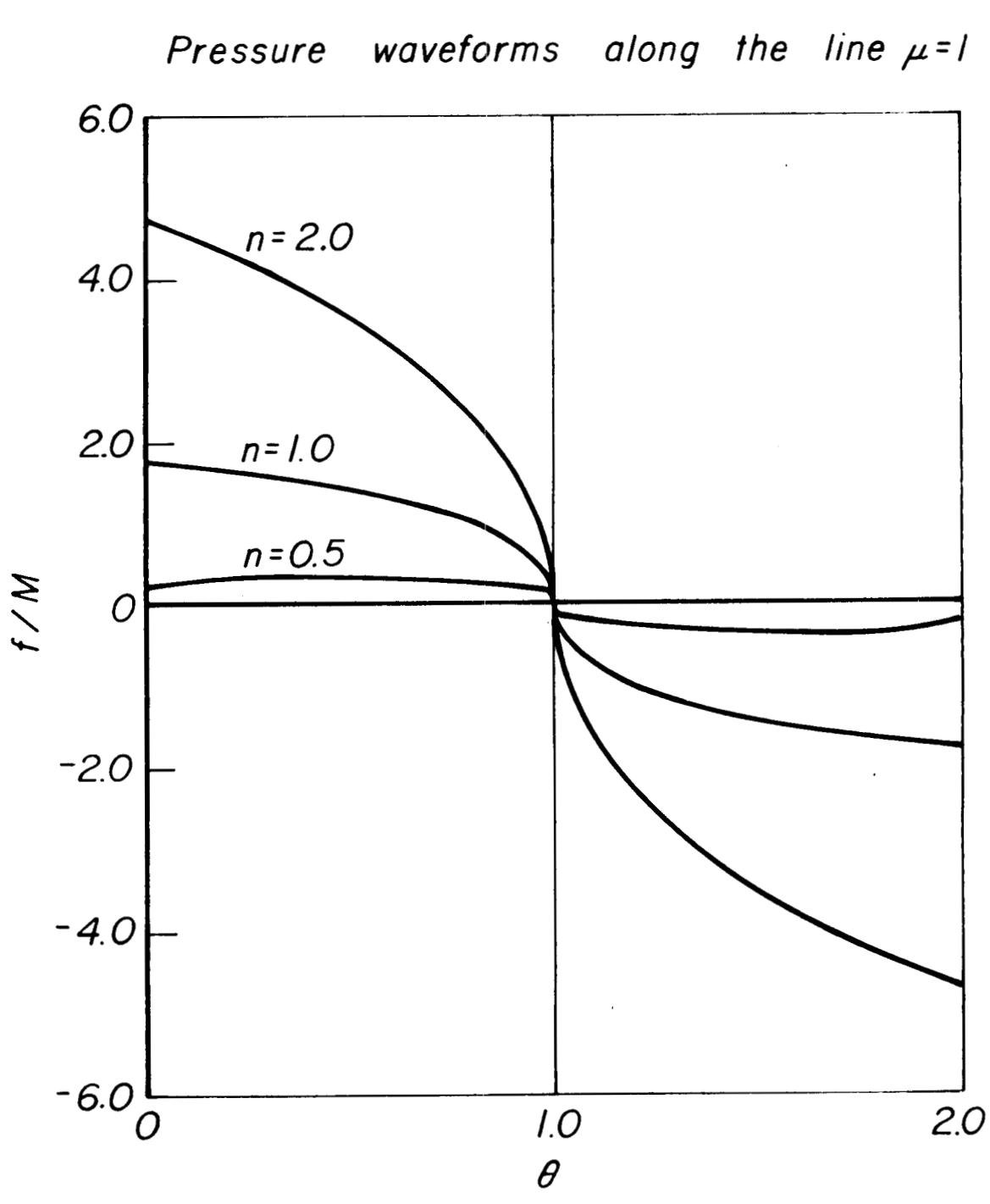
Pressure waveforms along the line μ=1
6.0
4.0
2.0
0
-2.0
-4.0
-6.0
f/M
n=2.0
n=1.0
n=0.5
0
1.0
2.0
θ

Figure 4

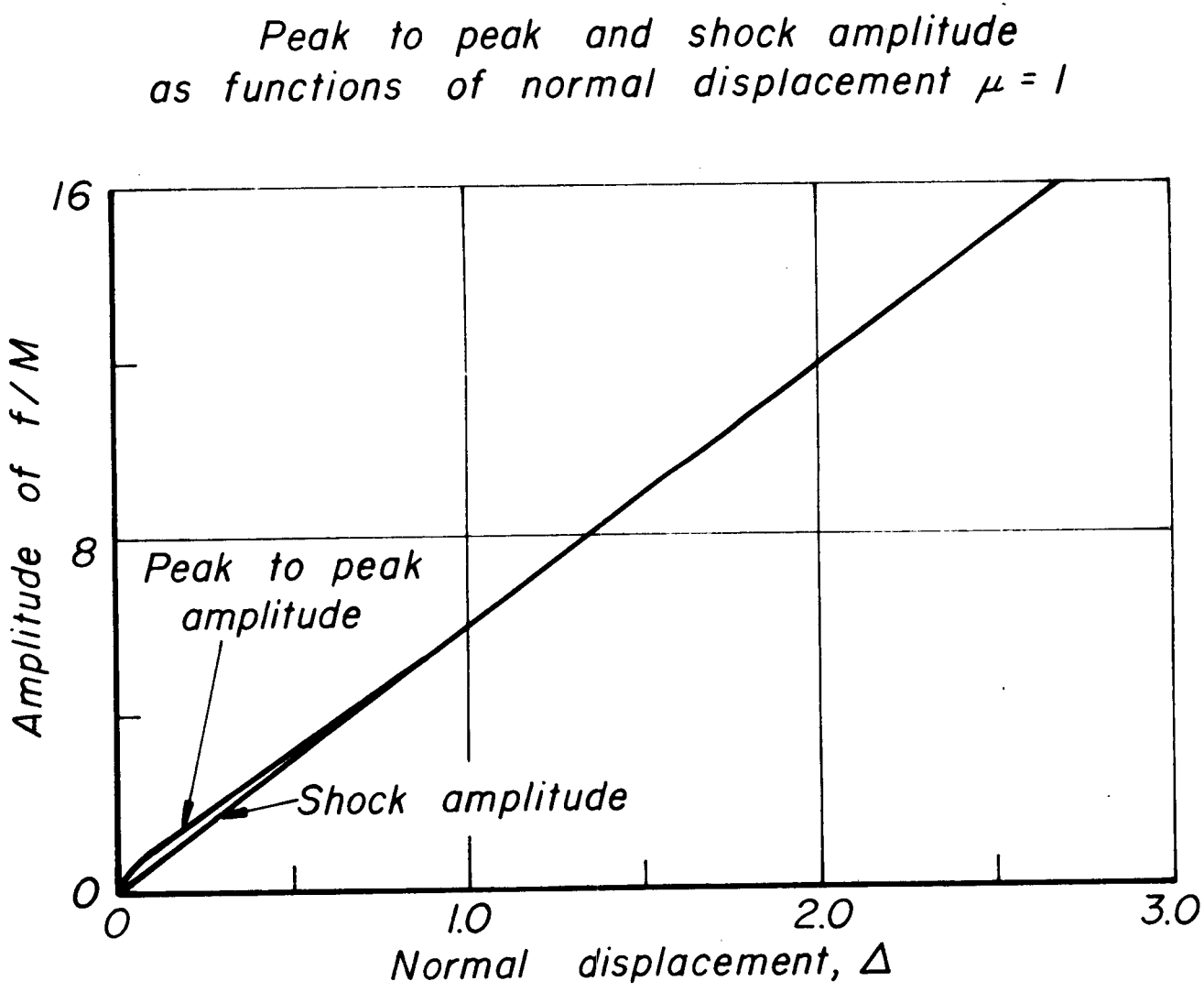
Peak to peak and shock amplitude
as functions of normal displacement $\mu = 1$
16
8
0
Amplitude of f/M
Peak to peak
amplitude
Shock amplitude
0
1.0
2.0
3.0
Normal displacement, Δ

Figure 5

Pressure wave forms along the line $\mu = 1$

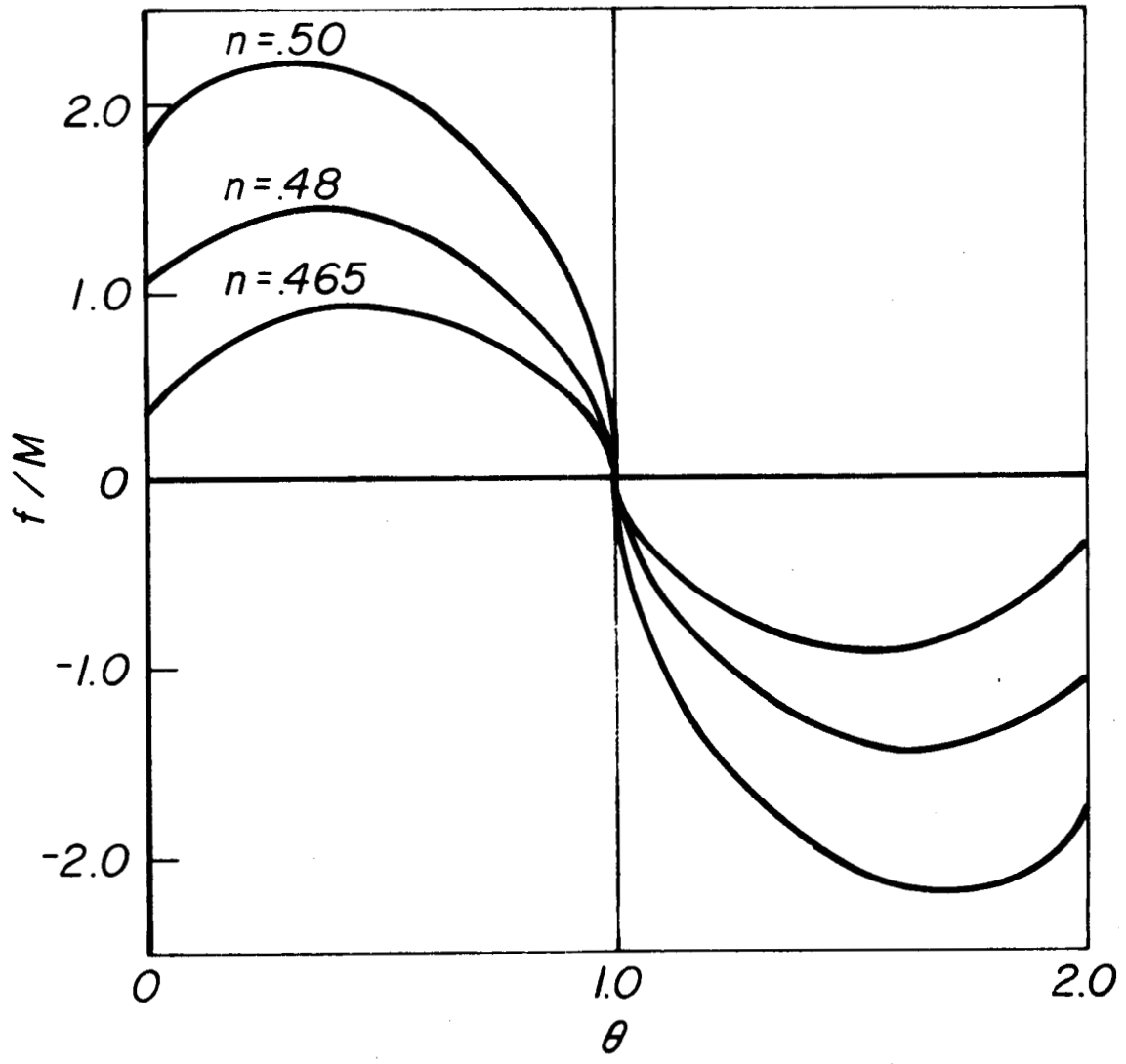

Figure 6

JP21-4213-67

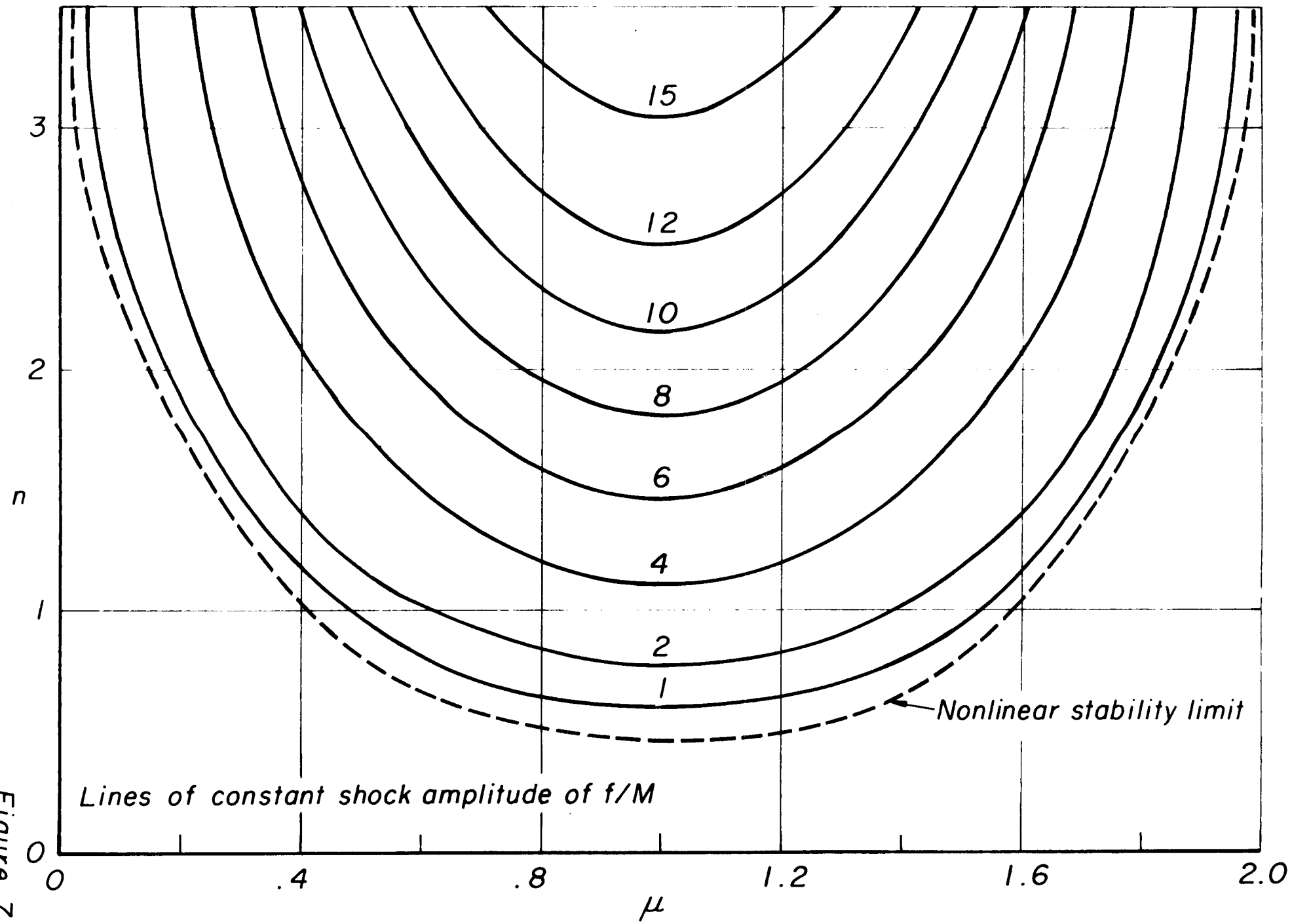

Figure 7

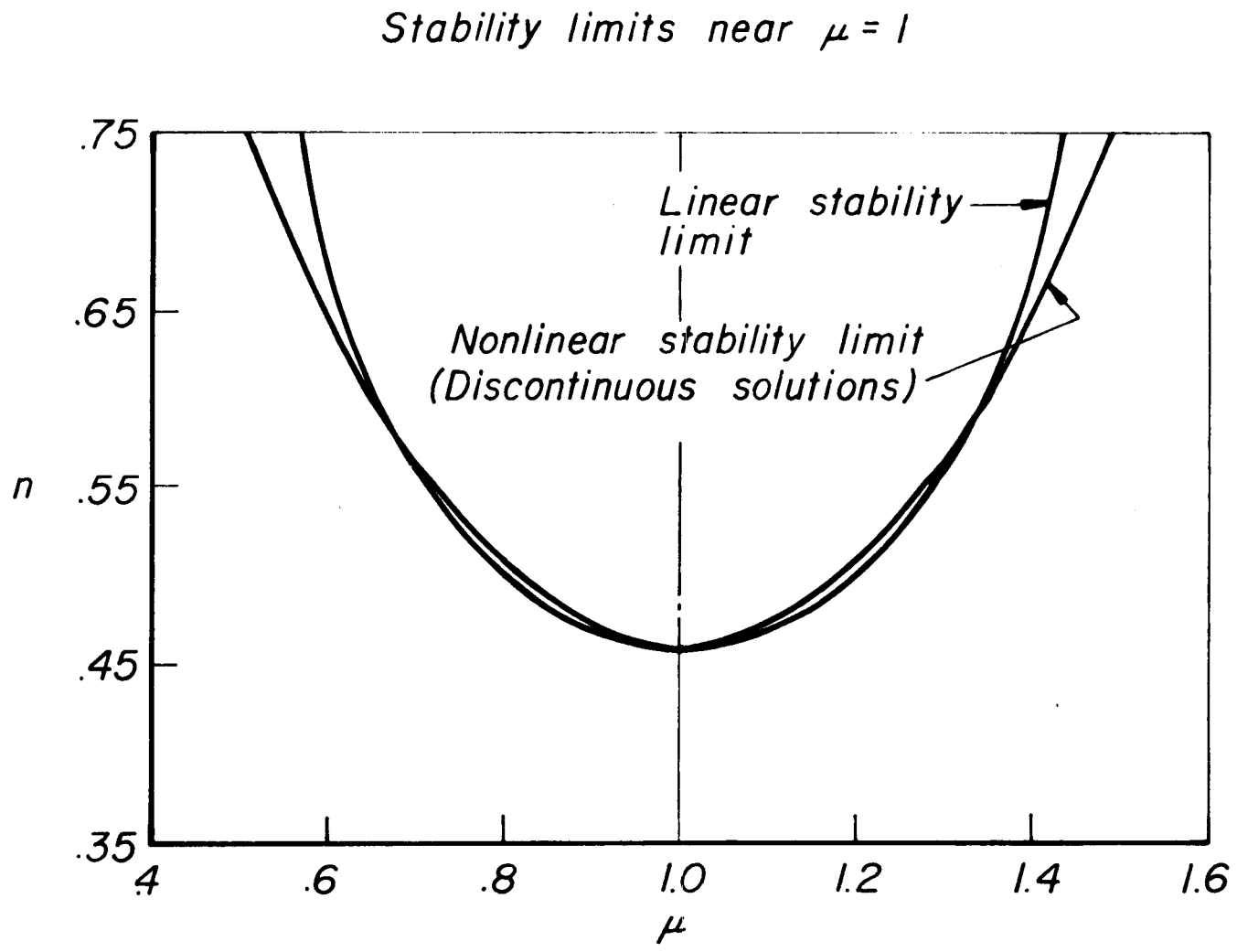
Stability limits near $\mu = 1$
.75
.65
.55
.45
.35
n
.4
.6
.8
1.0
1.2
1.4
1.6
μ
Linear stability limit
Nonlinear stability limit
(Discontinuous solutions)

Figure 8

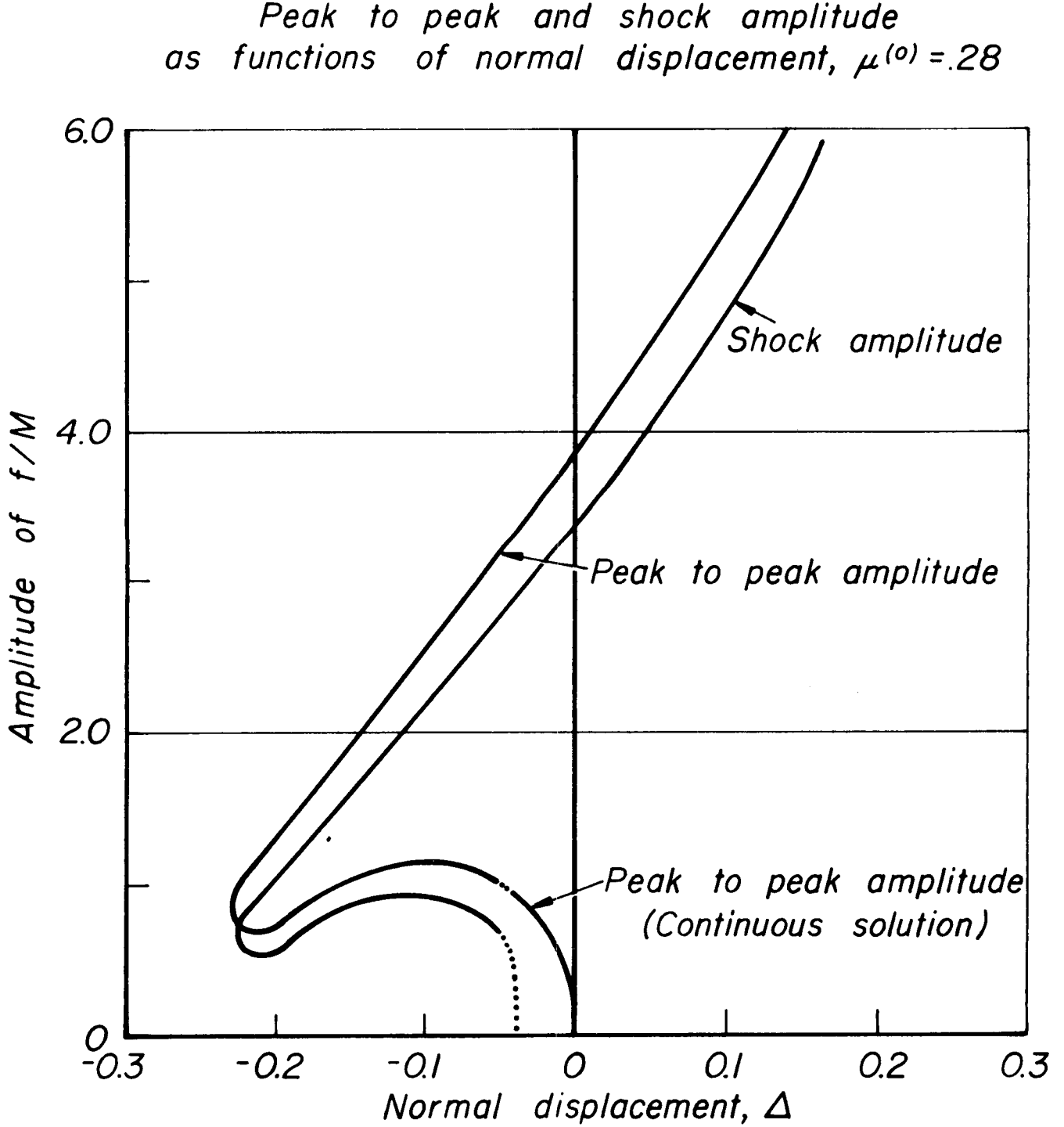
Peak to peak and shock amplitude
as functions of normal displacement, $\mu^{(o)} = .28$
6.0
4.0
2.0
0
Amplitude of f/M
Shock amplitude
Peak to peak amplitude
Peak to peak amplitude
(Continuous solution)
-0.3
-0.2
-0.1
0
0.1
0.2
0.3
Normal displacement, Δ

Figure 9

$\mathcal{D}$, The displacement factor, as a function of $\mu^{(o)}$

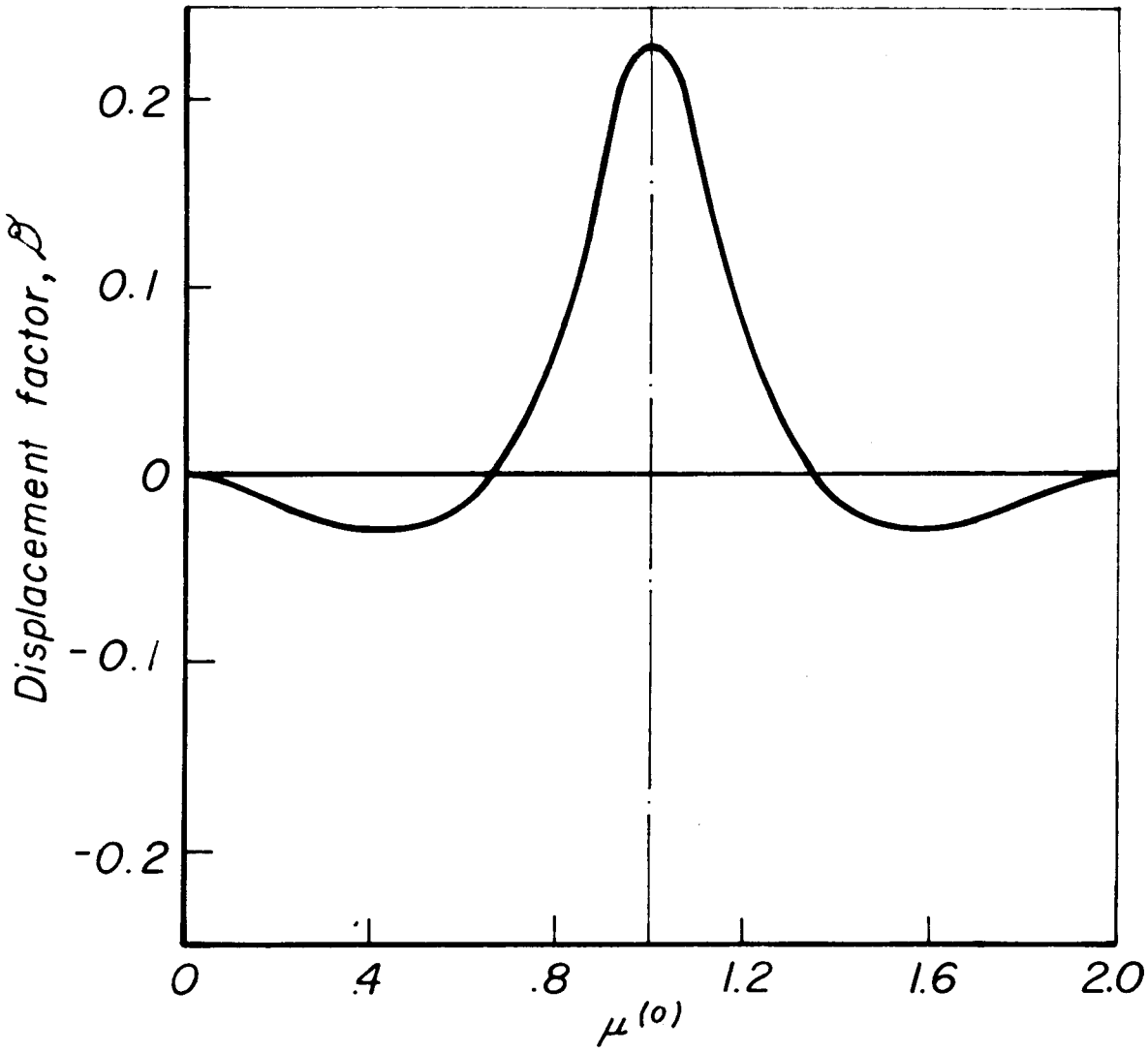

Figure 10

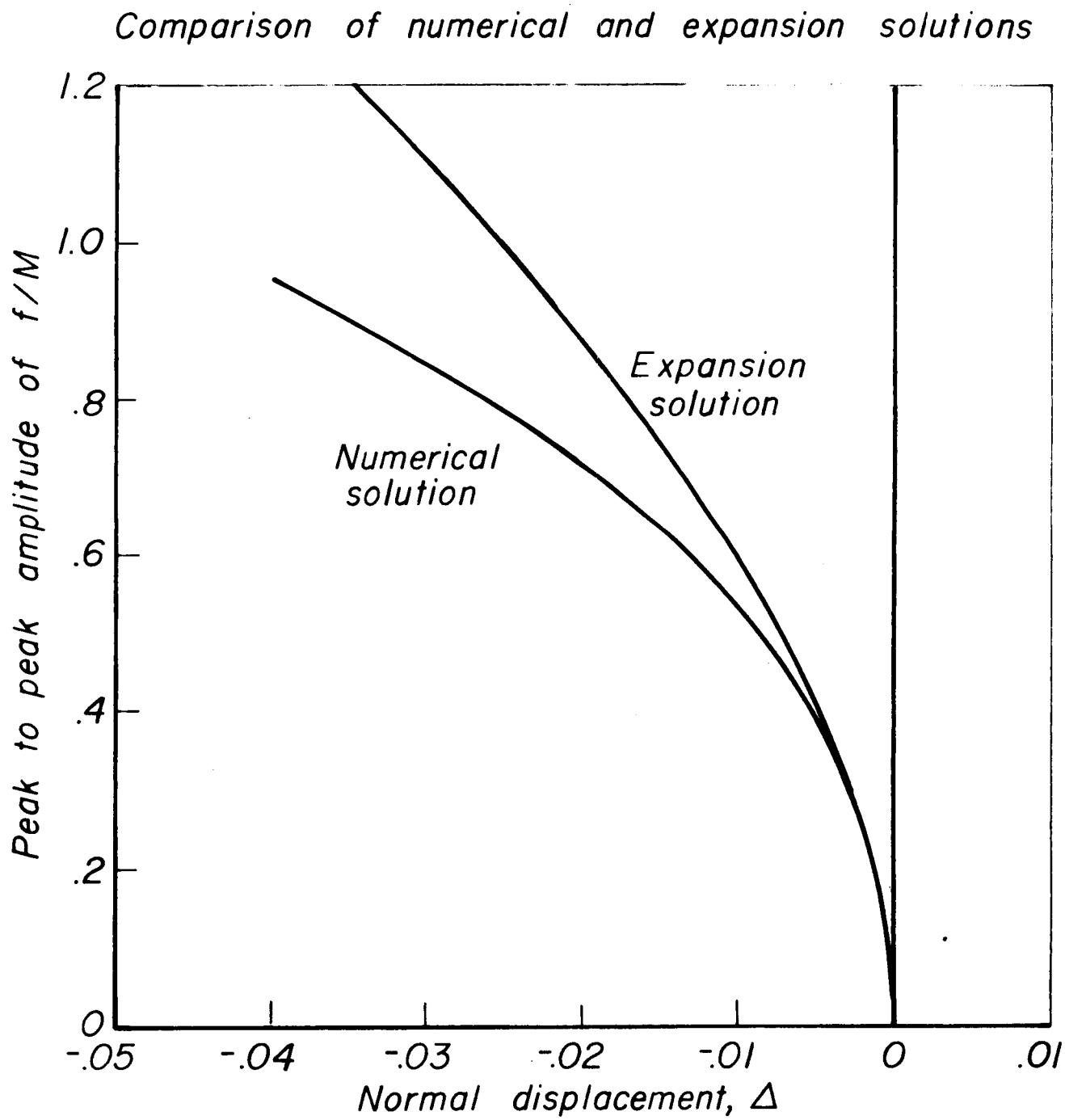
Comparison of numerical and expansion solutions
Peak to peak amplitude of f/M
1.2
1.0
.8
.6
.4
.2
0
-.05
-.04
-.03
-.02
-.01
0
.01
Normal displacement, Δ
Expansion solution
Numerical solution

Figure 11

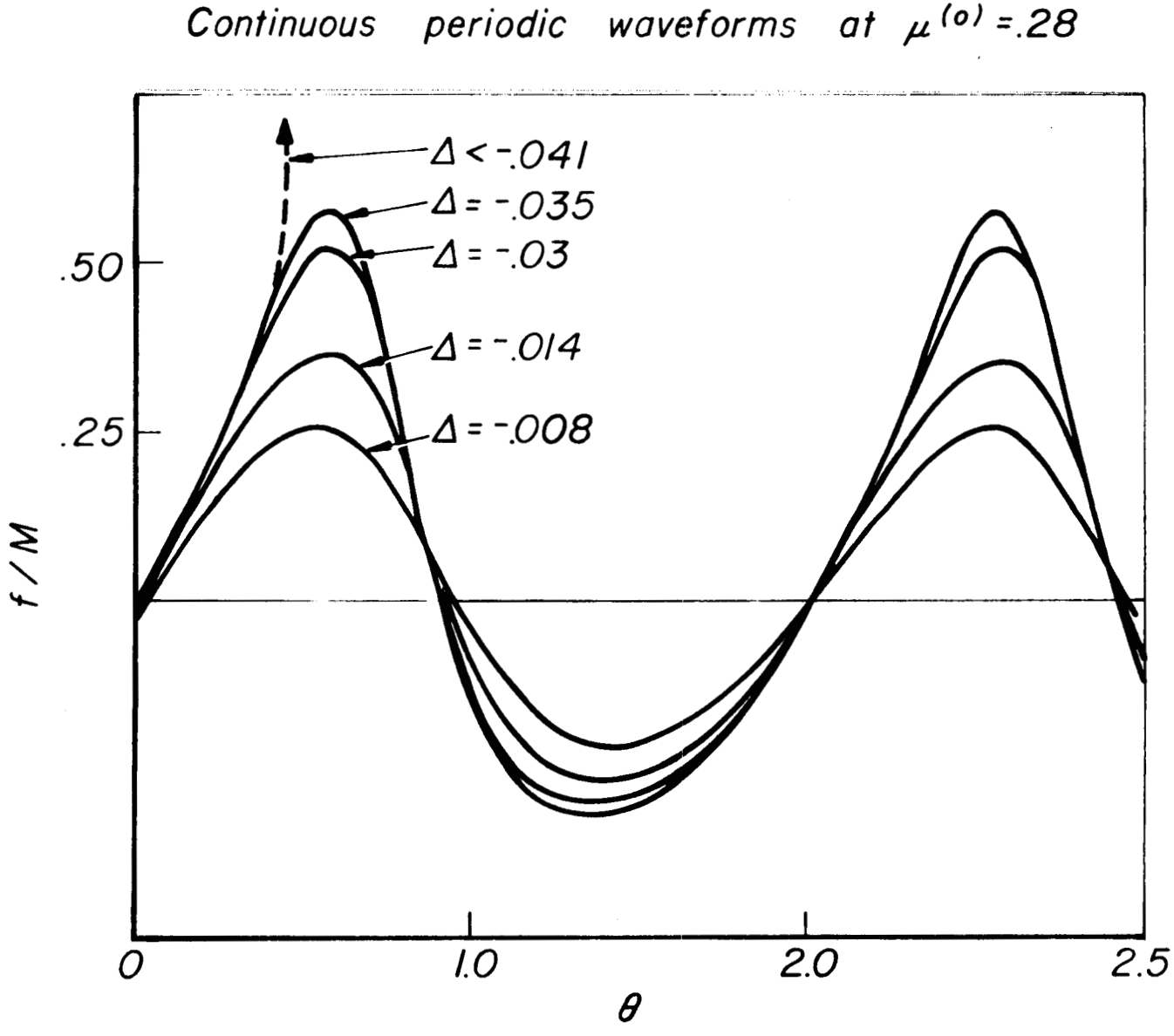
Continuous periodic waveforms at $\mu^{(o)} = .28$
$\Delta < -.041$
$\Delta = -.035$
$\Delta = -.03$
$\Delta = -.014$
$\Delta = -.008$
.50
.25
f / M
0
1.0
2.0
2.5
θ

Figure 12

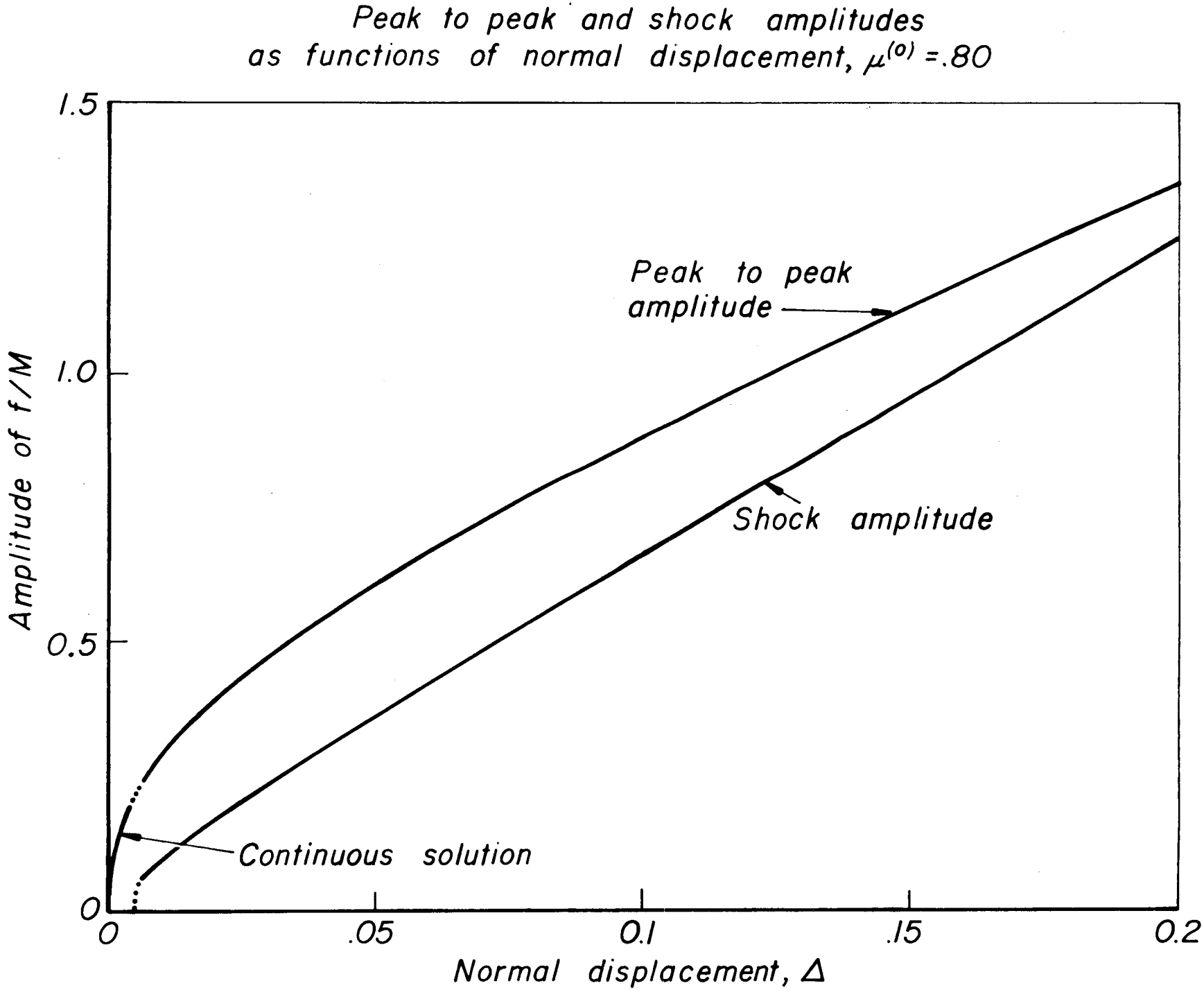
Peak to peak and shock amplitudes
as functions of normal displacement, $\mu^{(o)} = .80$
1.5
1.0
0.5
0
Amplitude of f/M
Peak to peak
amplitude
Shock amplitude
Continuous solution
0
.05
0.1
.15
0.2
Normal displacement, Δ

Figure 13

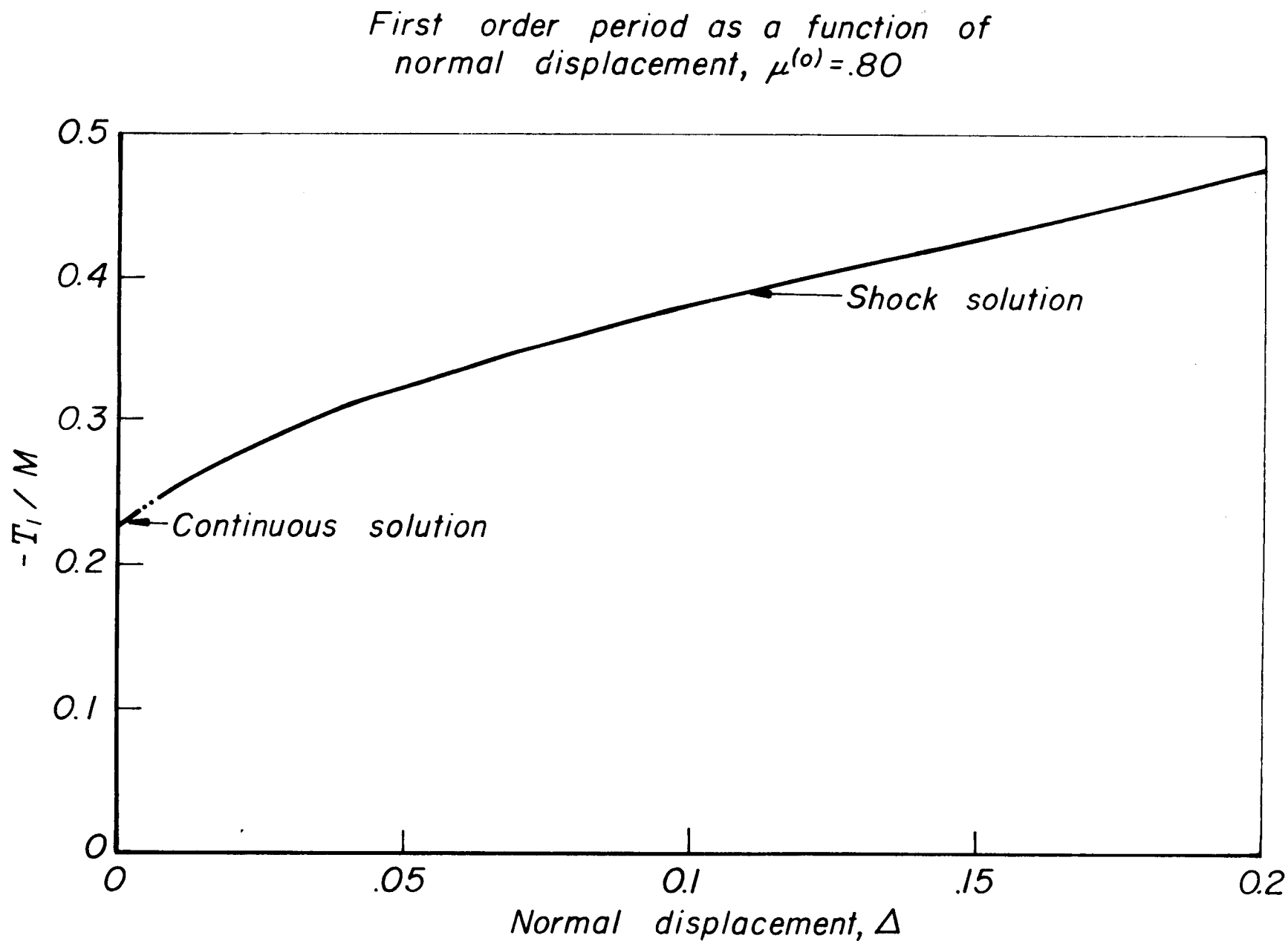
First order period as a function of normal displacement, $\mu^{(o)} = .80$
0.5
0.4
0.3
0.2
0.1
0
$-T_1 / M$
Shock solution
Continuous solution
0
.05
0.1
.15
0.2
Normal displacement, Δ

Figure 14

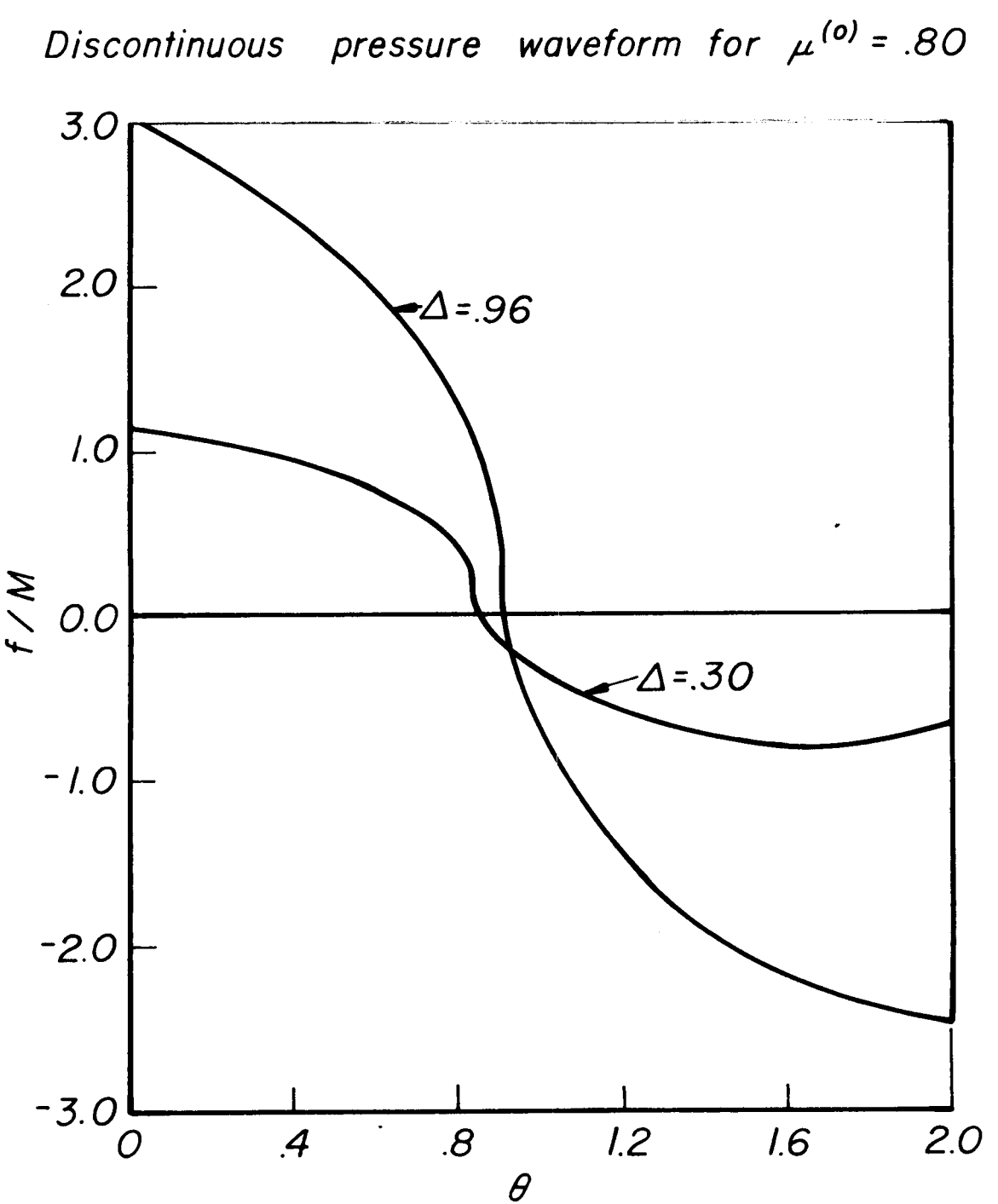
Discontinuous pressure waveform for $\mu^{(o)} = .80$
3.0
2.0
1.0
0.0
-1.0
-2.0
-3.0
f / M
Δ=.96
Δ=.30
0
.4
.8
1.2
1.6
2.0
θ

Figure 15

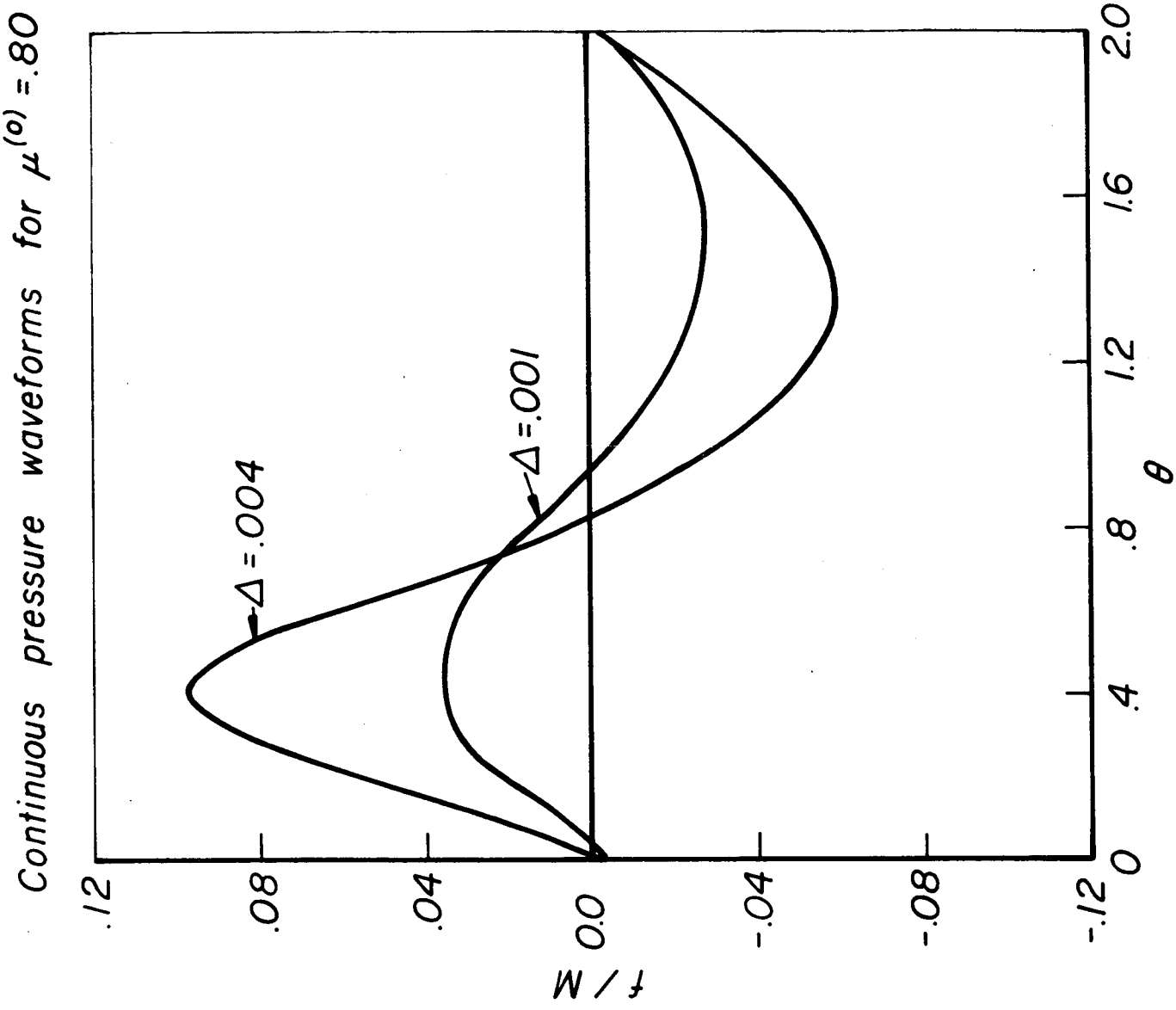
Continuous pressure waveforms for $\mu^{(o)} = .80$
Δ = .004
Δ = .001
f / M
θ
.12
.08
.04
0.0
-.04
-.08
-.12
0
.4
.8
1.2
1.6
2.0

Figure 16

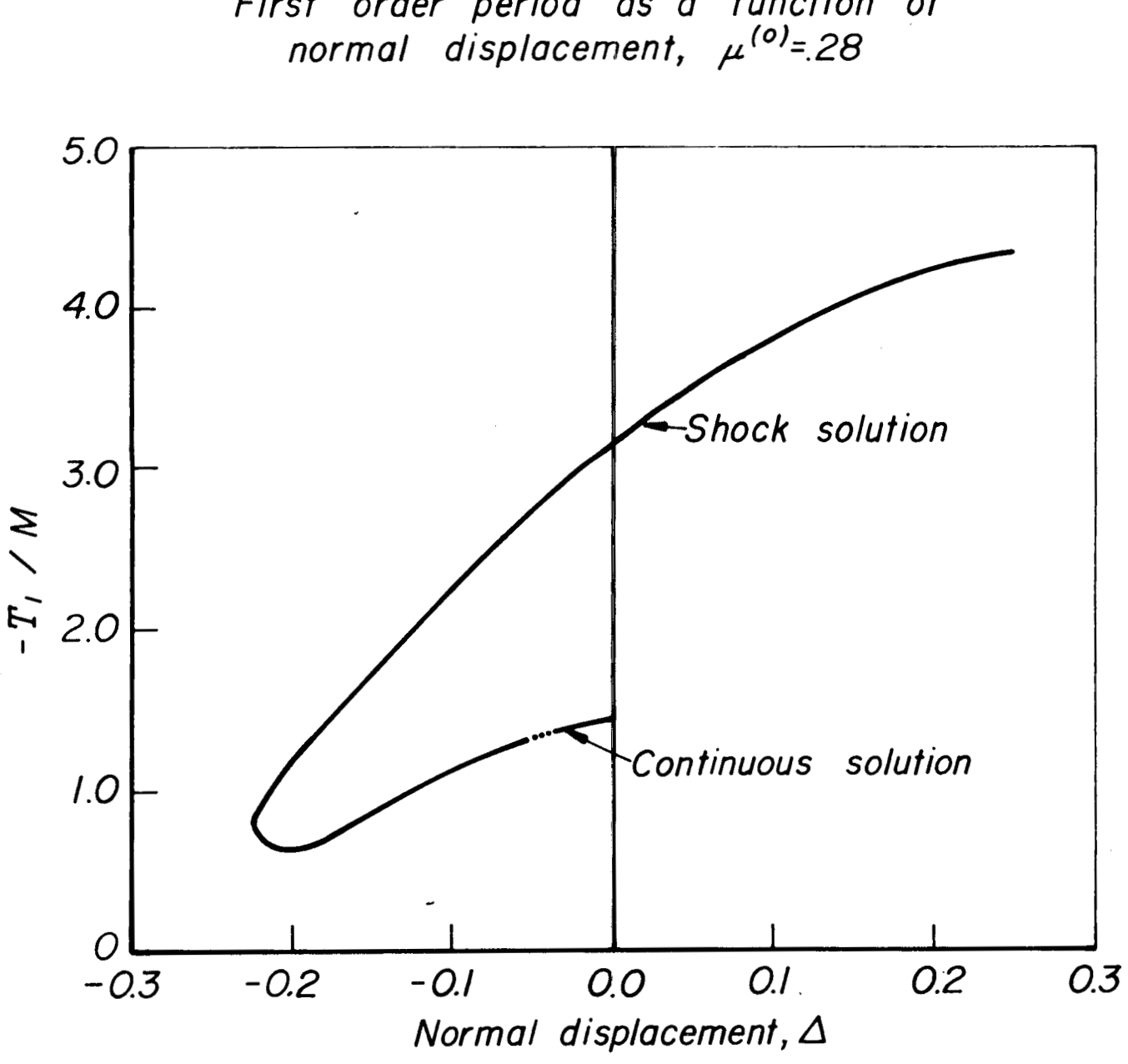
First order period as a function of normal displacement, $\mu^{(o)}=.28$
5.0
4.0
3.0
2.0
1.0
0
$-T_1 / M$
Shock solution
Continuous solution
-0.3
-0.2
-0.1
0.0
0.1
0.2
0.3
Normal displacement, Δ

Figure 17

Discontinuous pressure waveforms for $\mu^{(0)} = .28$

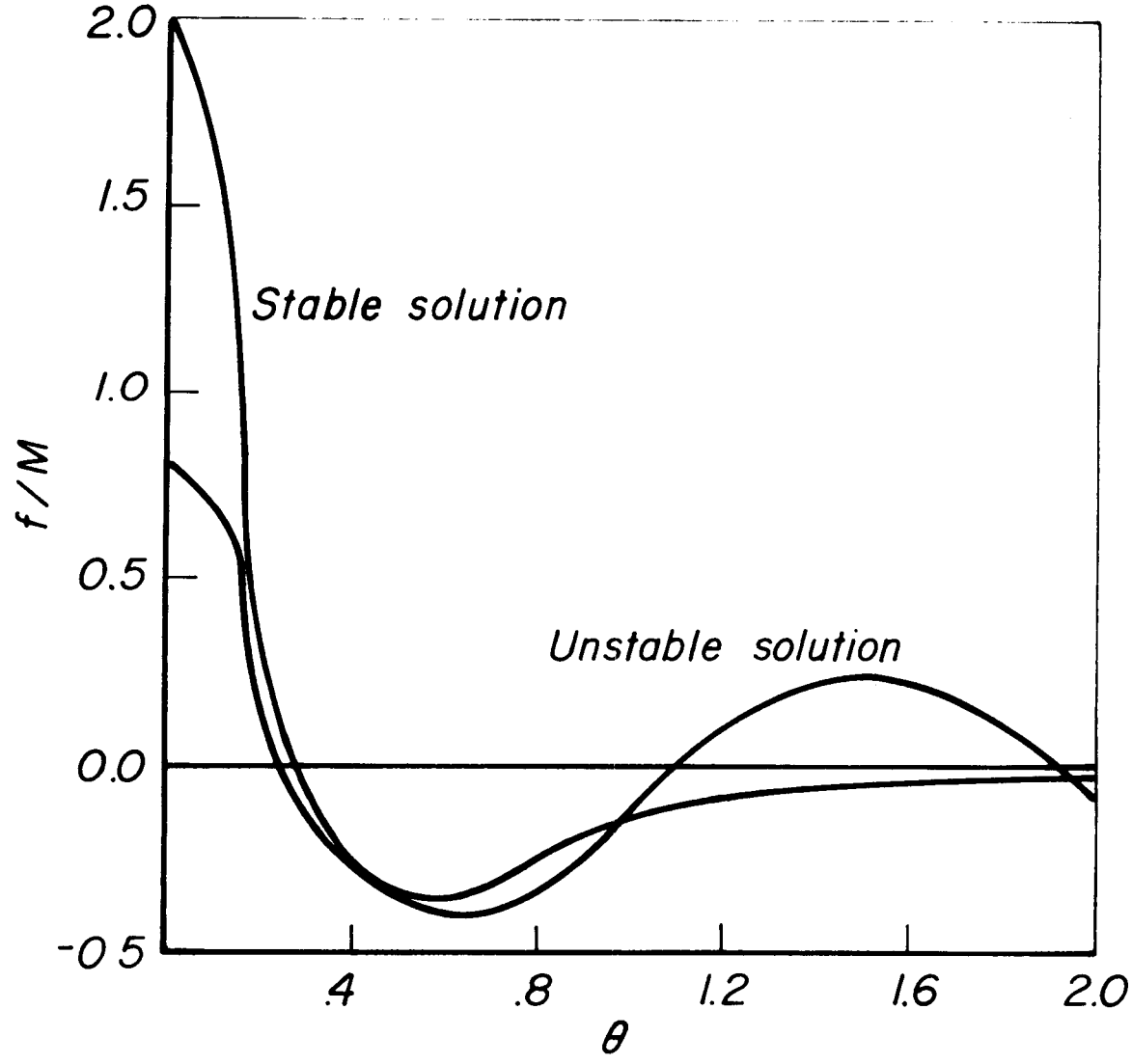

Figure 18

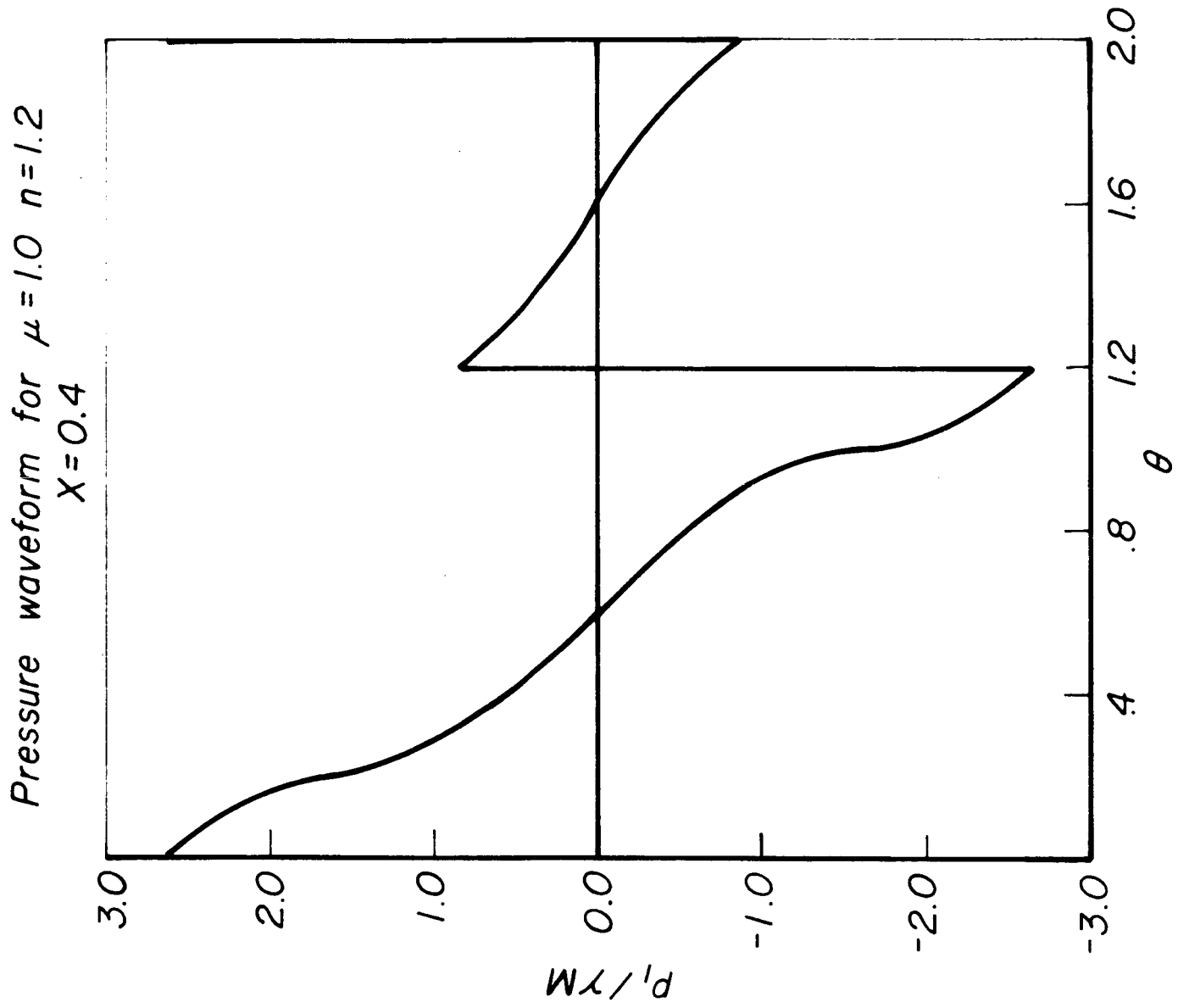
Pressure waveform for $\mu = 1.0$ $n = 1.2$
$X = 0.4$
$p_1/\gamma M$
3.0
2.0
1.0
0.0
-1.0
-2.0
-3.0
.4
.8
1.2
1.6
2.0
θ

Figure 19

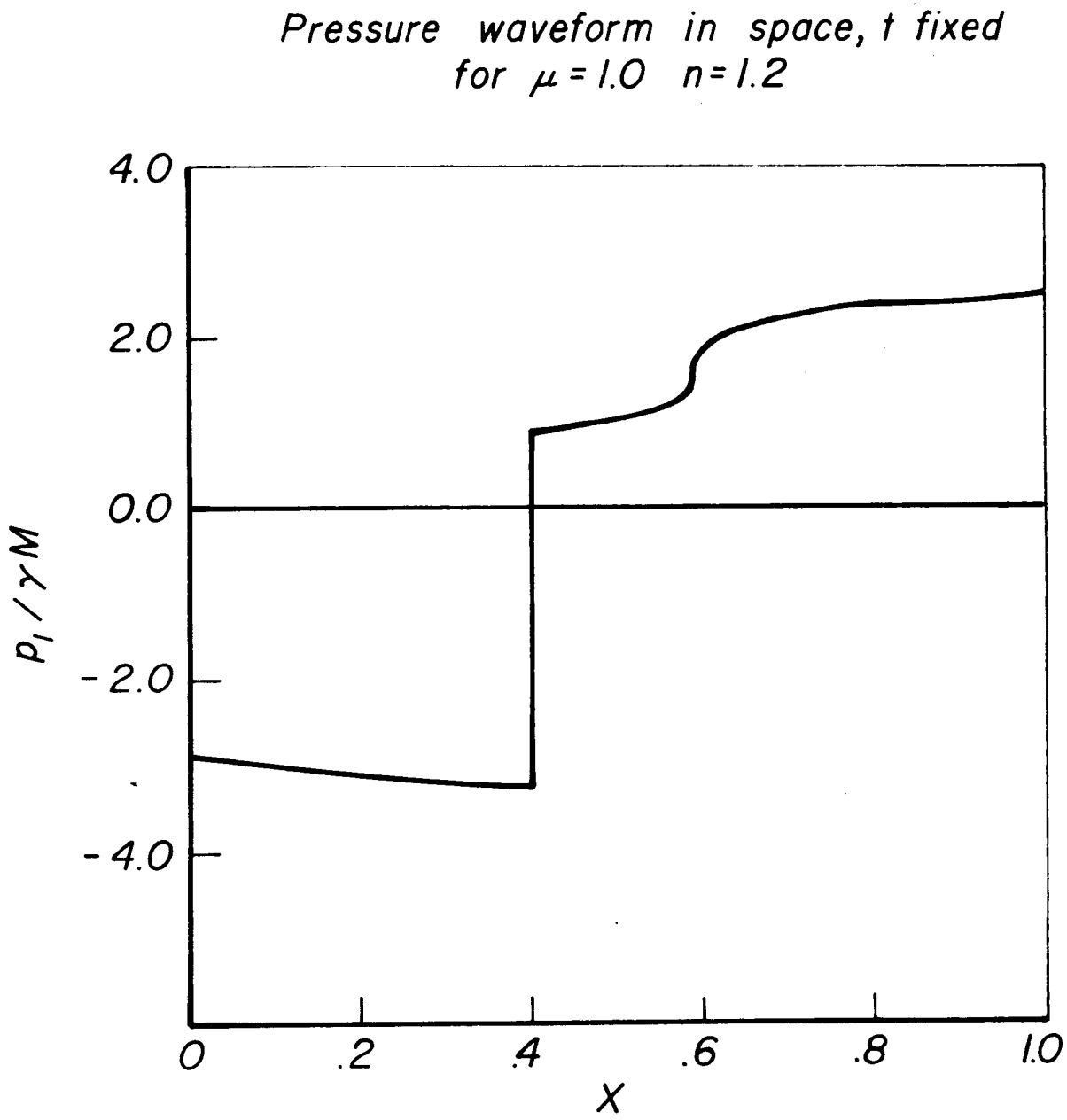
Pressure waveform in space, t fixed
for μ = 1.0 n = 1.2
4.0
2.0
0.0
-2.0
-4.0
p1 / γM
0
.2
.4
.6
.8
1.0
X

Figure 20

SP21-4229-67

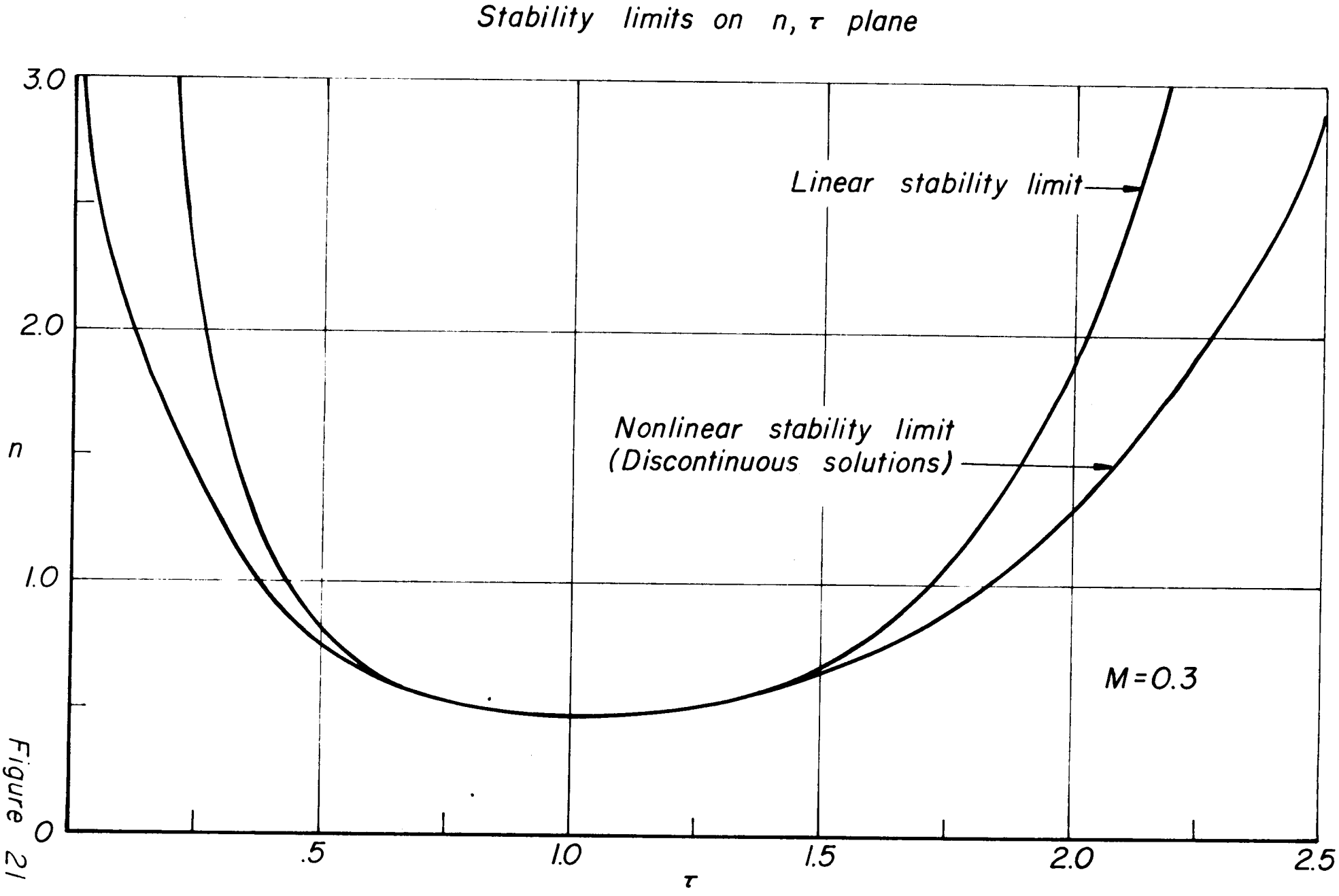

Figure 21

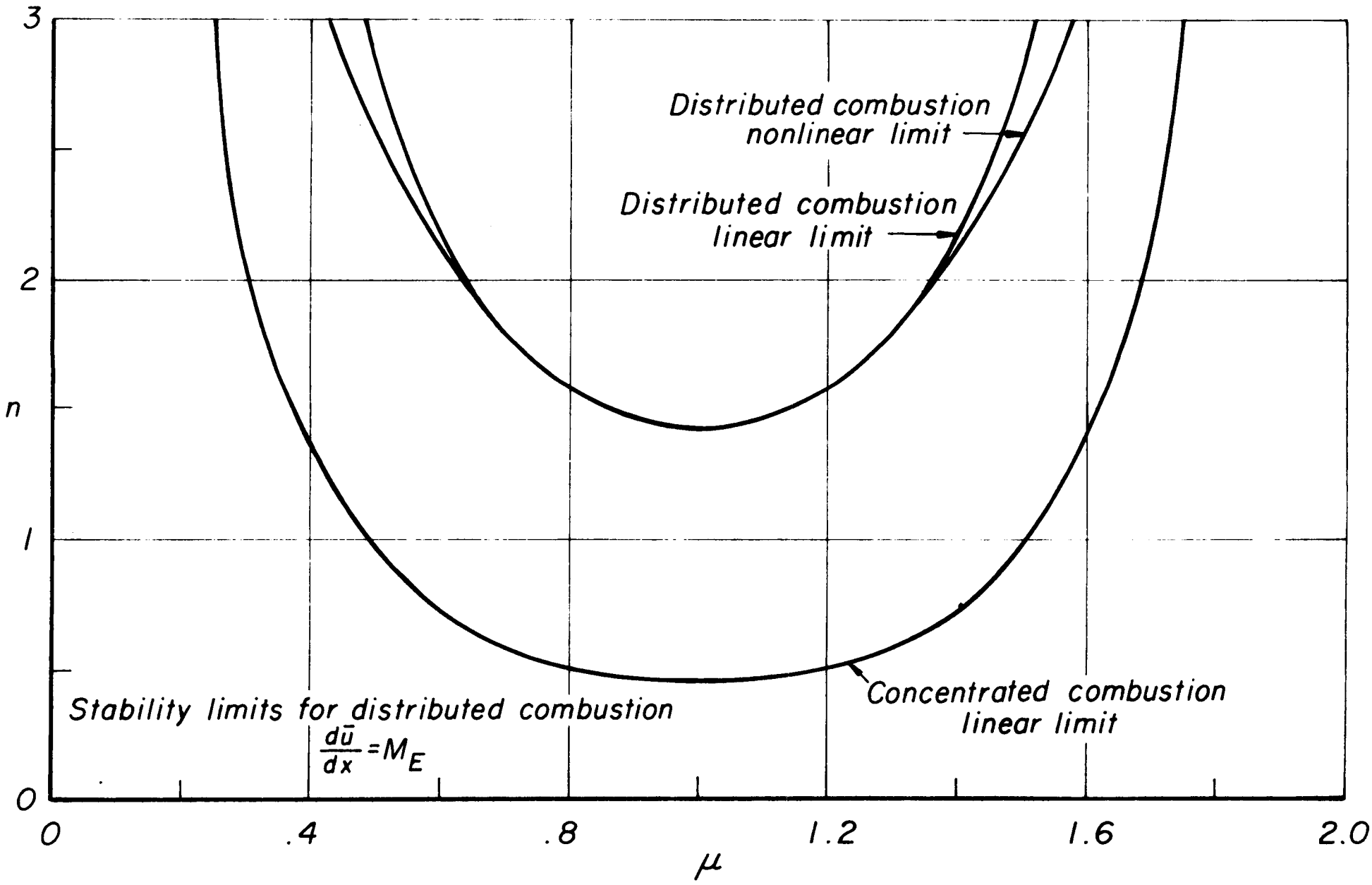
3
2
1
0
n
0
.4
.8
1.2
1.6
2.0
μ
Distributed combustion nonlinear limit
Distributed combustion linear limit
Concentrated combustion linear limit
Stability limits for distributed combustion
$\frac{d\bar{u}}{dx} = M_E$

Figure 22

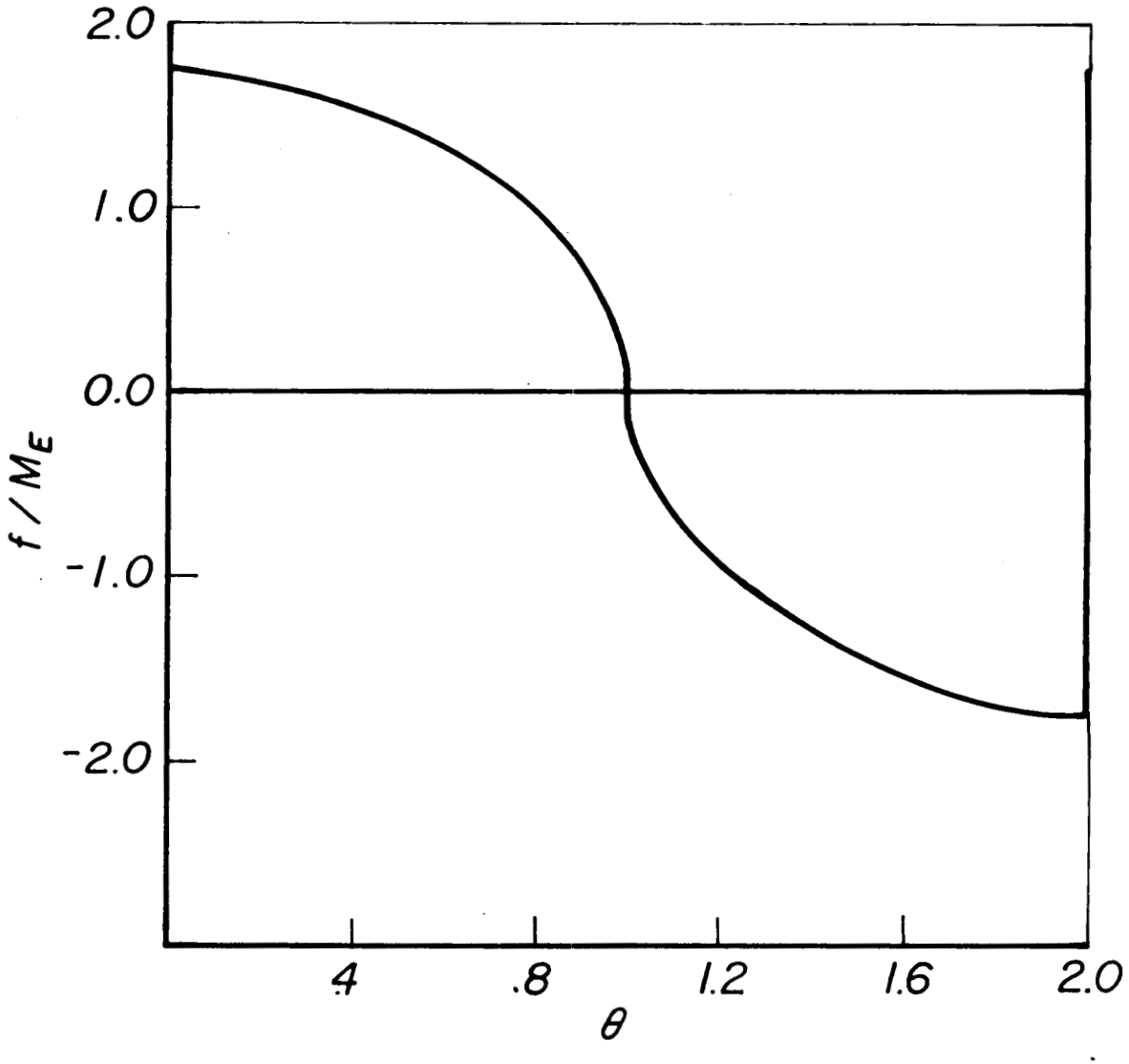
Pressure waveform for $\mu = 1.0$ $n = 2.5$
Distributed combustion $d\bar{u}/dx = M_E$
2.0
1.0
0.0
-1.0
-2.0
f/M_E
.4
.8
1.2
1.6
2.0
θ

Figure 23

A comparison of theoretical and experimental waveforms

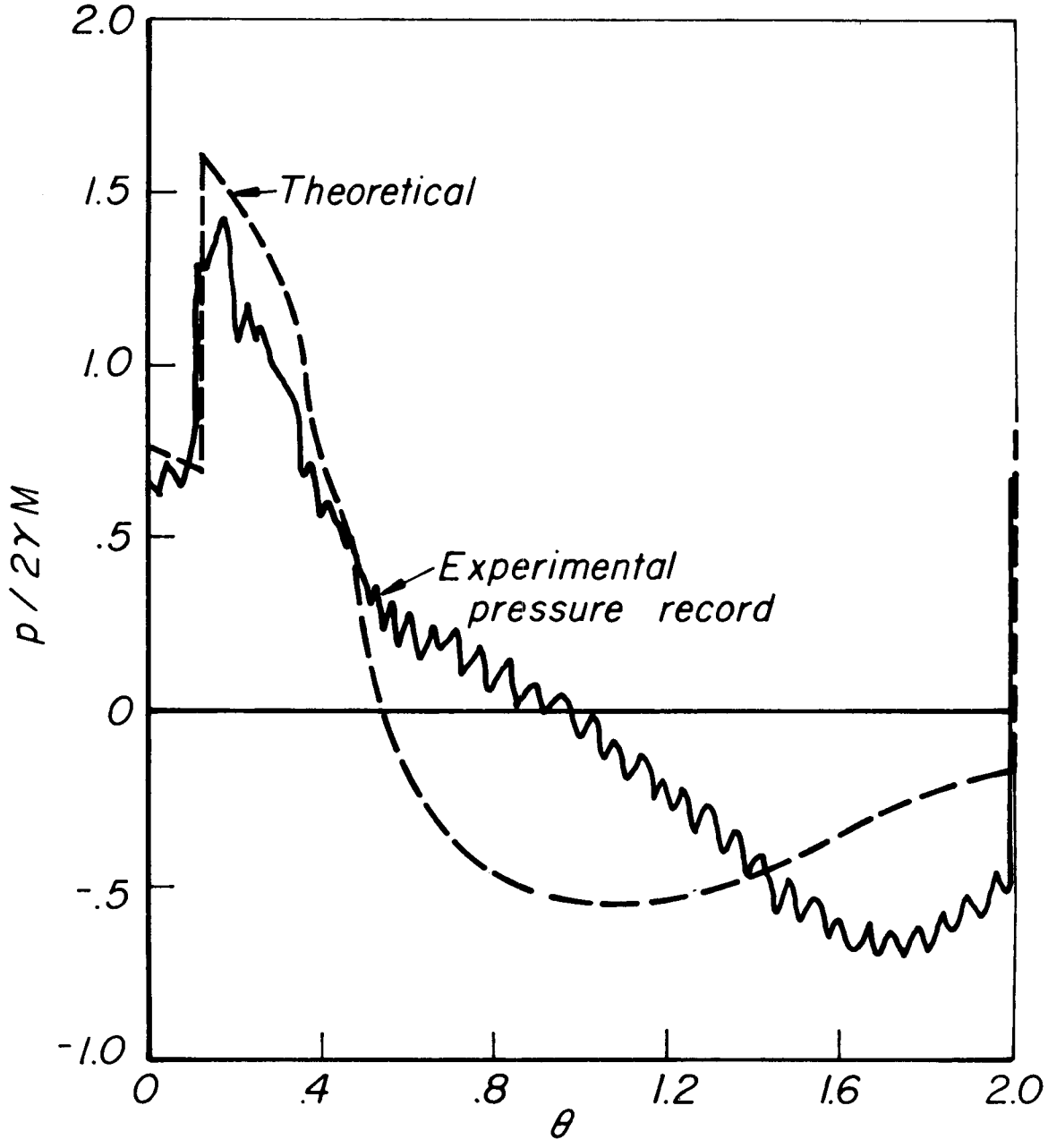

Figure 24

APPENDIX A: CALCULATION OF T_1

1. Calculation of T_1 Following the Shock Wave

It is well known (see for example page 159 of Reference 11) that to first order in shock amplitude the shock velocity is equal to the average of the propagation velocity of sound waves immediately before and after the shock. Thus for a right moving shock, say shock AB in Figure 1, $U_{AB} = \frac{1}{2}\left[u_{II} + a_{II} + u_I + a_I\right]$. Then, using the facts that (to first order in shock amplitude) $u = \bar{u} + u_1$, $a = 1 + a_1$, U_{AB} may be rewritten

$$U_{AB} = \bar{u} + 1 + \tfrac{1}{2}\left(u_{1II} + a_{1I}\right) + \tfrac{1}{2}\left(u_{1I} + a_{1I}\right) \tag{A-1}$$

Similarly, for a left moving shock, say, BC in Figure 1, $U_{BC} = \frac{1}{2}\left[u_I - a_I + u_{II} - a_{II}\right]$ or

$$U_{BC} = \bar{u} - 1 + \tfrac{1}{2}\left(u_{1I} - a_{1I}\right) + \tfrac{1}{2}\left(u_{1II} - a_{1II}\right) \tag{A-2}$$

(a) Concentrated Combustion

When the concentrated combustion model is used, the first order velocity and pressure are given by the following expressions (Equations (I-53) and (I-54))

$$u_1 = f(\theta - x) - f(\theta + x) \tag{A-3}$$

$$a_1 = \frac{\gamma - 1}{2}\left(f(\theta - x) + f(\theta + x)\right) \tag{A-4}$$

Substituting these in Equation (A-1) yields

$$U_{AB} = M + 1 + \frac{\gamma+1}{4}\left(f(0) + f(2)\right) - \frac{3-\gamma}{2} f(2\theta) \quad + O(M^2) \tag{A-5}$$

where $f(0)$ is the value of f immediately following the shock and $f(2)$ is the value of f immediately before the shock, and where it has been noted that $\bar{u} = M$. A similar substitution in Equation (A-2) produces the following first order expression for U_{BC}

$$U_{BC} = M - 1 - \frac{\gamma+1}{4}\left(f(0) + f(2)\right) + \frac{3-\gamma}{4} f(2\theta) \quad + O(M^2) \tag{A-6}$$

The quantity we are seeking to determine is T_1, the first order correction to the acoustic period, 2. The period is simply the sum of the wave travel time from A to B, T_{AB} added to the wave travel time from B to C, T_{BC}. Consequently, we may say $T_1 = T_{AB1} + T_{BC1}$, where T_{AB1} is the first order correction to the wave travel time from A to B and T_{BC1} is the first order correction to the wave travel time from B to C. Clearly, then

$$1 = \int_0^1 dx' = \int_0^{T_{AB}} U_{AB}\, d\theta' = 1 + \int_0^1 U_{AB1}\, d\theta' \quad + T_{AB1} \quad + O(M^2) \tag{A-7}$$

and

$$-1 = \int_1^0 dx' = \int_{T_{AB}}^{T_{AB}+T_{BC}} U_{BC}\, d\theta' = -1 + \int_1^2 U_{BC1}\, d\theta' - T_{BC1} \quad + O(M^2) \tag{A-8}$$

where $U_{AB1} = U_{AB} - 1$, and $U_{BC1} = U_{BC} + 1$, are the first order correction to the wave velocity. Equation (A-7) and (A-8) can be combined to yield the following relation for T_1

$$T_1 = T_{AB1} + T_{BC1} = \int_1^2 U_{BC1}\, d\theta' - \int_0^1 U_{AB1}\, d\theta' \tag{A-9}$$

The integrals on the right hand side of the equation above are evaluated as follows

$$\int_0^1 U_{AB1}\, d\theta' = M + \frac{\gamma+1}{4}\left(f(0) + f(2)\right) - \frac{3-\gamma}{4}\int_0^2 f(\theta')\, d\theta' \tag{A-10}$$

and

$$\int_1^2 U_{BC1}\, d\theta' = M - \frac{\gamma+1}{4}\left(f(0) + f(2)\right) + \frac{3-\gamma}{4}\int_0^2 f(\theta')\, d\theta' \tag{A-11}$$

Finally, substituting Equations (A-10) and (A-11) into (A-9) gives the expression for the first order correction to the period

$$T_1 = -\frac{\gamma+1}{2}\left(f(0) + f(2)\right) + \frac{3-\gamma}{2}\int_0^2 f(\theta')\, d\theta' \tag{A-12}$$

(b) Distributed Combustion

In the case of Distributed Combustion, regardless of velocity

profile as long as $\frac{d\bar{u}}{dx} = M_E$, the following expressions for u_1 and p_1 resulted from first order analysis (in shock strength)

$$p_1 = \gamma \left(f(\theta - x) + f(\theta + x) \right) \tag{A-13}$$

$$u_1 = f(\theta - x) + f(\theta + x) \tag{A-14}$$

p_1 is related to a_1 by the following expression, $a_1 = \frac{\gamma - 1}{2\gamma} p_1 + \frac{s_1}{2}$, where s_1 is the (constant) deviation of the entropy from its steady-state value. Substituting Equations (A-13) and (A-14) into (A-1) and (A-2) yields

$$U_{AB} = \bar{u} + 1 + \frac{\gamma+1}{4} \left(f(0) + f(2) \right) - \frac{3-\gamma}{2} f(2\theta) + \frac{s_1}{2} + O(M_E^2) \tag{A-15}$$

and

$$U_{BC} = \bar{u} - 1 - \frac{\gamma+1}{4} \left(f(0) + f(2) \right) + \frac{3-\gamma}{2} f(2\theta) - \frac{s_1}{2} + O(M_E^2)$$

Again separating T_1 into T_{AB1} and T_{BC1} one finds

$$T_{AB1} = -\int_0^1 U_{AB1} \, d\theta' = -\int_0^1 \bar{u} \, dx' - \frac{\gamma+1}{4} \left(f(0) + f(2) \right) + \frac{3-\gamma}{4} \int_0^2 f(\theta') \, d\theta' - \frac{s_1}{2} \tag{A-16}$$

$$T_{BC1} = \int_1^2 U_{BC1} \, d\theta' = \int_0^1 \bar{u} \, dx' - \frac{\gamma+1}{4} \left(f(0) + f(2) \right) + \frac{3-\gamma}{4} \int_0^2 f(\theta') \, d\theta' - \frac{s_1}{2} \tag{A-17}$$

Addition of (A-16) and (A-17) produces the final expression for T'_1

$$T'_1 = -\frac{\gamma+1}{2}\left(f(0)+f(2)\right) + \frac{3-\gamma}{2}\int_0^2 f(\theta')\,d\theta' - S_1$$

2. An Alternative Method of Calculating T'_1

A second method of calculating T'_1 based on extensions, by Crocco,[23] of some developments by Cantrell and Hart[4] will now be presented. In this case consideration will be limited, for simplicity, to the case of concentrated combustion, though the method is equally applicable to the case of distributed combustion.

Cantrell and Hart studied the stability of acoustic fields under the assumption that the flow in the cavity under consideration was isentropic. They manipulated the equations of motion in such a way that second order, stability determining equations, only containing first order quantities, were obtained. Crocco extended their approach to include non isentropic flow fields and the possibility of a discontinuity in the cavity. His treatment is general in that he derived equations of the nth order containing quantities of only the (n - 1) order and did not limit himself to second order equations composed of first order quantities as was the case in the work of Cantrell and Hart. He also found that it is possible to include source terms and chemically reacting species and still produce equations with the character of being one order higher than the quantities composing them. It is hoped that in the future a paper giving the details of this method in complete generality will be forthcoming.

For the purposes of the present work, however, the potentially

powerful technique will be employed simply to derive the first order correction to the period for the case where no sources are present in the chamber and the flow is homentropic through second order. For a one dimensional flow field under the restrictions imposed in the first chapter, the equations describing the conservation of mass, momentum and energy in the field may be written in non dimensional form, using the non dimensionalizing system of Chapter I, as

$$\frac{\partial \rho}{\partial t} + \frac{\partial \rho u}{\partial x} = 0 \tag{A-18}$$

$$\rho \frac{\partial u}{\partial t} + \rho u \frac{\partial u}{\partial x} = -\frac{1}{\gamma} \frac{\partial p}{\partial x} \tag{A-19}$$

$$\frac{\partial}{\partial t}\left(\rho h_s - \frac{\gamma-1}{\gamma} p\right) + \frac{\partial}{\partial x}\left(\rho u h_s\right) = 0 \tag{A-20}$$

where $h_s = \dfrac{h^*}{C_p^* \bar{T}^*} + \dfrac{\gamma - 1}{2} \left(\dfrac{u^*}{\bar{a}^*}\right)^2$

Because the gas composition is uniform, the following relation obtained from the second law of thermodynamics applies

$$T \frac{\partial s}{\partial x} = \frac{\partial h}{\partial x} - \frac{\gamma-1}{\gamma} \frac{1}{\rho} \frac{\partial p}{\partial x} \tag{A-21}$$

where $s = \dfrac{s^*}{C_p^*}$

If (A-21) and (A-19) are combined, the following equation results

$$\frac{\partial u}{\partial t} + \frac{1}{\gamma-1}\frac{\partial h_s}{\partial x} = \frac{T}{\gamma-1}\frac{\partial s}{\partial x} \qquad \text{(A-22)}$$

Multiplying Equation (A-18) by $\bar{h}_s = 1 - \frac{\gamma-1}{2}M^2$, Equation (A-21) by $(\gamma-1)M$ and subtracting the two equations that result from Equation (A-20) yields

$$\frac{\partial}{\partial t}\left(\rho h_s - \frac{\gamma-1}{\gamma}p - \bar{h}_s\rho - Mu\right) + \frac{\partial}{\partial x}\left(\rho u h_s - \bar{h}_s\rho u - M h_s\right) = -MT\frac{\partial s}{\partial x} \qquad \text{(A-23)}$$

Two quantities that are combinations of the physical variables are introduced

$$q \equiv \rho h_s - \frac{\gamma-1}{\gamma}p - \rho\bar{h}_s - (\gamma-1)Mu - s \qquad \text{(A-24)}$$

$$Q \equiv (\rho u - M)(h_s - \bar{h}_s) \qquad \text{(A-25)}$$

Then, adding and subtracting $\rho uT\frac{\partial s}{\partial x}$ and $u\frac{\partial s}{\partial x}$ to the right hand side of Equation (A-23) and noting that under the assumptions employed $\frac{Ds}{Dt} = 0$, the following expression is obtained

$$\frac{\partial q}{\partial t} + \frac{\partial Q}{\partial x} = \Phi \qquad \text{(A-26)}$$

where $$\Phi \equiv (\rho u - M)\frac{\partial s}{\partial x} - (\rho T - 1)u\frac{\partial s}{\partial x}$$

It is clear upon inspection that if $\mathcal{D}$ or Q is to be of second order in Mach number, only first order variations in the quantities ρ, u, h, T, and s can be considered. Similarly, if $\mathcal{D}$ and Q are of nth order, the physical quantities composing them must be of order $n-1$, $n-2$, $n-3$ - - - - - etc. The quantity q also displays this characteristic, however a little effort must be expended in order to see this. First q is rewritten as follows

$$q = \left(h - \frac{\gamma-1}{\gamma} p - s\right) + (\beta-1)(h_s - \bar{h}_s) + \frac{\gamma-1}{2}(u-M)^2 \qquad \text{(A-27)}$$

The second and third terms above obviously have the desired property of being one order of magnitude smaller than the quantities which compose them. The relationship between h, p and s must be investigated in order to show that this is also true of the first term. Say

$$h = 1 + h_1 + h_2 + - - - -$$

$$p = 1 + p_1 + p_2 + - - - -$$

$$s = s_1 + s_2 + - - - -$$

where subscript one means a quantity of $O(M)$, subscript 2 means a quantity of $O(M^2)$ etc. Recognizing that, in general, $h = h(p, s)$, h may be represented as follows

$$h = h_0 + \left(\frac{\partial h}{\partial p}\right)_0 p_1 + \left(\frac{\partial h}{\partial s}\right)_0 s_1 + \left(\frac{\partial^2 h}{\partial p^2}\right)_0 \frac{p_1^2}{2} + \left(\frac{\partial h}{\partial p}\right)_0 p_2$$

$$+ \left(\frac{\partial^2 h}{\partial p \partial s}\right)_0 p_1 s_1 + \left(\frac{\partial h}{\partial s}\right)_0 s_2 + \left(\frac{\partial^2 h}{\partial s^2}\right)_0 \frac{s_1^2}{2} + \cdots$$

where the subscript zero means that the derivative is to be evaluated in the reference state.

$$h_1 = \left(\frac{\partial h}{\partial p}\right)_0 p_1 + \left(\frac{\partial h}{\partial s}\right)_0 s_1$$

$$h_2 = \left(\frac{\partial^2 h}{\partial p^2}\right)_0 \frac{p_1^2}{2} + \left(\frac{\partial h}{\partial p}\right)_0 p_2 + \left(\frac{\partial^2 h}{\partial p \partial s}\right)_0 p_1 s_1 + \left(\frac{\partial h}{\partial s}\right)_0 s_2 + \left(\frac{\partial^2 h}{\partial s^2}\right)_0 \frac{s_1^2}{2}$$

$$\vdots$$

$$h_n = \left(\frac{\partial h}{\partial p}\right)_0 p_n + \left(\frac{\partial h}{\partial s}\right)_0 s_n + \text{terms of order } n \text{ composed of } (n-1) \text{ order quantities (or lower)}$$

Now,

$$dh = T\,ds + \frac{\gamma - 1}{\gamma}\,\frac{dp}{\rho} \tag{A-28}$$

and

$$dh = \left(\frac{\partial h}{\partial s}\right)_p ds + \left(\frac{\partial h}{\partial p}\right)_s dp \tag{A-29}$$

Therefore, combining Equations (A-28) and (A-29)

$$\left(\frac{\partial h}{\partial s}\right)_p = T \;;\; \left(\frac{\partial h}{\partial s}\right)_0 = 1 \tag{A-30}$$

$$\left(\frac{\partial h}{\partial p}\right)_s = \frac{\gamma - 1}{\gamma \rho} \;;\; \left(\frac{\partial h}{\partial p}\right)_0 = \frac{\gamma - 1}{\gamma} \tag{A-31}$$

This means that

$$h_1 = \frac{\gamma - 1}{\gamma}\, p_1 + s_1$$

$$\vdots$$

$$h_n = \frac{\gamma - 1}{\gamma}\, p_n + s_n + \text{terms of order n composed of products of n-1 order quantities (or lower)}$$

The term $(h - \frac{\gamma - 1}{\gamma} p - s)$ therefore is seen to satisfy the condition that, when it is of order n, the physical quantities composing it, p and s, are order $(n - 1)$ or larger.

Finally, then, Equation (A-26) has the property that to second order in Mach number it is composed of physical quantities which must satisfy the first order conservation equations, to third order it is composed of physical quantities that must satisfy the second order conservation equations and to nth order it is composed only of terms that must satisfy the $n - 1$ order conservation equations.

Consider now a chamber with a shock in it as shown in Figure 1. The cavity is divided into two regions, regions I and II, to the left and to the right of the shock, respectively. In region I

$$\frac{\partial q_I}{\partial t} + \frac{\partial Q_I}{\partial x} = \Phi_I \tag{A-32}$$

and in region II

$$\frac{\partial q_{II}}{\partial t} + \frac{\partial Q_{II}}{\partial x} = \Phi_{II} \tag{A-33}$$

Equation (A-32) is integrated with respect to x from $x = 0$ to $x = \xi$ where ξ is the distance of the shock from the injector, $x = 0$. This yields

$$\int_0^{\xi} \frac{\partial q_I}{\partial t} dx' + Q_I(x=\xi) - Q_I(x=0) = \int_0^{\xi} \Phi_I \, dx' \tag{A-34}$$

Similarly, Equation (A-33) is integrated from $x = \xi$ to $x = 1$

$$\int_{\xi}^{1} \frac{\partial q_{II}}{\partial t} dx' + Q_{II}(x=1) - Q_{II}(x=\xi) = \int_{\xi}^{1} \Phi_{II} dx' \tag{A-35}$$

Using the chain rule for differentiation one finds

$$\int_{0}^{\xi} \frac{\partial q_I}{\partial t} dx' = \frac{d}{dt} \int_{0}^{\xi} q_I dx' - q_{I,\xi} U_{sh} \tag{A-36}$$

and

$$\int_{\xi}^{1} \frac{\partial q_{II}}{\partial t} dx' = \frac{d}{dt} \int_{\xi}^{1} q_{II} dx' + q_{II,\xi} U_{sh} \tag{A-37}$$

where U_{sh} is the shock velocity and $q_{I,\xi}$ and $q_{II,\xi}$ represent, respectively, the value of q_I at $x = \xi$ and the value of q_{II} at $x = \xi$. Adding Equation (A-34) to Equation (A-35) and making use of the relationships (A-36) and (A-37), the following expression is obtained

$$\frac{d}{dt} \int_{0}^{1} q \, dx' + Q(x=1) - Q(x=0) = \Psi + \int_{0}^{1} \Phi \, dx' \tag{A-38}$$

where $\Psi = Q_{II,\xi} - Q_{I,\xi} + U_{sh} (q_{I,\xi} - q_{II,\xi})$.

Using the definitions of Q and q, Ψ may be written

$$\Psi = (\rho_{II} u_{II} - M)(h_{sII} - \bar{h}_s) - (\rho_I u_I - M)(h_{sI} - \bar{h}_s)$$

$$+ U_{sh}\left(\rho_I h_{sI} - \rho_{II} h_{sII} - \frac{\gamma-1}{\gamma}(p_I - p_{II})\right)$$

$$- U_{sh}\left((\rho_I - \rho_{II})\bar{h}_s - (\gamma-1) M (u_I - u_{II}) - (S_I - S_{II})\right) \qquad \text{(A-39)}$$

where all quantities are evaluated at the shock in either region I or region II. The conservation equations for mass, momentum and energy are now written across the normal shock.

mass:

$$\rho_{II}\left(U_{sh} - u_{II}\right) = \rho_I\left(U_{sh} - u_I\right) \equiv m \qquad \text{(A-40)}$$

momentum:

$$\frac{p_{II}}{\gamma} + \rho_{II}\left(U_{sh} - u_{II}\right)^2 = \frac{p_I}{\gamma} + \rho_I\left(U_{sh} - u_I\right)^2 \qquad \text{(A-41)}$$

energy:

$$h_{II} + \frac{\gamma-1}{2}\left(U_{sh} - u_{II}\right)^2 = h_I + \frac{\gamma-1}{2}\left(U_{sh} - u_I\right)^2 \qquad \text{(A-42)}$$

After some manipulation Ψ can be rewritten in the following form

$$\psi = M\left[\left(h_{sI} - (\gamma-1)\,U_{sh}\,u_I\right) - \left(h_{sII} - (\gamma-1)\,U_{sh}\,u_{II}\right)\right]$$

$$+\ \bar{h}_s\left[\rho_{II}\left(U_{sh} - u_{II}\right) - \rho_I\left(U_{sh} - u_I\right)\right]$$

$$+\ m\left[\left(h_{sII} - (\gamma-1)\,U_{sh}\,u_{II}\right) - \left(h_{sI} - (\gamma-1)\,U_{sh}\,u_I\right)\right]$$

$$-\ U_{sh}(\gamma-1)\left[\left(\frac{p_I}{\gamma} + m u_I\right) - \left(\frac{p_{II}}{\gamma} + m u_{II}\right)\right] - U_{sh}\left(s_I - s_{II}\right)$$

(A-43)

The first and third terms on the right hand side of the above expression vanish because of Equation (A-42), the second term because of Equation (A-40) and the fourth term because of Equation (A-41). Therefore, Equation (A-43) reduces to

$$\psi = -\left(s_{II} - s_I\right) U_{sh} \tag{A-44}$$

It is convenient to rewrite this as

$$\psi = -\Delta s\,\left|U_{sh}\right| \tag{A-45}$$

where Δs represents the positive jump in the value of the entropy across the shock wave. Using Equation (A-45), Equation (A-38) becomes

$$\frac{d}{dt}\int_0^1 q\,dx' + Q(x=1) - Q(x=0) = \int_0^1 \Phi\,dx' - \Delta s\,\left|U_{sh}\right|$$

(A-46)

Since a second order analysis was performed in Chapter 1, we wish to find a relationship between first and second order quantities that will determine T_1. To do this Equation (A-46) must be written out correct through third order in the Mach number. Because s, the entropy, is of order M^3, the term $\int_0^1 \Phi \, dx'$ is seen to be of $O(M^4)$ or smaller. Consequently, this term can be dropped to third order. If the transformation from t to θ is used then Equation (A-46) is written

$$T_1 \frac{d}{d\theta} \int_0^1 q_2 \, dx' + \frac{d}{d\theta} \int_0^1 (q_2 + q_3) \, dx' + (Q_2 + Q_3)\Big|_{x=0}^{x=1} = -\Delta S + O(M^4)$$

where

$$\theta = \frac{2}{T} t \quad , \quad T = T_1 + T_2 + \cdots \tag{A-47}$$

In the above equation the definitions $q = q_2 + q_3 + O(M^4)$, and $Q = Q_2 + Q_3 + O(M^4)$ have been used, where q_2 is $O(M^2)$, q_3 is $O(M^3)$ etc. Also, to third order $|U_{sh}|$ has been taken to be equal to the steady-state sound velocity, (unity in non dimensional form) since ΔS is of $O(M^3)$.

If the physical quantities of interest (p, u, a, h, s etc.) are to be periodic to second order in θ with period two, then, also, q must be periodic in two. Thus, it must be so that $\int_\theta^{\theta+2} \left[\frac{d}{d\theta'} \int_0^1 q \, dx \right] d\theta' = 0$. Then, integrating Equation (A-47) from $\theta = \theta$ to $\theta = \theta + 2$, yields

$$\int_\theta^{\theta+2} \left[Q_3(x=1) - Q_3(x=0) \right] d\theta = -\int_\theta^{\theta+2} \Delta S \, d\theta$$

(A-48)

where it has been noted that, since $u_1(x = 0) = u_1(x = 1) = 0$, $Q_2(x = 1) = Q_2(x = 0) = 0$. It is well known (see for instance Ref. 12) that the increase in entropy across a normal shock can be related to the strength of the shock in the following way

$$s^* = \frac{R^*(\gamma + 1)}{12\gamma^2} \left| \frac{\Delta p^*}{p^*} \right|^3$$

or, in nondimensional form, to $O(M^3)$ $\Delta s = \frac{(\gamma^2 - 1)}{12\gamma^2} |\Delta p_1|^3$. Moreover, from the results of Chapter 1 it is known that to the present order of approximation the strength of the shock is the same whether moving toward the injector or the nozzle and is given by $|\Delta p_1| = \gamma (f(0) - f(2))$. Thus, Equation (A-48) may now be written

$$\int_{\theta}^{\theta+2} \left[Q_3(x=1) - Q_3(x=0) \right] d\theta = -\frac{(\gamma+1)}{6} \left[f(0) - f(2) \right]^3$$

(A-49)

It will be recalled that Q was defined as $Q = (\rho u - M)(h + \frac{\gamma - 1}{2} u^2 - \bar{h}_s)$. It is desired now to find Q in terms of f. In general $h = h(p_1 s)$. However, since $s_1 = s_2 = 0$ we may write

$$h = 1 + \left(\frac{\partial h}{\partial p}\right)_0 p_1 + \left(\frac{\partial h}{\partial p}\right)_0 p_2 + \left(\frac{\partial^2 h}{\partial p^2}\right)_0 \frac{p_1^2}{2} + O(M^3)$$

Then, since $\left(\frac{\partial h}{\partial p}\right)_0 = \frac{\gamma - 1}{\gamma}$, and $\left(\frac{\partial^2 h}{\partial p^2}\right)_0 = \left(\frac{\partial \frac{1}{s}}{\partial p}\right)_0 = \frac{\gamma - 1}{\gamma}$

(see Equation (A-31)), the following expression for h_1 results

$$h = \frac{\gamma-1}{\gamma} p_1 + \frac{\gamma-1}{\gamma} p_2 - \frac{\gamma-1}{\gamma} \frac{p_1^2}{2} + O(M^3)$$

(A-50)

Using this in the definition of Q it is found that, to third order

$$Q_3 = (\rho_1 M + \rho_1 u_1 + u_2)\left(\frac{\gamma-1}{\gamma} p_1\right) + u_1\left[\frac{\gamma-1}{\gamma} p_2 - \frac{\gamma-1}{2\gamma} p_1^2 + (\gamma-1) M u_1 + (\gamma-1) u_1^2\right]$$

(A-51)

At $x = 0$ and $x = 1$, $u_1 = 0$, consequently the second term on the right hand side vanishes at these locations. The quantities ρ_1 and p_1 can be related to a_1 by using the isentropic condition. Q_3 at either the injector or nozzle may then be written $Q_3 = 2a_1\left(\frac{2}{\gamma - 1} a_1 M + u_2\right)$ where a_1 and u_2 are to be evaluated at either $x = 1$ or $x = 0$. At the injector the condition on u_2 due to the combustion occurring there, is $u_2(x = 0) = \frac{2}{\gamma - 1} M \left[a_1 - \gamma n\, a_1(\theta - \mu)\right]$. This combustion zone boundary condition was presented in the first chapter. Substituting this relationship for u_2 into the expression for Q_3 yields

$$Q_3(x=0) = \frac{4}{\gamma-1} M a_1 \gamma n \left(a_1 - a_1(\theta-\mu)\right)$$

(A-52)

Similarly, the constant Mach number requirement at $x = 1$, $u_2 = Ma_1$, means that

$$Q_3(x=1) = \frac{2}{\gamma-1}(\gamma+1) M a_1^2$$

(A-53)

Expressing a_1 and u_1 in terms of f (see Equations (I-53) and (I-54)) Equations (A-52) and (A-53) become respectively

$$Q_3(x=0) = 4(\gamma-1) M \gamma n \left(f^2(\theta) - f(\theta) f(\theta-\mu)\right)$$

(A-54)

$$Q_3(x=1) = 2(\gamma^2-1)Mf^2$$

(A-55)

Now, from Equation (I-76)

$$ff(\theta-\mu) = \frac{f}{2\gamma nM}\left[\frac{df}{d\theta}\left(T_1 + (\gamma+1)f - \frac{3-\gamma}{2}\int_0^2 f(\eta)\,d\eta\right) - \left((\gamma+1)-2\gamma\eta\right)Mf\right]$$

(A-56)

Consequently, Q_3 at $x = 0$ can be written

$$Q_3(x=0) = 2(\gamma^2-1)Mf^2 - 2(\gamma-1)\left[\frac{df}{d\theta}\left(T_1 + (\gamma+1)f - \frac{3-\gamma}{2}\int_0^2 f(\eta)\,d\eta\right)\right]f$$

(A-57)

Substituting Equation (A-57) and (A-55) into Equation (A-49) and performing the integration on the left hand side yields

$$2(\gamma-1)\left\{\left[T_1 - \frac{3-\gamma}{2}\int_0^2 f(\eta)\,d\eta\right]\left(\frac{f^2(2)}{2} - \frac{f^2(0)}{2}\right) + (\gamma+1)\left(\frac{f^3(2)}{3} - \frac{f^3(0)}{3}\right)\right\}$$

$$= \frac{\gamma^2-1}{6}\left(f(2)-f(0)\right)^3$$

(A-58)

This may be rewritten

$$3X^3 - 3y^2 + X^2(6\alpha+3y) - y^2(6\alpha+3X) = 0$$

(A-59)

where $\alpha = \frac{T_1}{\gamma+1} - \frac{3-\gamma}{2(\gamma+1)}\int_0^2 f(\eta)\,d\eta$, $X = f(2)$, $y = f(0)$

In order for this expression to hold for all periodic solutions, it must hold for all values of x and y, ($f(2)$ and $f(0)$). Thus, one must solve Equation (A-59) for α. This is easily done and the following value for α is obtained

$$\alpha = -\frac{1}{2}(x+y) = \frac{1}{2}\left[f(0) + f(2)\right] \tag{A-60}$$

Using the definition of α following Equation (A-59), then gives the final expression for T_1

$$T_1 = -\frac{\gamma+1}{2}\left(f(0)+f(2)\right) + \frac{3-\gamma}{2}\int_0^2 f(\eta)\,d\eta \tag{A-61}$$

This is precisely the same result found using the first method.

It is clear that somewhat more manipulation is required in order to find T_1 using the second method presented above. To the order of approximation necessary for the present work, that is, in order to find T_1, this extra effort can hardly be justified. However, the second method can easily and consistently be extended in order to determine the higher order corrections to the period. This is not true for the first method since it was dependent on the fact that, to lowest order in shock strength, the velocity of the shock is the average velocity of sound waves immediately before and after the shock. Of course, for higher order analyses this would no longer be true. Thus, because the second technique is more general, and can be applied to higher order analyses, it is felt that the presentation of the second method is appropriate.

DISTRIBUTION FOR THIS REPORT

NASA

NASA Headquarters
Washington, D.C. 20546
Attn: Alfred Gessow
Robert S. Levine RPL (3)
A. O. Tischler RP

NASA
Universal North Building
Connecticut & Florida Avenues
Washington, D.C.
Attn: T.L. Smull, Director
Grants & Space Contracts (10)

NASA Scientific & Technical
Information Facility
P.O. Box 33
College Park, Maryland 20740 (15)

NASA Headquarters
Washington, D.C. 20546
Attn: E.L. Gray, Director
Advanced Manned Missions, MT
Office of Manned Space Flight

Attn: V.L. Johnson, Director
Launch Vehicles & Propulsion, SV
Office of Space Science

Ames Research Center
Moffett Field
California 94035
Attn: Technical Librarian
Designee: Harold Hornby
Mission Analysis Division

Goddard Space Flight Center
Greenbelt, Maryland 20771
Attn: Technical Librarian
Designee: Merland L. Moseson
Code 620

Jet Propulsion Laboratory
California Institute of Technology
4800 Oak Grove Drive
Pasadena, California 91103
Attn: J.H. Rupe

Attn: Technical Librarian
Designee: Henry Burlage, Jr.
Propulsion Div., 38

John F. Kennedy Space Center, NASA
Cocoa Beach, Florida 32931
Attn: Technical Librarian
Designee: Kurt H. Debus

Langley Research Center
Langley Station
Hampton, Virginia 23365
Attn: Technical Librarian
Designee: Floyd L. Thompson, Director

NASA
Lewis Research Center
21000 Brookpark Road
Cleveland, Ohio 44135
Attn: M.F. Heidmann (Technical Monitor)
R.J. Priem
E. Conrad

Attn: Technical Librarian
Designee: A. Silverstein, Director

Manned Spacecraft Center
Houston, Texas 77001
Attn: G. Spencer

Attn: Technical Librarian
Designee: Robert R. Gilruth, Director

Marshall Space Flight Center
R-P&VED
Huntsville, Alabama 35812
Attn: Jerry Thomson
R.J. Richmond

Attn: Technical Librarian
Designee: Hans G. Paul

GOVERNMENT INSTALLATIONS

Headquarters, U.S. Air Force
Washington 25, D.C.
Attn: Technical Librarian
Designee: Col. C.K. Stambaugh
AFRST

Aeronautical Systems Division
Air Force Systems Command
Wright-Patterson Air Force Base
Dayton, Ohio 45433
Attn: Technical Librian
Designee: D.L. Schmidt
Code ASRCNC-2

Air Force Missile Test Center
Patrick Air Force Base
Florida
Attn: Technical Librarian
Designee: L.J. Ullian

Air Force Office of Scientific Research
Propulsion Division
Washington, D.C.
Attn: B.T. Wolfson

Air Force Rocket Propulsion Laboratory
Research & Technology Division
Air Force Systems Command
Edwards, California 93523
Attn: R.R. Weiss, RPRR

Attn: Technical Librarian
Designee: H. Main

Air Force Systems Division
Air Force Unit Post Office
Los Angeles 45, California
Attn: Technical Librarian

ARL (ARC)
Building 450
Wright-Patterson Air Force Base
Dayton, Ohio
Attn: K. Scheller

Arnold Engineering Development Center
Arnold Air Force Station
Tullahoma, Tennessee
Attn: Technical Librarian
Designee: H.K. Doetsch

Department of the Navy
Bureau of Naval Weapons
Washington, D.C.
Attn: Technical Librarian
Designee: J. Kay
RTMS-41

Department of the Navy
Office of Naval Research
Washington, D.C. 20360
Attn: R.O. Jackel

Defense Documentation Center Headquarters
Cameron Station, Building 5
5010 Duke Street
Alexandria, Virginia 22314
Attn: TISIA

Naval Ordnance Station
Research & Development Dept.
Indian Head, Maryland 20640
Attn: Lionel A. Dickinson

Picatinny Arsenal
Dover, New Jersey 07801
Attn: E. Jenkins

Attn: Technical Librarian
Designee: I. Forsten, Chief
Liquid Propulsion Lab.
SMUPA-DL

Redstone Scientific Information
Building 4484
Redstone Arsenal
Huntsville, Alabama
Attn: Technical Librarian

RTNT
Bolling Field
Washington, D.C. 20332
Attn: L. Green, Jr.

U.S. Army Missile Command
Redstone Arsenal
Huntsville
Alabama 35809
Attn: J. Connaughton

Attn: Technical Librarian
Designee: Walter Wharton

U.S. Atomic Energy Commission
Technical Information Services
Box 62
Oak Ridge, Tennessee
Attn: Technical Librarian
Designee: A.P. Huber
Gaseous Diffusion Plant
(ORGDP) P.O. Box P

U.S. Naval Ordnance Test Station
China Lake
California 93557
Attn: E.W. Price

Attn: Technical Librarian
Designee: Code 4562
Chief,
Missile Propulsion Div.

CPIA

Chemical Propulsion Information Agency
Applied Physics Laboratory
The John Hopkins University
8621 Georgia Avenue
Silver Spring, Maryland 20910
Attn: T.W. Christian

Attn: Technical Librarian
Designee: Neil Safeer

INDUSTRY CONTRACTORS

Aerojet-General Corporation
P.O. Box 296
Azusa, California 91703
Attn: Technical Librarian
Designee: L.F. Kohrs

Aerojet-General Corporation
P.O. Box 1947
Sacramento, California 95809
Attn: R.J. Hefner

Attn: Technical Librarian
Bldg. 2015, Dept. 2410
Designee: R. Stiff

Aeronutronic
Philco Corporation
Ford Road
Newport Beach, California 92663
Attn: Technical Librarian
Designee: D.A. Carrison

Aerospace Corporation
P.O. Box 95085
Los Angeles, California 90045
Attn: O.W. Dykema

Attn: Technical Librarian
Designee: John G. Wilder
MS-2293
Propulsion Dept.

Astrosystems International, Inc.
1275 Bloomfield Avenue
Fairfield, New Jersey 07007
Attn: Technical Librarian
Designee: A. Mendenhall

Atlantic Research Corporation
Edsall Road and Shirley Highway
Alexandria, Virginia 22314
Attn: Technical Librarian
Designee: A. Scurlock

Autonetics
Div. of North American Aviation, Inc.
3370 Miraloma Avenue
Anaheim, California 92803
Attn: Dr. Ju Chin Chu

Battelle Memorial Institute
505 King Avenue
Columbus 1, Ohio
Attn: Charles E. Day,
Classified Rept. Librarian

Bell Aerosystems Company
P.O. Box 1
Buffalo 5, New York 14240
Attn: K. Berman
J. Senneff

Attn: Technical Librarian
Designee: W.M. Smith

Boeing Company
P.O. Box 3707
Seattle, Washington 98124
Attn: Technical Librarian
Designee: J.D. Alexander

Bolt, Berenak & Newman, Inc.
Cambridge, Mass.
Attn: Dr. Dyer

Chrysler Corporation
Missile Division
P.O. Box 2628
Detroit, Michigan 48231
Attn: Technical Librarian
Designee: John Gates

Curtiss-Wright Corporation
Wright Aeronautical Division
Wood-Ridge, New Jersey 07075
Attn: Technical Librarian
Designee: G. Kelley

Defense Research Corporation
6300 Hollister Avenue
P.O. Box 3587
Santa Barbara, California 93105
Attn: B. Gray
C.H. Yang

Douglas Aircraft Company
Missile & Space Systems Division
3000 Ocean Park Boulevard
Santa Monica, California 90406
Attn: Technical Librarian
Designee: R.W. Hallet
Advanced Space Tech.

Douglas Aircraft Company
Astropower Laboratory
2121 Paularino
Newport Beach, California 92663
Attn: Technical Librarian
Designee: George Moc
Director, Research

Dynamic Science Corporation
1445 Huntington Drive
South Pasadena, California
Attn: M. Beltran

General Dynamics/Astronautics
Library & Information Services (128-00)
P.O. Box 1128
San Diego, California 92112
Attn: Technical Librarian
Designee: Frank Dore

General Electric Company
Advanced Engine & Technology Dept.
Cincinnati, Ohio 45215
Attn: Technical Librarian
Designee: D. Suichu

General Electric Company
Malta Test Station
Ballstan Spa, New York
Attn: Alfred Graham, Manager
Rocket Engines

General Electric Company
Re-Entry Systems Department
3198 Chestnut Street
Philadelphia, Pennsylvania 19101
Attn: Technical Librarian
Designee: F.E. Schultz

Geophysics Corporation of America
Technical Division
Bedford, Massachusetts
Attn: A.C. Toby

Grumman Aircraft Engineering Corp.
Bethpage
Long Island, New York
Attn: Technical Librarian
Designee: Joseph Gavin

Institute for Defense Analyses
RESD
400 Army-Navy Drive
Arlington, Virginia
Attn: Warren C. Strahle

Ling-Temco-Vought Corporation
Astronautics
P.O. Box 5907
Dallas, Texas 75222
Attn: Technical Librarian
Designee: Warren C. Trent

Arthur D. Little, Inc.
20 Acorn Park
Cambridge, Massachusetts 02140
Attn: E. Karl Bastress
Attn: Technical Librarian

Lockheed Missiles & Space Co.
P.O. Box 504
Sunnyvale, California 94088
Attn: Technical Information Center
Designee: Y.C. Lee

Lockheed Propulsion Company
P.O. Box 111
Redlands, California 91409
Attn: Technical Librarian
Designee: H.L. Thackwell

McDonnell Aircraft Corporation
P.O. Box 516
Municipal Airport
St. Louis, Missouri 63166
Attn: Technical Librarian
Designee: R.A. Herzmark

The Marquardt Corporation
16555 Saticoy Street
Van Nuys, California 91409
Attn: Technical Librarian
Designee: Warren P. Boardman, Jr.

Martin Marietta Corporation
Denver Division
P.O. Box 179
Denver, Colorado 80201
Attn: Technical Librarian
Designee: J.D. Goodlette (A-241)

Multi-Tech. Inc.
Box 4186 No. Annex
San Fernando, California
Attn: F. B. Cramer

Northrup Space Laboratories
3401 West Broadway
Hawthorne, California
Attn: Technical Librarian
Designee: William Howard

Rocket Research Corporation
520 South Portland Street
Seattle, Washington 98108
Attn: Technical Librarian
Designee: Foy McCullough, Jr.

Rocketdyne
Division of North American Aviation
6633 Canoga Avenue
Canoga Park, California 91304
Attn: R. Fontaine
R.B. Lawhead

Attn: Technical Librarian
(Library 586-306)
Designee: E.B. Monteath

Space & Information Systems Division
North American Aviation, Inc.
12214 Lakewood Boulevard
Downey, California 90241
Attn: Technical Librarian
Designee: H. Storms

Rohm & Haas Company
Redstone Arsenal
Huntsville, Alabama
Attn: Librarian

Stanford Research Institute
333 Ravenswood Avenue
Menlo Park, California 94025
Attn: Technical Librarian
Designee: G. Marxman

Thiokol Chemical Corporation
Huntsville Division
Huntsville, Alabama
Attn: Technical Librarian
Designee: John Goodloe

Thiokol Chemical Corporation
Reaction Motors Division
Denville, New Jersey 07832
Attn: D. Mann

Attn: Technical Librarian
Designee: Arthur Sherman

TRW Systems
One Space Park
Redondo Beach, California 90278
Attn: G.W. Elverum
Attn: Donald H. Lee

Attn: Technical Librarian
Designee: Sam J. Van Grouw

United Technology Center
Division of United Aircraft Corporation
P.O. Box 358
Sunnyvale, California 94088
Attn: R.H. Osborn
Attn: Technical Librarian

Pratt & Whitney Aircraft Company
Division of United Aircraft Corp.
West Palm Beach
Florida
Attn: G. Lewis

Pratt & Whitney Aircraft Company
Division of United Aircraft Corp.
Engineering, Building 1-F
East Hartford, Connecticut
Attn: D.H. Utvik

Research Laboratories
Division of United Aircraft Corp.
400 Main Street
East Hartford, Connecticut 06108
Attn: Technical Librarian
Designee: Erle Martin

Walter Kidde and Company
Aerospace Operations
567 Main Street
Belleville, New Jersey 07109
Attn: Technical Librarian
Designee: R. J. Hanville

Warner-Swasey Company
Control Instrument Division
32-16 Downing Street
Flushing, New York 11354
Attn: R.H. Tourin

UNIVERSITIES

California Institute of Technology
204 Karman Laboratory
Pasadena, California 91109
Attn: Fred E. Culick

Case Institute of Technology
Engineering Division
University Circle
Cleveland, Ohio 44106
Attn: C.R. Klotz

Dartmouth University
Hanover
New Hamshire
Attn: P.D. McCormack

Georgia Institute of Technology
Aerospace School
Atlanta 13
Georgia
Attn: Ben T. Zinn

Illinois Institute of Technology
10 W. 35th Street
Chicago, Illinois
Attn: P.T. Torda

The John Hopkins University
Applied Physics Laboratory
8621 Georgia Avenue
Silver Spring, Maryland
Attn: W.G. Berl

Massachusetts Institute of Technology
Cambridge 39
Massachusetts
Attn: T.Y. Toong
Dept. of Mechanical Engineering
Attn: Gail E. Partridge, Librarian
Engineering Projects Laboratory

New York University
Dept. of Chemical Engineering
New York 53, New York
Attn: P.F. Winternitz

Ohio State University
Rocket Research Laboratory
Dept. of Aeronautical & Astronautical Eng.
Columbus 10, Ohio
Attn: Technical Librarian

Polytechnic Institute of Brooklyn
Graduate Center
Route 110
Farmingdale, New York
Attn: V.D. Agosta

Purdue University
School of Mechanical Engineering
Lafayette, Indiana
Attn: J.R. Osborn

Sacramento State College
Engineering Division
60000 J. Street
Sacramento, California 95819
Attn: F.H. Reardon

Sheffield University
Research Laboratories
Harpur Hill
Buxton, Derbyshire
England
Attn: V.J. Ibberson

University of California
Institute of Engineering Research
Berkeley, California
Attn: A.K. Oppenheim

University of Michigan
Aeronautical & Astronautical Eng. Labs.
Aircraft Propulsion Lab.
North Campus
Ann Arbor, Michigan
Attn: J.A. Nicholls

University of Southern California
Dept. of Mechanical Engineering
University Park
Los Angeles, California 90007
Attn: M. Gerstein

University of Wisconsin
Dept. of Mechanical Engineering
1513 University Avenue
Madison, Wisconsin
Attn: P.S. Myers

Yale University
Dept. of Engineering & Applied Science
Mason Laboratory
400 Temple Street
New Haven, Connecticut
Attn: B.T. Chu